Earth-Science Reviews 102 (2010) 159–206

Contents lists available at ScienceDirect

Earth-Science Reviews

journal homepage: www.elsevier.com/locate/earscirev

Lithosphere tectonics and thermo-mechanical properties: An integrated modelling approach for Enhanced Geothermal Systems exploration in Europe

S. Cloetingh [a,*], J.D. van Wees [a,b], P.A. Ziegler [c], L. Lenkey [d], F. Beekman [a], M. Tesauro [a], A. Förster [e], B. Norden [e], M. Kaban [e], N. Hardebol [a], D. Bonté [a], A. Genter [f], L. Guillou-Frottier [g], M. Ter Voorde [a], D. Sokoutis [a], E. Willingshofer [a], T. Cornu [a], G. Worum [a]

[a] Faculty of Earth and Life Sciences, VU University, De Boelelaan 1085, 1081 HV Amsterdam, The Netherlands
[b] TNO, PO Box 80015, 3508 TA Utrecht, The Netherlands
[c] Department of Earth Sciences, University of Basel, Bernoullistrasse 32, 4056 Basel, Switzerland
[d] Department of Geophysics, Loránd Eötvös University, Ludovika tér 2, 1083 Budapest, Hungary
[e] GeoForschungsZentrum Potsdam (GFZ), Telegrafenberg, 14473 Potsdam, Germany
[f] EIGE Heat Mining, France
[g] BRGM, 3av. Claude Villemin, Orleans, France

ARTICLE INFO

Article history:
Received 18 August 2009
Accepted 19 May 2010
Available online 8 June 2010

Keywords:
geothermal
EGS
tectonics
basin models

ABSTRACT

Knowledge of temperature at drillable depth is a prerequisite in site selection for geothermal exploration and development of enhanced geothermal systems (EGS). Equally important, the thermo-mechanical signature of the lithosphere and crust provides critical constraints for the crustal stress field and basement temperatures where borehole observations are rare. The stress and temperature field in Europe is subject to strong spatial variations often linked to polyphase extensional and compressional reactivation of the lithosphere, in different modes of deformation. The development of innovative combinations of numerical and analogue modelling techniques is key to thoroughly understand the spatial and temporal variations in crustal stress and temperature. In this paper we present an overview of advances in developing and applying analogue and numerical thermo-mechanical models to quantitatively assess the interplay of lithosphere dynamics and basin (de)formation. Field studies of kinematic indicators and numerical modelling of present-day and paleo-stress fields in selected areas yield new constraints on the causes and the expression of intraplate stress fields in the lithosphere, driving basin (de)formation. The actual basin response to intraplate stress is strongly affected by the rheological structure of the underlying lithosphere, the basin geometry, fault dynamics and interplay with surface processes. Integrated basin studies show that the rheological structure of the lithosphere plays an important role in the spatial and temporal distribution of stress-induced vertical motions, varying from subtle faulting to basin reactivation and large wavelength patterns of lithospheric folding. These findings demonstrate that sedimentary basins are sensitive recorders of the intraplate stress field. The long lasting memory of the lithosphere, in terms of lithospheric scale weak zones, plays a far more important role in basin formation and reactivation than hitherto assumed. A better understanding of the 3-D linkage between basin formation and basin reactivation is, therefore, an essential step in connecting lithospheric forcing and upper mantle dynamics to crustal vertical motions and stress, and their effect on sedimentary systems and heat flow. Vertical motions in basins can become strongly enhanced, through coupled processes of surface erosion/sedimentation and lower crustal flow. Furthermore, patterns of active thermal attenuation by mantle plumes can cause a significant spatial and modal redistribution of intraplate deformation and stress, as a result of changing patterns in lithospheric strength and rheological layering. The models provide useful constraints for geothermal exploration and production, including understanding and predicting crustal stress and basin and basement heat flow.

* Corresponding author. Tel.: +31 205987341.
E-mail address: sierd.cloetingh@falw.vu.nl (S. Cloetingh).

0012-8252/$ – see front matter © 2010 Elsevier B.V. All rights reserved.
doi:10.1016/j.earscirev.2010.05.003

Contents

1. Introduction

At upper crustal levels (<10 km) the Earth contains a significant amount of heat, which allows the extraction of geothermal energy through producing hot water from the subsurface used for heating and electricity production. The Enhanced Geothermal System (EGS) concept (Gérard et al., 2006, Fig. 1) consists essentially of drilling at least two boreholes (a "doublet") into deep fractured rock, extracting hot fluid from a production well and injecting the cooled fluid back into the fractured reservoir through an injection well. To this end, both boreholes have been stimulated to connect the two wells to the natural surrounding geothermal reservoir by artificially enhancing the permeability of the natural network of fractures in their vicinity. This may imply some direct connections between the wells through natural fractures. The EGS, in theory, will provide abundant environmentally friendly quantities of heat or electricity in the future. In the USA it has been estimated that EGS can most likely provide about 5–10 % of electricity demand in 2050 (e.g. Tester et al., 2007).

Contrary to conventional hydrothermal reservoirs, Enhanced Geothermal Systems require hydraulic stimulation, since the rock mass permeability in the vicinity of the boreholes is generally too low for economic heat recovery. Stimulation proved successful in the Soultz research project in eastern France (Gérard et al., 2006, Fig. 1) and in the commercial project of Landau (Palatinate, western Germany). Temperature conditions are critical for the potential of electricity production, as both influence the thermal power and the efficiency of electricity generation (e.g. DiPippo, 2007). Currently at temperatures of ca 120 °C, relatively high flow rates of ca 150 l s^{-1} are capable to deliver a power of about 3 MWe (Schoenwiesner-Bozkurt, 2006). On the other hand at much higher temperatures of 150–200 °C flow rates of 50–100 l s^{-1} are sufficient to deliver the same amount of power. Given the notion that higher reservoir temperatures both increase efficiency and thermal power it is important to identify prospects with relatively high temperatures, and/or flow rate capable of sustaining power production over the lifetime of the geothermal project. For hydraulic stimulation prediction of the stress field orientation and magnitude is required for optimizing well planning during exploitation. Success of hydraulic stimulation is dependent on the thermo-mechanical properties of the crust. Critically stressed regions, marked by active deformation, require little excess pressure for stimulation and are therefore favoured. In addition such regions are marked by pre-existing faults and fractures, forming preferential pathways for stimulated flow.

At the same time, critically stressed regions are often also marked by high density of natural earthquakes. In the deep heat mining projects in Soultz (France) and Basel (Switzerland), it has been observed that 'felt' microseismic events occur after shut-in of the hydraulic stimulation (Charléty et al., 2007; Häring et al., 2008). In Basel after shutting in the well for about 5 h, a seismic event of M_L 3.4 occurred during preparations for bleeding off the well to hydrostatic

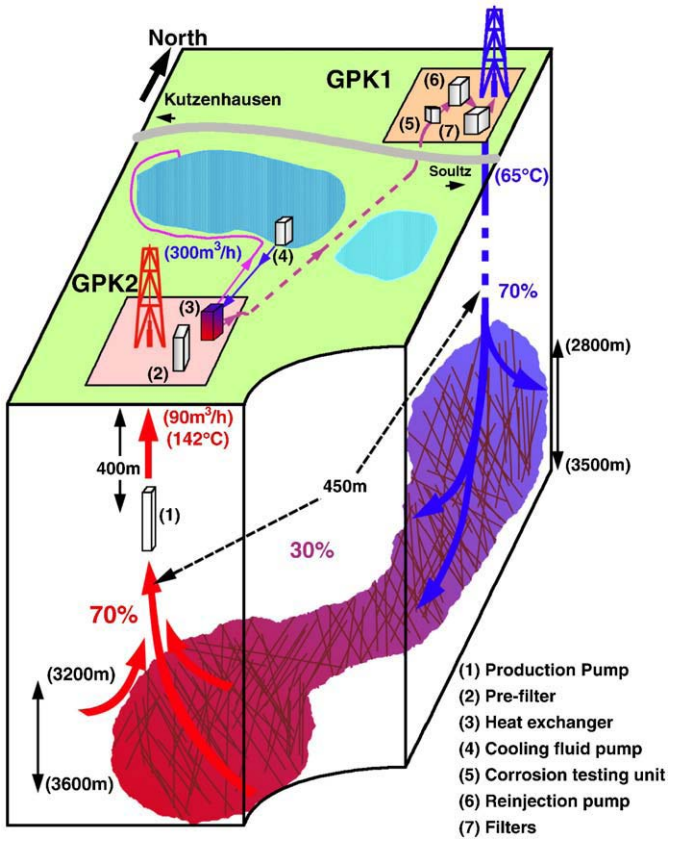

Fig. 1. Schematic block diagram of the 1997 Enhanced geothermal System (EGS) circulation test performed at Soultz (Upper Rhine Graben, eastern France) when heat was extracted at a rate of 10MW$_{th}$. GPK1 and GPK2 are the injection and production well, respectively. The pumps used to circulate the fluids consumed less than 250 kW of electricity (from Gérard et al., 2006).

conditions. Over the following 56 days, three aftershocks of $M_L>3$ were recorded. At present the project is suspended but not abandoned pending an independent risk analysis and identification of acceptable ways of reservoir enhancement (Häring et al., 2008). Favourable conditions of tectonic stress are required to allow hydraulic stimulation of the naturally fractured rock mass with limited injection pressure.

In recent years EGS conditions have been identified at drillable depths in many locations within Europe (e.g. Genter et al., 2003, Fig. 2). These areas have been selected largely on the basis of observations of high near surface temperature gradients derived from surface heat flow values and magmatism (e.g. volcanic areas such as Iceland and Tuscany in central Italy) and or relatively high temperatures assessed in deep boreholes drilled mainly for hydrocarbon exploration and production (e.g. Soultz-sous-Forêt, Landau). In addition geological information (Fig. 3), world stress map information (Heidbach et al., 2008, Fig. 4) and natural seismicity (Fig. 5) can be used to identify active deforming basins and basement areas which are critically stressed. Microseismic monitoring shows that critically stressed pre-existing faults and fractures are preferential pathways for hydraulic stimulation, marked by a shear mode of fracturing (e.g. Häring et al., 2008). From exploration and production wells it appears that deep and widespread convective hydrothermal systems in the basement rock in favourable settings are capable of enhancing local heat flow. In the basement, natural fracture networks are conduits for fluid flow (e.g. Sanjuan et al., 2006).

Assessment of exploration potential of continental intraplate regions for EGS is generally not taking into account lithosphere-scale tectonic models. At the same time, tectonics has been recognized to be of prime importance for the creation of favourable thermo-mechanical conditions (e.g. Genter et al., 2003). To fill in this gap, we review in this paper the relevance of quantitative assessment of tectonic processes for EGS exploration. In this context, we will demonstrate that tectonic models can be used for the following purposes:

- To understand the relationship between proven favourable conditions for EGS and underlying tectonic processes. Through this relationship new prospective EGS areas can be outlined in areas where near surface (well) data are missing. This integrated lithosphere scale approach sets the stage for more detailed follow up local analyses for targeted exploration purposes.
- To discriminate between regional tectonic heat flow and local hydrothermal and magmatic anomalies. This allows improving the robustness of vertical and horizontal extrapolation of temperatures, where no well control is available.
- To constrain crustal rheology and stress regimes. At large scale, tectonic models are capable to quantitatively assess active deformation zones as a function of intraplate stress field and layered lithosphere rheology. In more detail, tectonic models are capable to quantitatively predict the interplay of crustal stress and rheology (faults and fractured zones). These play an important role in fracture formation and opening of pre-existing fractures, induced (and triggered) seismicity and natural permeability of fractured rock mass.

In order to illustrate these points, we review key geodynamic factors, controlling the thermal state and stress conditions in Europe's continental lithosphere. In doing so, we first introduce basic concepts on the compositional structure of the lithosphere and its relationship with thermal structure of the Earth up to ca. 100 km depth. We show how first order thermal constraints from surface heat flow and deep subsurface geophysical data sets can be jointly used to build and constrain thermal models of the lithosphere beyond well control. First order patterns can be well explained by both compositional controls and active tectonic processes. We also demonstrate that modelled tectonic heat flows are limited to values of about 100 mW m^{-2}, but can occur in large areas which share the same geodynamic context. Higher values, observed locally are most likely the result of hydrothermal processes and magmatism.

Subsequently, we explain how the thermal and compositional structure of the lithosphere controls the mechanical or so called rheological properties (e.g. Cloetingh et al., 2005; Burov, 2007). The drivers for earth deformation are plate boundary forces, resulting in relatively uniform intraplate stress conditions. Consequently rheological models for Europe can be validated by testing if spatial distributions of relatively low strength, predicted by the model, correspond with zones of active deformation, whereas relatively strong zones are shielded from deformation. We will demonstrate that first order thermal and rheological model predictions fit in general very well with overall patterns of earthquake distribution, and localization of deformation and associated partioning of relative rigid zones in Europe derived from geodetic measurements. The combined interpretation of the thermal and rheological state of the lithosphere is in close agreement with independent other geophysical data such as the gravity field. The thermo-mechanical make-up of Europe reflects a complex polyphase evolution through geological times (Fig. 6), involving pervasive extensional and compressional deformation. It serves as a framework to distinguish actively deforming areas sharing extensional and strike slip settings favourable for EGS, and gives in-depth insight in the relationship of stress–strain interactions on geological timescales and spatial distribution of natural seismicity. In more detail, validation of rheological models through analogue and numerical modelling of deformation processes over geological timescales demonstrates that first order rheological models fail to take into account lithosphere and crustal scale weak zones which are inherited from previous deformation. These weak zones/faults play an important role in distributing

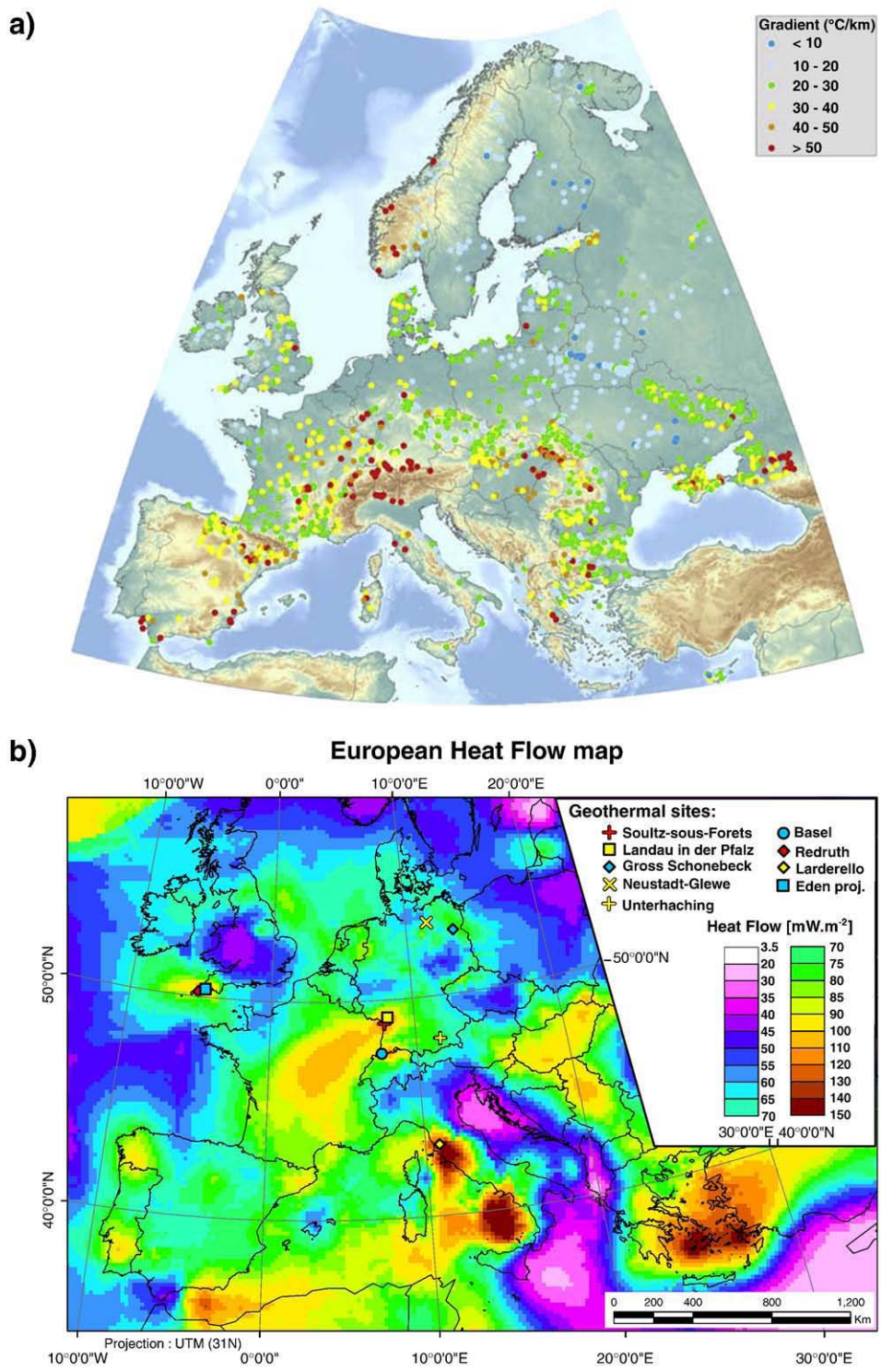

Fig. 2. Thermal signatures of Europe, described by measured temperature gradients and interpolated heat flow data. (a) Temperature gradient values (°C/km) in Europe extracted from the international heat flow database http://www.heatflow.und.edu and separated in 6 classes; (b) Corresponding surface heat flow extended with additional data (Haenel et al., 1988; Hurtig et al., 1992; Hurter and Haenel, 2002).

stress and strain in the upper crust representing the top 10 km in the Earth. Detailed geomechanical models linking crustal stresses and sub basin fault fabrics allow a validation of stress distributions in basins. This type of modelling aids in predicting critically stressed faults and fractures. Active faults that most likely represent active hydrothermal zones enhance the probability of EGS favourable conditions, both in terms of hydraulic stimulation as well as natural fracture permeability).

The added value of tectonic modelling is highlighted for selected tectonic settings, marked by a specific deformation style. For these settings we discuss the relationship between key-factors in tectonic evolution and geothermal prospectivity. This relationship allows to approach in a rational fashion continent-scale exploration for geothermal resources and building hypotheses for thermal and mechanical characterization at depth.

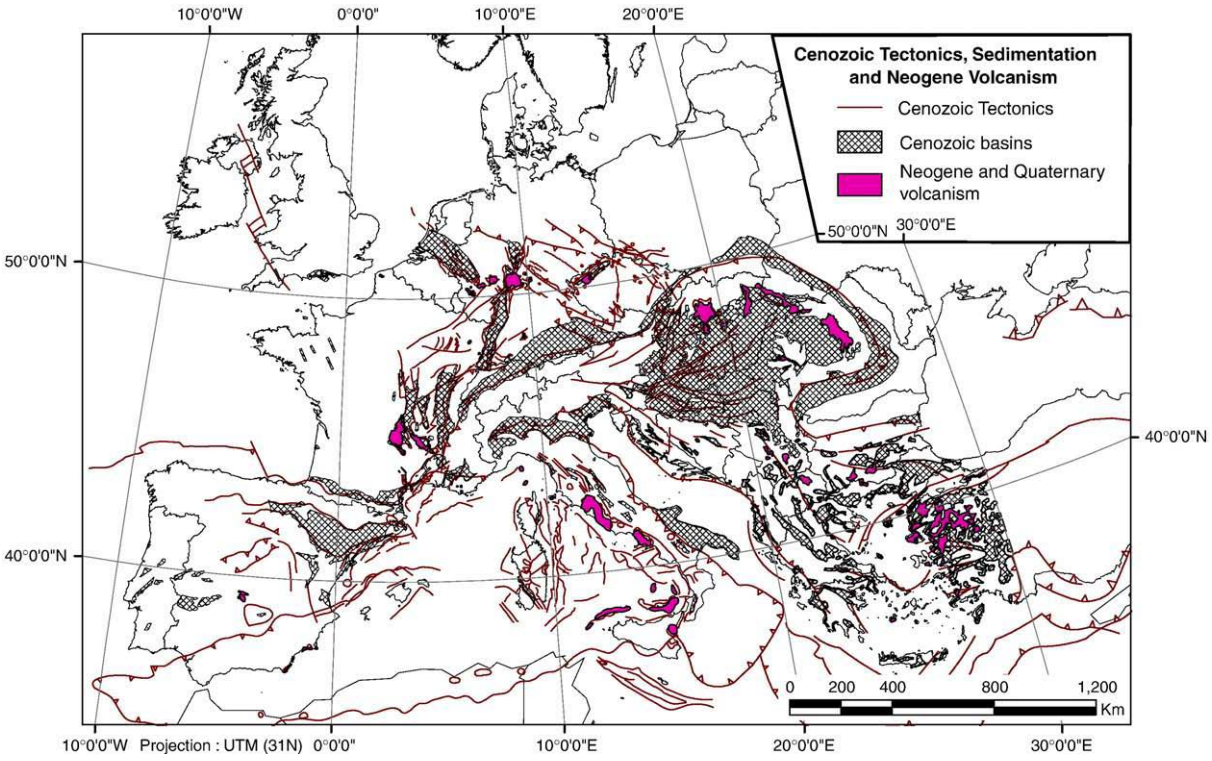

Fig. 3. Major tectonic fault zones, Cenozoic sedimentary basin configuration and distribution of Neogene and Quaternary volcanism in Europe.

2. Thermal structure of Europe's lithosphere

2.1. Basic definitions and concepts

The thickness of the lithosphere depends on the concept by which it is determined. From the viewpoint of mantle convection the lithosphere can be regarded as the upper thermal boundary layer of the convecting mantle (e.g. Turcotte and Oxburgh, 1967; Sleep, 2006). In the lithosphere heat is transported primarily by conduction, in contrast to the underlying asthenosphere, where heat is transported primarily by convection (e.g. Jaupart and Mareschal, 2007a). In steady state, the lithosphere is characterized by a nearly linear temperature-

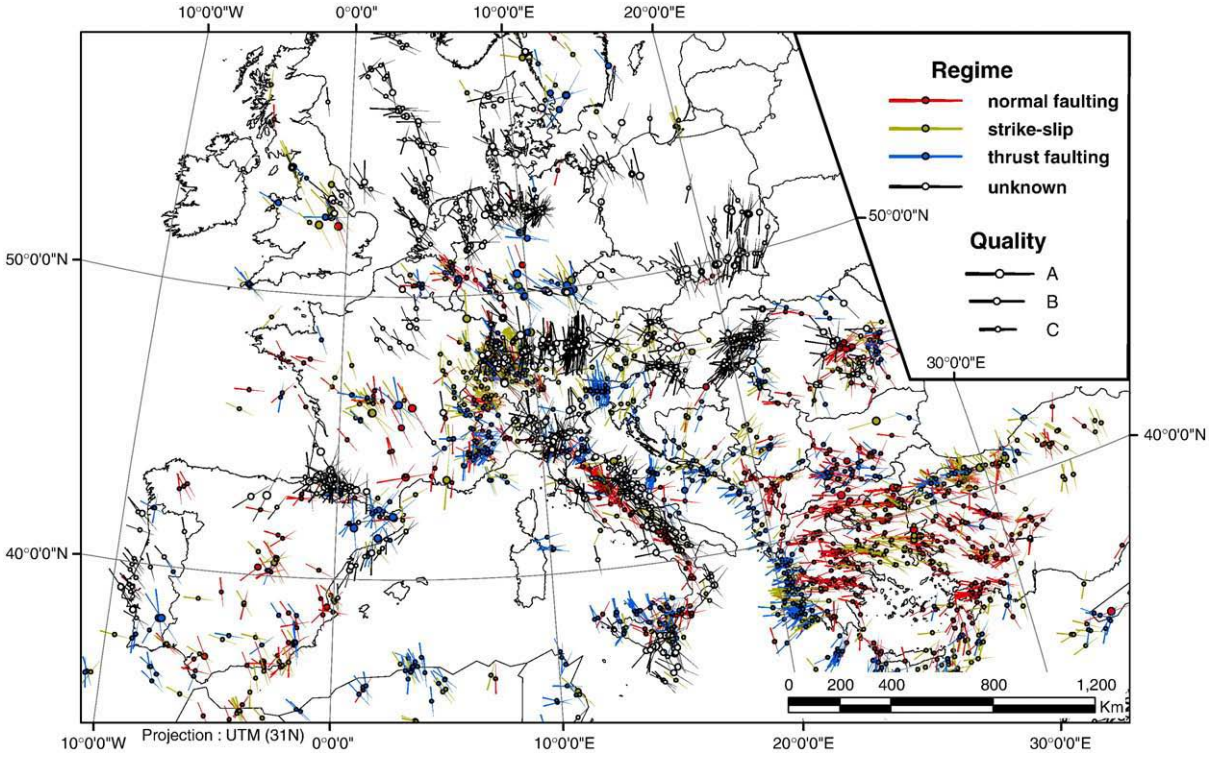

Fig. 4. Intraplate stress map for Europe, displaying the present-day orientation of the maximum horizontal stress (SHmax). Different colours stand for different stress regimes. Stress map data are extracted from the World Stress Map database (Heidbach et al., 2008).

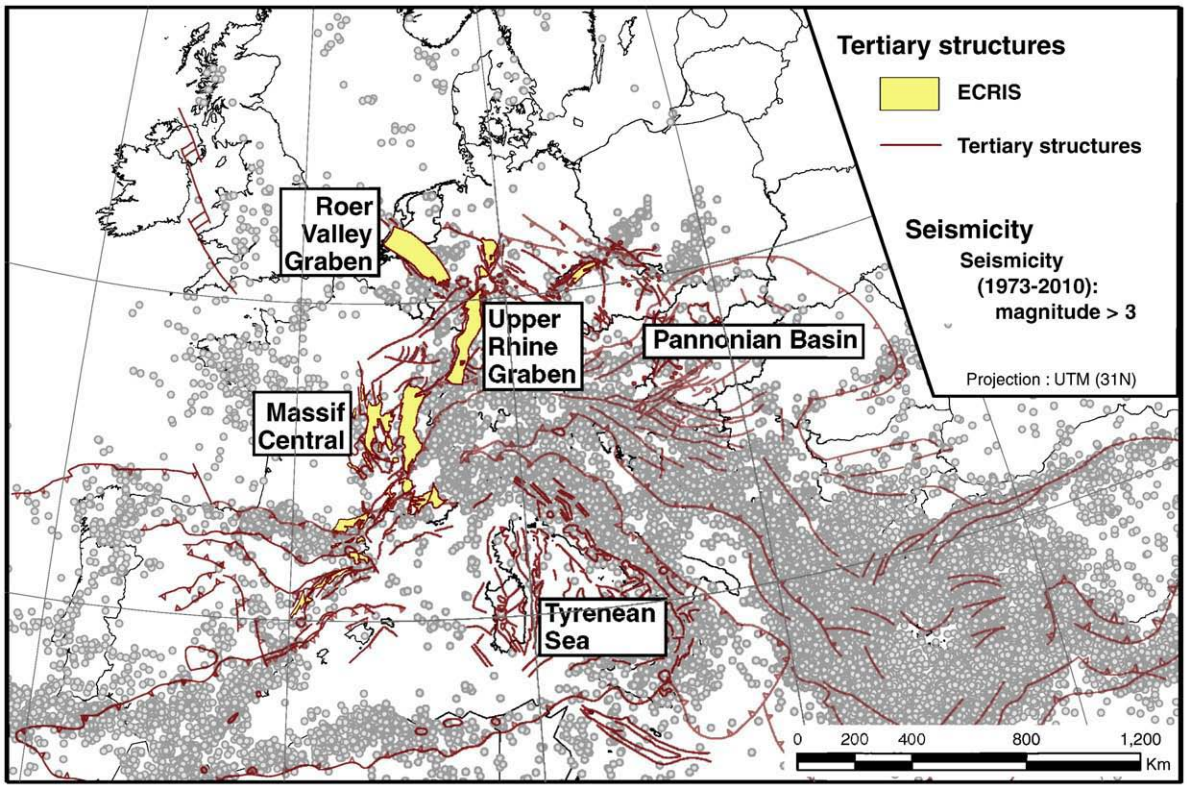

Fig. 5. Natural seismicity and main tectonic provinces in Europe discussed in the text in the context of EGS. ECRIS = European Cenozoic Rift System.

depth profile (e.g. Pollack and Chapman, 1977; Sleep, 2005). There is no sharp boundary between the lithosphere and the asthenosphere. Between the purely conductive and purely convective regimes a transition zone is located where temperature tends asymptotically to the fully convective profile (e.g. McKenzie et al., 2005). Usually, the base of the lithosphere is defined to be at well-mixed convective mantle temperatures along an isentropic 'oceanic' temperature profile with a potential temperature of 1300 °C.

In contrast, the mechanical lithosphere is defined by the outermost shell of the Earth in which stresses can be transmitted on geological time scales (e.g. McKenzie, 1967; Ziegler and Cloetingh, 2004). The viscosity of rocks depends strongly on the temperature and therefore the mechanical behaviour of the lithosphere is related to its thermal condition. At lower temperatures the rocks are solid. As temperature increases the rocks begin to deform in a ductile way, and therefore they are unable to sustain stresses on geological time scales.

Considering its chemical composition the continental lithosphere consists of a crust and a mantle part. The present day continents consist largely of Proterozoic continental lithosphere, which has been reworked in many places and on which younger terranes were accreted in post-Proterozoic times. The continental crust is chemically more differentiated and has a higher content in radioactive elements than the mantle lithosphere (e.g. Rudnick et al., 1998). The mantle part of the continental lithosphere consists of material similar to the underlying asthenospheric mantle, however acts like a solid due to its lower temperature.

2.2. Steady state lithosphere temperatures and thickness

The temperature profile or geotherm is a model of the thermal structure of the lithosphere. The simplest assumption is that the continental lithosphere is in thermal equilibrium, and the geotherm is steady state. In this case the temperature gradient in sediments and underlying crust and mantle is often approximated assuming a layered geotherm based on surface heat flow ($q_{surface}$, Fig. 2), rock thermal conductivity (k) and heat production (A) (cf. Table 1; Fig. 7). In the lithosphere, A varies with depth according to the distribution of radiogenic isotopes and k varies with composition and with both pressure and temperature. However, the algorithm incorporated in this study uses the analytical solution of Poisson's equation for $T(z)$ with restrictive requirements. For a layer of the lithosphere with fixed A (A_{layer}) and k, the analytical steady state temperature is

$$T(z) = T_{top} + q_{top}\frac{z}{k} - 0.5A_{layer}\frac{z^2}{k} \quad (1)$$

where T_{top} and q_{top} correspond to the temperature and heat flow at the top of the layer. The heat flow decreases towards the base of the layer or top of the next layers as:

$$q_{base} = q_{top} - A_{layer}{}^{*}\Delta z_{layer} \quad (2)$$

Eqs. (1) and (2) are applied to successive layers, resetting T_{Top} and q_{Top} at the top of each new layer with the values T_B and q_B solved for the bottom of the previous layer. Thermal conductivity k (z, T) is incorporated in each layer in an iterative way.

If surface heat flow values are free of modifying effects such as paleoclimate, topography changes, heat refraction due to complicated geology, fluid flow etc. they represent the heat from depth. Thus on a large scale and at steady state, the variability in surface heat flow must then be entirely attributed to Eq. (1) the composition of the lithosphere and its radiogenic heat production and Eq. (2) the heat from the asthenospheric mantle. This means, the surface heat flow is in equilibrium with the heat flowing into the lithosphere at its base plus the heat generated by radioactive decay within the lithosphere.

Using surface heat flow, Moho depth (crustal thickness) and sediment thickness in Europe, recent studies (Fig. 8) have presented generalized depth maps of the thermally defined base of the lithosphere (depth of the 1300 °C isotherm) (Figs. 7, 8). Such

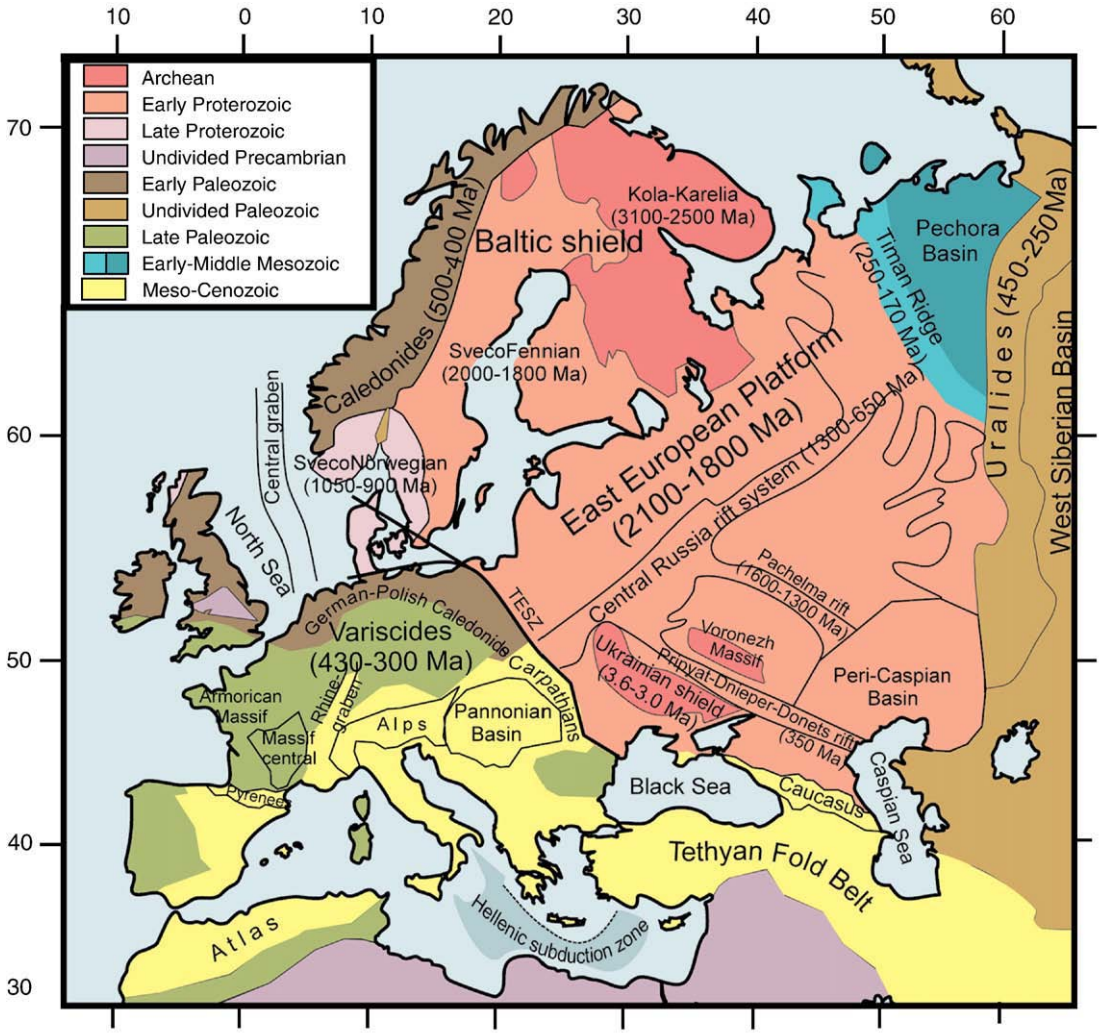

Fig. 6. Simplified tectonic map of Europe. TESZ, Trans-European Suture Zone (from Artemieva et al., 2006).

approach uses a standard lithosphere neglecting any changes in lithospheric composition laterally and vertically. Hence the resulting base of thermal lithosphere (Fig. 8) may diverge locally from results gained if a model based on careful consideration of compositional and thermal properties were used. Nevertheless, Fig. 8 shows for the European lithosphere an overall trend of large variation in lithosphere thickness to be associated with large temperature variation at depth.

Sediment and crustal thickness are an important constraint for generalized thermo-mechanical models for the lithosphere as the crust has strong contrasting thermo-mechanical properties compared to subcrustal mantle material (Table 1). Dèzes and Ziegler (2004) have integrated the results of crustal studies that were carried out since the publication of Moho depth maps by Meissner et al. (1987), Ziegler (1990) and Ansorge et al. (1992) to obtain a better

Table 1
Rheological model parameters (Carter and Tsenn, 1987; Brace and Kohlstedt, 1980).

Parameter	Symbol	Units	Sediment	Upper crust	Lower crust	Upper mantle
Dominant mineralogical composition			Various	Quartzite (dry)	Diorite (wet)	Olivine (dry)
Density	ρ	kg m^{-3}	2400	2650	2900	3300
Thermal conductivity	k	W m^{-1} K^{-1}	2.3	2.5	2.8	3.5
Specific heat	C_p	J kg^{-1} K^{-1}	1050	1050	1050	1050
Heat production	H	μ W.m^{-3}	1.5	2.0	0.5	0
Exponential decay rate of heat production	z_H	km	20	20	20	0
Power law exponent	n	–	–	2.72	2.4	3.0
Power law activation energy	E_p	kJ mol^{-1}	134	212	510	
Power law strain-rate	A_p	Pa^{-N}s^{-1}	6.03e−24	1.26e−16	7.0e−14	
Dorn law activation energy	E_D	kJ mol^{-1}	–	–	–	535
Dorn law strain-rate	A_D	s^{-1}	–	–	–	5.7e11
Dorn law stress	σ_D	Pa	–	–	–	8.5e9
Creep equations						
Power law creep	$\sigma_{creep} = (\dot{\varepsilon} \cdot A_p)^{1/n} \cdot \exp\,[Ep/nRT]$					
Dorn law creep	$\sigma_{creep} = \sigma_D\{1-[1-(RT/E_D)\ln(\dot{\varepsilon}/A_D)]^{1/2}\}$					

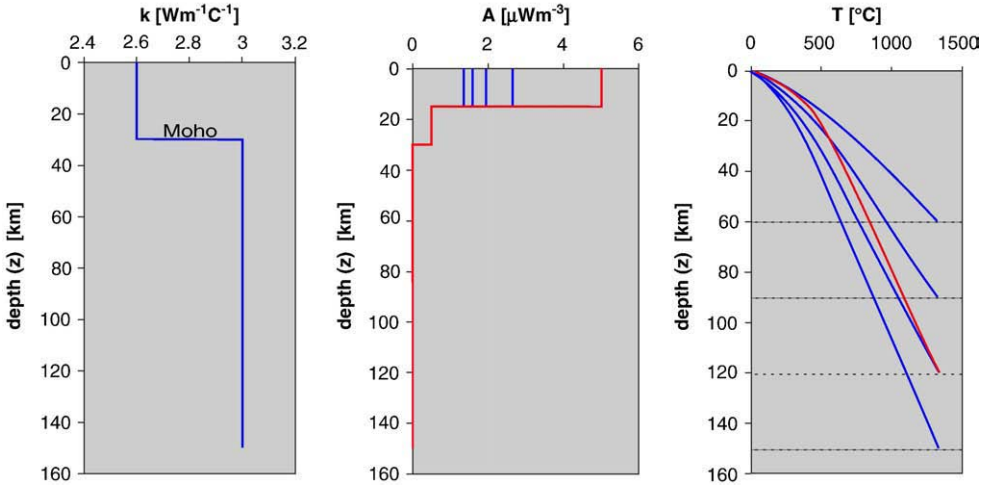

Fig. 7. Construction of a conduction dominated continental lithosphere geotherm (right) from the steady state relation between surface heat flow, stratified conductivity (left), and heat production (middle) in crust and mantle lithosphere . For various values of lithospheric thickness (60, 90,120, 150 km).Crustal thickness is 30 km. Lithosphere parameters after van Wees et al. (2009), assuming 40% of the surface heat flow is caused by radiogenic heat production in the upper crust. The surface heat flow corresponds to 100, 74, 60, 51 mW m^{-2}. The red curve shows a geotherm of a 120 km thick lithosphere with the effect of abnormal high heat production in the upper crust as a consequence of granite intrusions such as observed in the Bohemian Massif marked by heat flow values up to 107 mW m^{-2} (Förster and Förster, 2000).

understanding of the present day crustal configuration of Western and Central Europe, and to analyze processes and their timing which controlled the evolution of the crust in the different parts of Europe. From the Moho depth map (Fig. 8), it is evident that the stable parts of the Precambrian Fennoscandian — East-European craton are characterized by a thick crust and Moho depths ranging up to 48 km, whereas in more mobile Phanerozoic Europe Moho depths range between 24 and 48 km and no longer bear any relation to the Caledonian and Variscan orogens. On the other hand, areas underlain by the Precambrian Hebridean craton are characterized by a crustal thickness in the range of 20 to 26 km, reflecting a strong overprinting by a Mesozoic rifting. By contrast, the Alpine chains, such as the Western and Central Alps, the Carpathians, Apennines, Dinarides, as well as the Betic Cordilleras and the Pyrenees, are characterized by more or less distinct crustal roots with Moho depths attaining values of up to 60 km. The present crustal configuration of Phanerozoic Europe reflects that the crustal roots of the Caledonides and Variscides were destroyed during post-orogenic times, and that their crust was repeatedly modified by Mesozoic and Cenozoic tectonic activities.

2.3. Validation of lithosphere temperatures and thickness by geophysical methods

In contrast to the upper crust, for which temperatures either can be measured directly in boreholes (to a maximum depth of 10 km) or extrapolated confidently from measurements of surface heat flow and known thermal properties of rocks, for mid-crustal, lower crustal and upper mantle depths the actual temperature estimate is less certain and depends on the accuracy of the used thermal properties. In addition, although large areas of Europe (the Precambrian shield and platform areas) presently are in thermal steady-state, other regions in Europe are under transient thermal conditions. For example, in areas having experienced young lithospheric-scale tectonic events, the thermal perturbations originating in the asthenosphere may not be expressed yet in the surface heat flow. Moreover, young geological processes, such as rapid burial by sedimentation, exhumation by erosion, burial by thrusting, extensional unroofing etc. affect the temperatures at drillable depths. Therefore, the surface heat flow determined in these areas diverges from the value representing a steady-state heat flow. Given this complexity in the temperature field, the surface heat flow mapped for Europe in general has to be screened and corrected for these different effects before it can be used to extrapolate temperature to greater depths. In addition, continental geotherms need to be constrained at great depth by additional data.

Independent constraints of deep temperatures can be provided by thermobarometric methods using minerals of xenoliths (e.g. Kukkonen and Peltonen, 1999) or by geophysical methods. In this paper we concentrate on the latter methods, which measure variations in different properties of the mantle: e.g. density, elastic moduli and conductivity, which are related to variations in composition, structure, mineral alignment and temperature. Global geophysical methods, such as seismic tomography or magnetotellurics, are able to determine the top of the convective regime just below the lithosphere base. The difference between the seismic lithosphere, defined as the seismic high velocity region on the top of the mantle, and the thermal lithosphere, derived from surface heat flow (Fig. 8) can be up to 40–50 km (Jaupart and Mareschal, 1999).

Significant advancements have been made in global travel time tomography. A new model parameterization technique and new 3-D ray tracing algorithms (Bijwaard and Spakman, 1999a) resulted in global mantle models that, for the first time, exhibit regional scale (60–100 km) detail (Bijwaard and Spakman, 2000, as a follow-up on Bijwaard et al., 1998). Improved focusing on lower mantle structures led to the first evidence for a whole mantle plume below Iceland (Bijwaard and Spakman, 1999b) and for up-welling of the lower mantle beneath Europe, which is proposed as the cause for long-standing central European volcanism (Goes et al., 1999). Future developments in tomography will be directed towards a more detailed structure (50 km) of the upper 1000 km, although the whole mantle is involved in the analyses (Fig. 9).

Goes et al. (2000a) developed a new inversion strategy which takes advantage of the fact that most of the variation in seismic wave velocities in the upper mantle is caused by variations in temperature. State-of-the-art seismological models and experimental data on the physical properties of mantle rocks are inverted for upper mantle temperatures, e.g. beneath Europe. Inferred mantle temperatures

Fig. 8. Steady state lithosphere thickness derived from surface heat flow and compositional input of the crust and mantle lithosphere (cf. Table 1, Fig. 6). Panel (a) Moho depth or crustal thickness (Dèzes and Ziegler, 2004); (b) surface heat flow and; (c) lithospheric thickness (Hardebol, 2010).

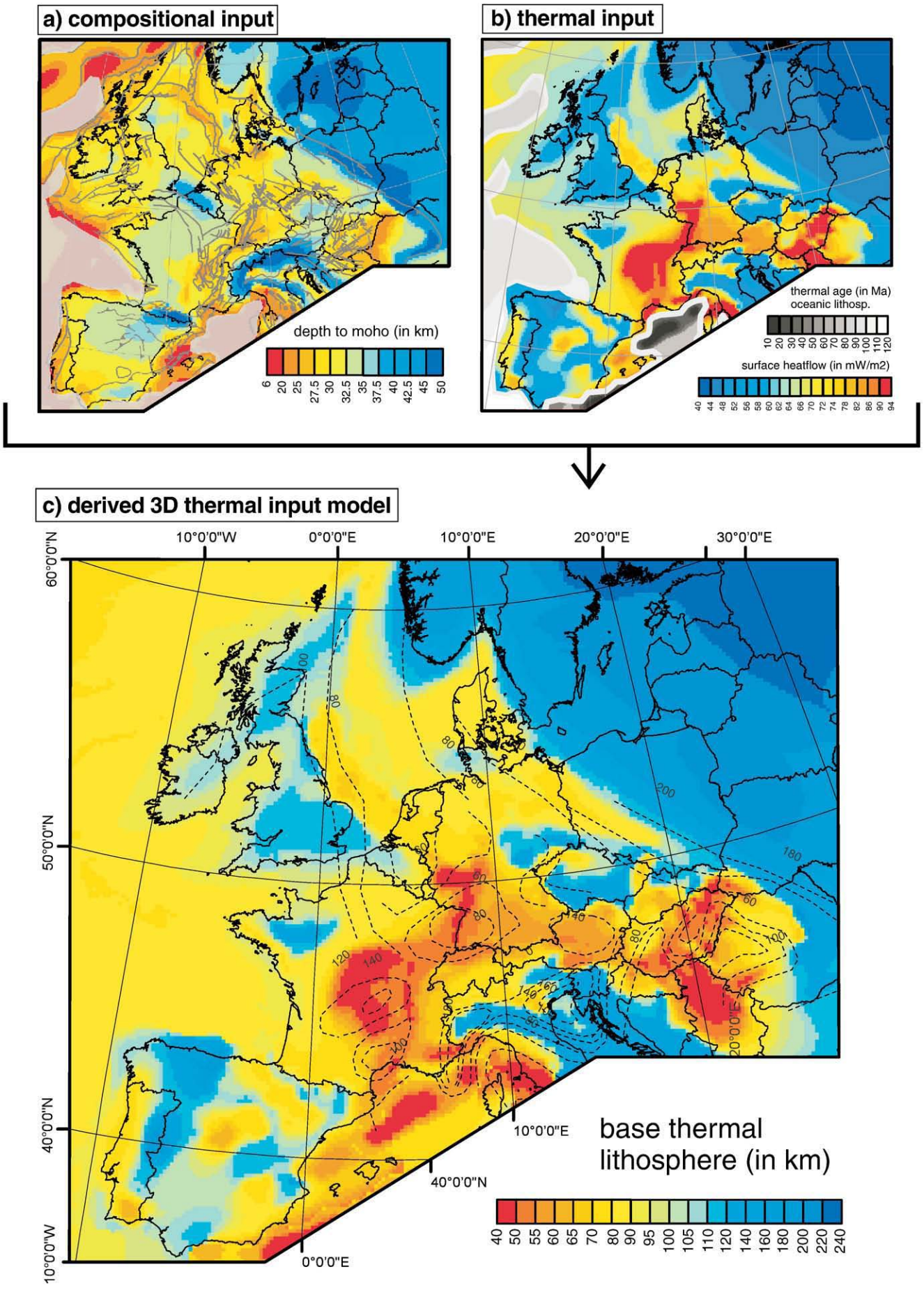
a) compositional input
depth to moho (in km)
6 20 25 27.5 30 32.5 35 37.5 40 42.5 45 50
b) thermal input
thermal age (in Ma)
oceanic lithosp.
10 20 30 40 50 60 70 80 90 100 110 120
surface heatflow (in mW/m2)
40 44 48 52 56 58 60 62 64 66 70 72 74 78 82 86 90 94
c) derived 3D thermal input model
10°0'0"W
0°0'0"E
10°0'0"E
20°0'0"E
30°0'0"E
60°0'0"N
50°0'0"N
40°0'0"N
10°0'0"W
0°0'0"E
10°0'0"E
40°0'0"N
20°0'0"E
base thermal
lithosphere (in km)
40 50 55 60 65 70 80 90 95 100 105 110 120 140 160 180 200 220 240

beneath Europe agree reasonably well with independent estimates from heat flow and general geological considerations (e.g. Dunai and Baur, 1995).

The most comprehensive overview to date of the lithospheric structure of the major tectonic provinces in Europe is given by Artemieva et al. (2006). The integrated model of the lithospheric thickness (Fig. 10) is based on P-wave seismic tomography models (Spakman, 1990; Kissling and Spakman, 1996; Bijwaard and Spakman, 2000; Piromallo and Morelli, 2003), surface-wave tomography models (Panza et al., 1986; Calcagnile, 1991; Du et al., 1998; Shapiro and Ritzwoller, 2002; Boschi et al., 2004), P-wave residuals (Babuška and Plomerová, 1992), thermal models (Balling, 1995; Cermak and Bodri, 1995; Artemieva, 2003), magnetotelluric studies (Ádám et al., 1982; Jones, 1984; Praus et al., 1990) and P–T data for mantle xenoliths (Coisy and Nicolas, 1978; Kukkonen and Peltonen, 1999).

2.4. Large scale spatial variation in heat flow and lithosphere thickness

The Precambrian part of Europe (Ukrainian shield, East European Platform, Baltic shield; for location see Fig. 6) is characterized by 40–50 km thick crust and 200–250 km thick high-velocity lithosphere. The surface heat flow value of 30–60 mW m^{-2} (Artemieva, 2003) is close to the global average for Precambrian cratons (Nyblade and Pollack, 1993; Sandiford and McLaren, 2006) and corroborates values from the Precambrian of North America (Mareschal and Jaupart, 2004; Jaupart et al., 2007). These areas have not been tectonically reactivated after their formation and are thermally in steady state. The variation in surface heat flow is linked to different factors. As was shown on the example of the North American craton, Mareschal and Jaupart (2004) observed heat flow variations on scales <500 km, linked to changes of local crustal structure, and on scales >500 km, linked to changes in crustal heat production. Based on the generally low heat flow values, the steady state thermal models predict for the Precambrian areas of Europe a cold, 170–280 km thick lithosphere (Pasquale et al., 2001; Artemieva, 2003). The high seismic velocity beneath the Baltic shield is only partly due to the low temperature in the upper mantle. Gravity and buoyancy constraints on mantle density (Artemieva, 2003; Kaban et al., 2003) reveal a strong density anomaly, which can be attributed to highly depleted lithospheric mantle. Palaeozoic rifts developed within the Precambrian part of Europe (the Oslo rift and Pripyat–Dnieper–Donets rift) have lithospheric thickness similar to the Variscan belt (100–140 km).

The Phanerozoic lithosphere of western and central Europe has uniform crustal thickness of 28–32 km, and the lithospheric thickness is in the range of 80–140 km with the larger values beneath the Proterozoic–early Palaeozoic terranes (the Armorican, Bohemian and Brabant Massifs, and the northern part of the Massif Central). The main tectonic events which profoundly affected the lithosphere were the Caledonian (500–400 Ma) and the Variscan (430–400 Ma) orogenies involving the triple plate collision of Baltica, Laurentia and Avalonia (Dewey, 1969). The thin crust in Europe, in places with seismically laminated lower crust and sharp sub horizontal Moho that crosses pre-existing terrane boundaries, and a lack of seismic signature in the lithospheric mantle suggest that a large portion of the lower crust and lithospheric mantle have been delaminated during the Palaeozoic orogenies (Ziegler et al., 2004) or following it (Nelson, 1992). Compared with the Palaeozoic orogens of Western Europe, the Uralides, which remained intact within the continental interior, have a thick crust (50–55 km) and thick lithosphere (170–200 km).

Surface heat flow in western and central Europe varies generally (apart from local anomalies) between 50 and 80 mW m^{-2} (Cermak, 1993) indicating a general trend of thinner thermal lithosphere and increased lithospheric temperature compared to the adjoining Precambrian terranes to the north (Fig. 8). In Fig. 11, on the example of the Northeast German Basin (NEGB), an integrated thermal 2-D model (Norden et al., 2008) is shown of the transition from western and central European lithosphere towards the Precambrian lithosphere to the northeast, which beneath the southern Baltic Shield is about 200 km thick. From a test of different models for the depth of the base of the lithosphere, the best-fit to surface heat flow was achieved with a base of lithosphere (1300 °C) between 75 km and 90 km beneath the basin. Data shown in Fig. 9 suggest that this estimate can be probably extended to the west, to the Northwest German Basin and adjoining areas and also to areas to the northwest. The S receiver function analysis by Heuer et al. (2007) performed to the south of the NEGB shows the lithosphere–asthenosphere boundary in the Saxothuringian and the northeastern Tepla–Barrandian units of the Bohemian Massif at 80–90 km and in the Moldanubian units at 120–130 km. The decrease of lithospheric thickness to the north is sharp and oriented E–W and could be the result of post-Variscan delamination of lithosphere triggered by the Alpidic orogeny. These new results for central Europe would slightly modify the lithospheric thickness pattern in Fig. 10.

Besides the large-scale pattern, Europe's surface heat flow exhibits small-scale variation that more likely correlate with crustal composition rather than with anomalies linked with lithospheric thickness changes. The most influential factor to surface heat flow and lithosphere temperature, independent of the tectonic age of a terrane, is the crustal heat production. Geophysical, petrological, and geochemical data provide important information about the composition of the crust that needs to be translated into radiogenic heat production for the calculation of geotherms.

Using various models of the K, Th, and U content for the bulk continental crust, Rudnick et al. (1998) determined for stable continental regions (crustal thickness of 41 km) a bulk heat production most likely on the order of 0.58–0.92 μW m^{-3} resulting in a crustal contribution to surface heat flow for Precambrian terranes of >50 %. In general, heat-producing elements decrease with depth in the crust owing to their depletion in felsic rocks caused by granulite facies metamorphism and an increase in the proportion of mafic rocks with depth (e.g. Rudnick and Fountain, 1995). However, the distribution of heat-producing elements within different continental regions is difficult to constrain. Early studies relying on an empirical relationship between surface heat flow and near-surface heat production (e.g. Birch et al., 1968) lead to many misinterpretations of the crustal heat production distribution. Rather than an exponential decrease of heat production with depth, it is now more common to use a step-wise assignation of values strongly linked to lithology changes (Jaupart and Mareschal, 2007a,b; Jaupart et al., 2007).

In-depth studies in areas exposing locally high surface heat flow have shown that the upper crust hosting granitic rocks may be exceptionally enriched in U and Th. These granites of exceptionally high heat production (HHP granites) are perspective sites for encountering high temperatures at shallow depth (red curve in Fig. 7), shallow enough to favour exploitation of geothermal energy.

HHP granites occur throughout Europe, although in different frequency and volume. Most HHP granites formed during the Variscan orogeny such as those from southwestern England, western France, the French Massif Central, and the Erzgebirge in the northern part of the Bohemian Massif. They also occur in older terranes as in the Scottish Caledonides and the Proterozoic shields of Fennoscandia, Baltica, and the Ukraine.

One of the best investigated areas, in which the interplay of surface heat flow, shallow and deep radiogenic heat sources and mantle heat flow was investigated in Europe is the Erzgebirge region in the northern part of the Bohemian Massif (Förster and Förster, 2000). Surface heat flow ranges between 61 and 108 mW m^{-2} and displays a strong relation with lithology. Sites of high heat flow correlate with the distribution of late Variscan granites that are on average between 5 and 8 km thick, those of lower heat flow refer to the outcropping early Variscan metamorphic basement. These major groups of upper crustal basement rocks are distinctly different in radiogenic heat

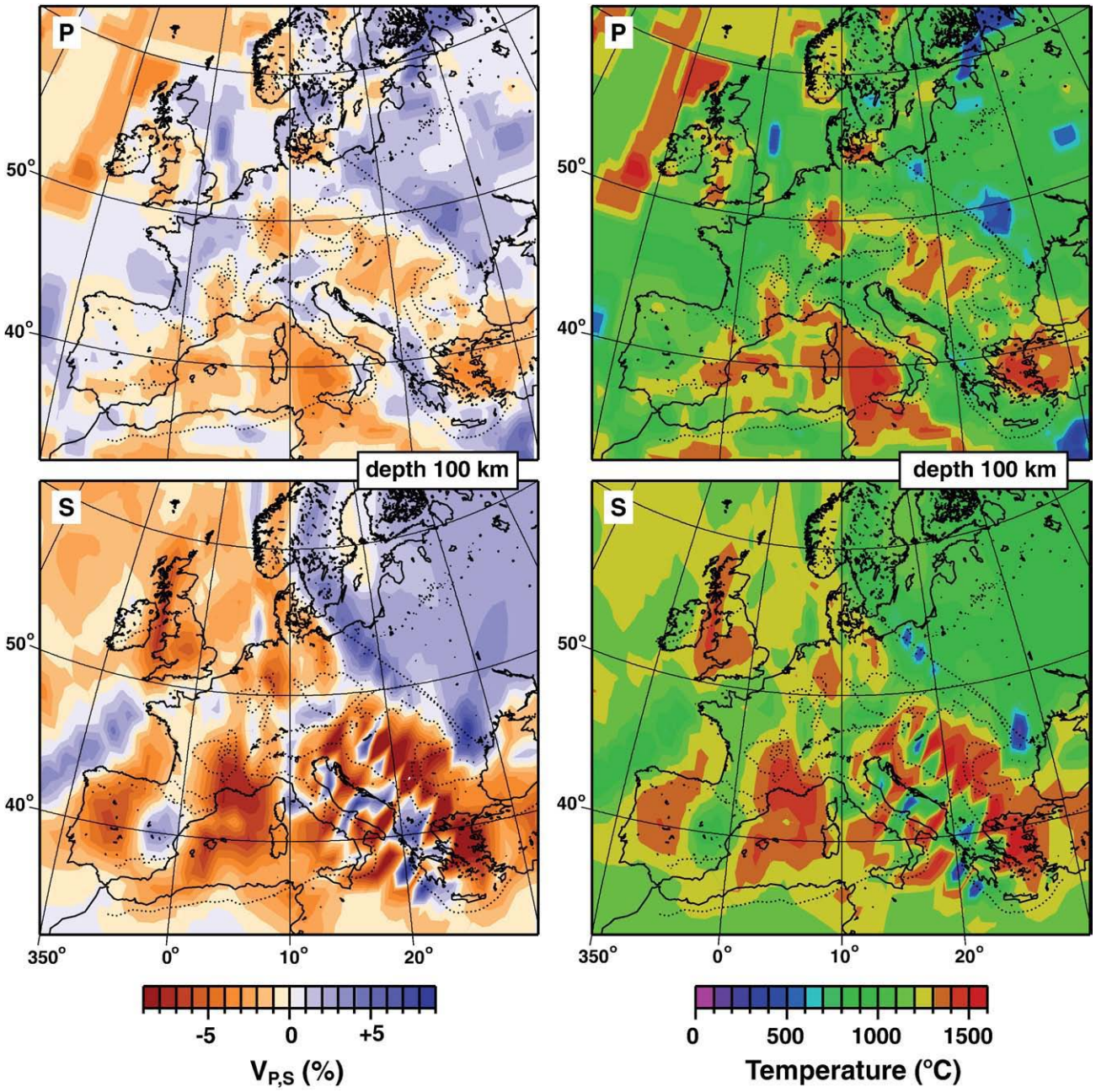

Fig. 9. Seismic velocity anomalies at 100 km under Europe for P waves (top left) and S waves (bottom left) (after Goes et al., 2000a). Panels on the right show temperatures at 100 km depth estimated from the P and S velocity anomalies. The assumption that all velocity anomalies can be attributed to variations in temperature appears to be reasonable in view of the similarity in thermal structure obtained from P- and S-wave velocities (after Goes et al., 2000a). However, high mantle velocities for the Baltic Shield, can be in part related to a highly depleted mantle composition, as demonstrated by independent gravity analysis (Artemieva, 2003; Kaban, 2004).

production: most granitic rocks are classified as HHP granites and display values of heat production usually between 4 and 10 $\mu W\ m^{-3}$ depending on geochemical type, intensity of alteration, and degree of magma differentiation. The heat production values of most of the Erzgebirge granites largely exceed those of average Phanerozoic granite (2.8 $\mu W\ m^{-3}$) and average felsic I- and S-type granites (3.0 $\mu W\ m^{-3}$). The values of upper crustal metamorphic rocks are distinctly lower and range between 1.5 and 3.5 $\mu W\ m^{-3}$, with the majority of values between 2 and 3 $\mu W\ m^{-3}$. The strong contrast in heat production between the igneous and metamorphic basement in a depth level of up to 8 km causes heat-refraction effects that should be accounted for if surface heat flow is used in geotherm calculations. In addition, the 30 km thick crust of the Erzgebirge shows a higher bulk heat production in both the off-granite areas (1.4 $\mu W\ m^{-3}$) and the on-granite areas (up to 3 $\mu W\ m^{-3}$) than global estimates of the bulk composition of continental crust (0.58–0.92 $\mu W\ m^{-3}$; Rudnick et al., 1998). Also the upper 15 km most enriched in radioactive elements exhibits in off-granite areas a slightly higher value of 2.2 $\mu W\ m^{-3}$ compared to the average heat production in the Earth's upper continental crust (1.8 $\mu W\ m^{-3}$; Taylor and McLennan, 1985). This example from the Erzgebirge shows that parts of the comparably thinner European crust may distinctively be hotter than a Precambrian crust, only because of different crustal composition.

The case of the Eger Rift (graben), a part of the European Cenozoic Rift System (ECRIS), is an interesting place to look at in terms of thermo-mechanics in conjunction with Alpine tectonics. The Eger Rift strikes NE–SW, just as the Erzgebirge/Krusne Hory to the north of it. Both are oriented oblique to the E–W striking lithosphere–

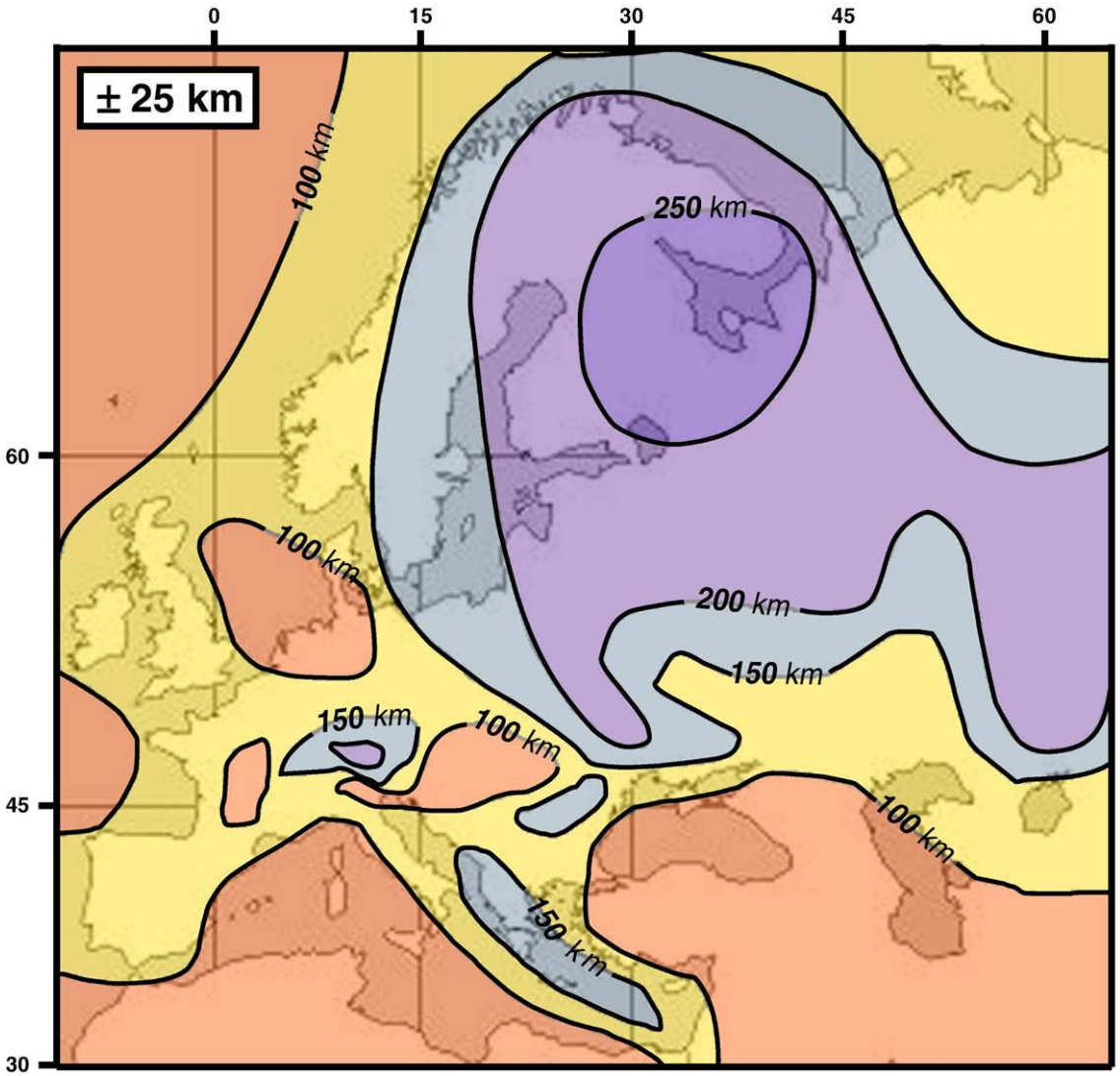

Fig. 10. Integrated model of lithospheric thickness in Europe, based on seismic, thermal, MT, electromagnetic and gravity interpretations. In general, a direct comparison of lithospheric thickness values, constrained by different techniques, is not valid, as they are based on measurements of diverse physical parameters. The difference between the thicknesses of 'seismic' and 'thermal' lithosphere can be up to 40–50 km (Jaupart and Mareschal, 1999), which approximately corresponds to the thickness of the transition zone between pure conductive and pure convective heat transfer (from Artemieva et al., 2006).

asthenosphere transition zone between Saxothuringian units and Moldanubian units (Heuer et al., 2007) located to the south. It is reasonable to assume that in response to far field stresses in Alpine time, the abnormal heat production in the crust of the Erzgebirge/Krusne Hory (Förster and Förster, 2000), which is responsible for a weak lithosphere, has had a bearing on the spatial configuration of the Eger rift that originated in the Cenozoic times. Uplift and erosion of the Erzgebirge was observed in different episodes of Earth history starting in the early Mesozoic (during breakup of Pangea). The most prominent late Cenozoic uplift and exhumation of the Erzgebirge (Ventura and Lisker, 2003) occurred in response to far field stresses linked to late Alpine orogenic phases. It is also interesting to note that this area is thermally characterized by a large temperature gradient (in excess of 40 °C/km) at a few hundred meters depth.

3. Large scale spatial variation in heat flow related to Alpine and Cenozoic tectonics

The Palaeozoic Variscan orogens have been significantly reworked and overprinted by the collision of the Eurasian and the African plates (Fig. 6). Consequently the lithospheric structure of the tectonically active areas in the Mediterranean region is very heterogeneous. The Cenozoic orogens of the Alps, Dinarides and Caucasus formed by continental subduction are characterized by crustal thickness which locally reaches 60–65 km and lithospheric thickness exceeding 150–200 km (Fig. 8). Coeval to the continental collision several smaller fragments of Tethyan ocean domains were subducted during the late Cenozoic to present time. It resulted in the formation of back-arc basins (e.g. the Tyrrhenian, Aegean and Pannonian basins. These basins have thin crust (20–30 km) and thin lithosphere (60–80 km). West and North of the Alps, tectonic and magmatic events are associated with the formation and development of the Cenozoic European Central Rift System (Ziegler and Dèzes, 2006).

The various extensional and compressive Cenozoic settings, which are to a large extent active up to the present day show a strong relationship with basin and basement temperatures and can well be correlated with spatial variations in heat flow, deep basin and basement temperature and lithosphere thickness.

Below we describe in more detail the Cenozoic evolution of the different tectonic settings including the back-arc basin settings in the Mediterranean and the Pannonian Basin, and the Central European Rift System.

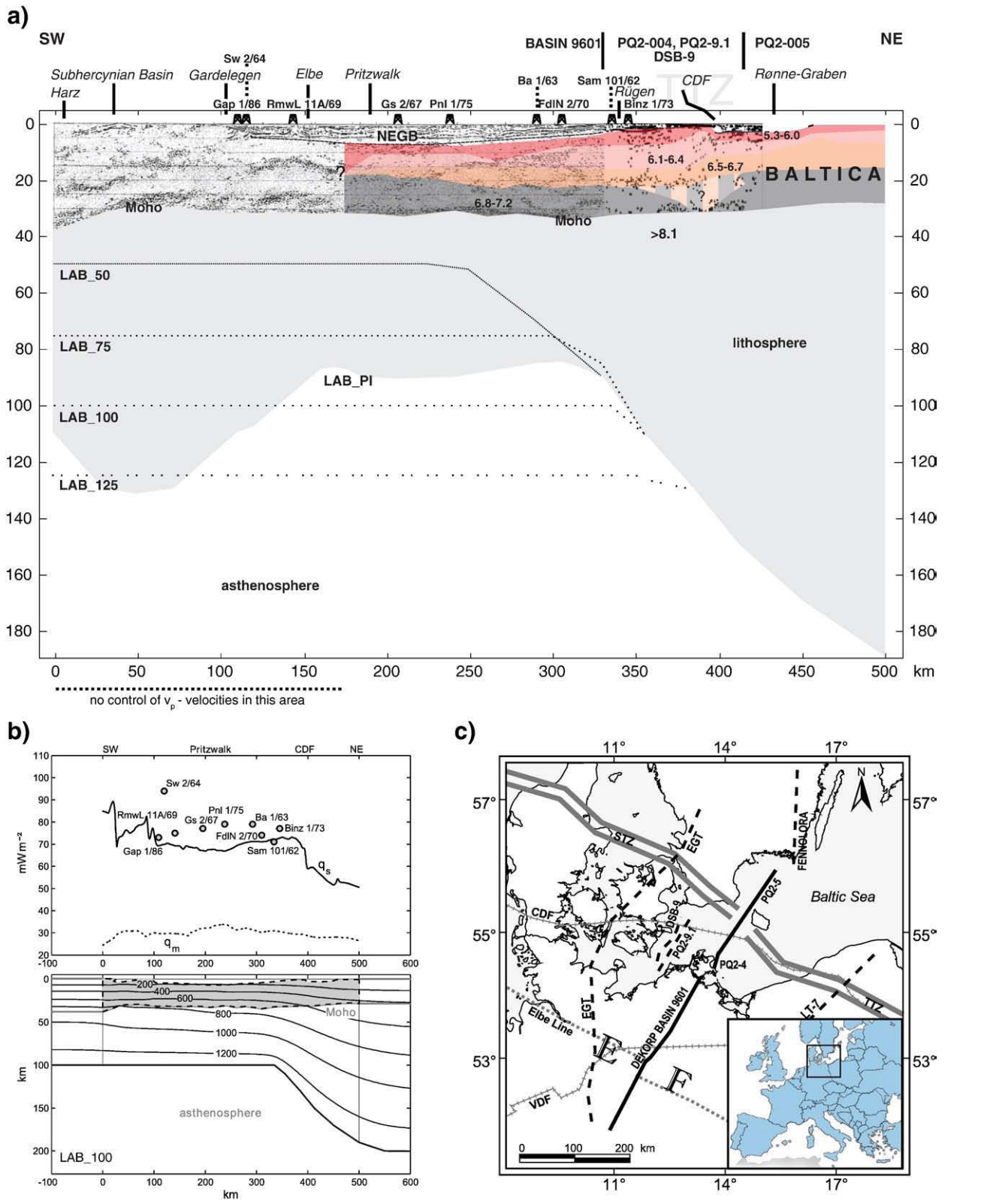

Fig. 11. Thermal lithosphere model of a 500-km section along the DEKORP-BASIN 9601 deep seismic line across the North East German Basin (NEGB), extended to the northeast across the Tornquist Zone (modified from Norden et al., 2008). (a) Details of crustal structure and different assumptions on lithosphere thickness used in thermal modelling; (b) Modelled temperatures and modelled heat flow in the best-fit scenario, which is based on a lithosphere–asthenosphere boundary at 75 km depth. q_s is surface heat flow, q_m is mantle heat flow, both in mW m^{-2}; (c) Location of the profile and of the sections used in this study. The average observed surface heat flow in the NEGB is 77 ± 3 mW m^{-2}.

3.1. Central European Rift System (ECRIS)

Development of the presently still active European Cenozoic rift system (ECRIS), which extends from the Dutch North Sea coast to the western Mediterranean, commenced during the late Eocene (Fig. 12, Ziegler and Dèzes, 2005). Its southern elements are the Valencia Trough, the graben systems of the Gulf of Lions, and the northerly striking Valence, Limagne and Bresse grabens; the latter two are superimposed

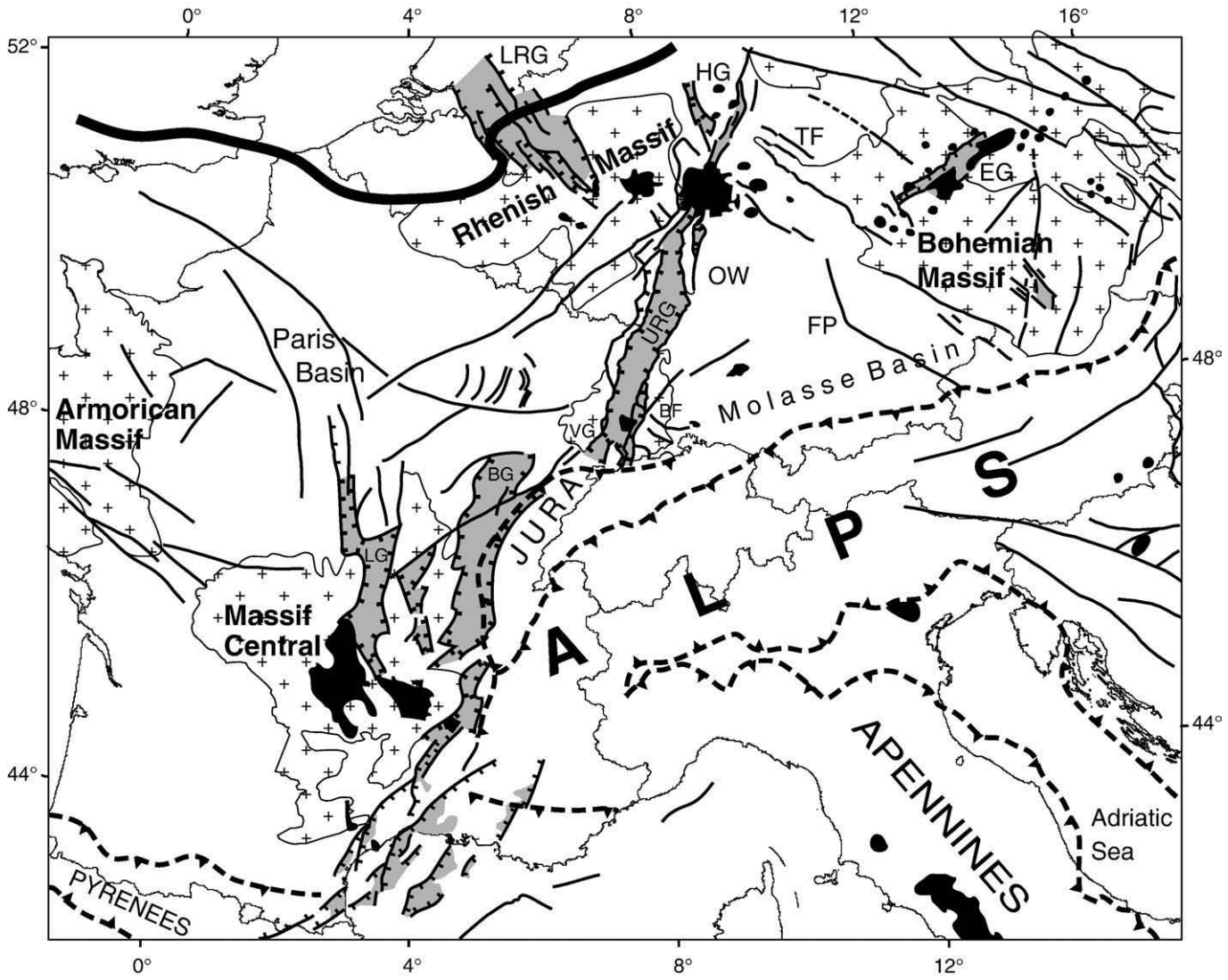

Fig. 12. Location map of the European Cenozoic rift system (ECRIS) in the Alpine and Pyrenean foreland, showing Cenozoic fault systems (black lines), rift-related sedimentary basins (light gray), Variscan massifs (cross pattern) and volcanic fields (black). Solid line: Variscan deformation front; stippled barbed line: Alpine deformation front. BF, Black Forest; BG, Bresse Graben; EG, Eger (Ohre) Graben; FP, Franconian Platform; HG, Hessian Grabens; LG, Limagne Graben, LRG, Lower Rhine (Roer Valley) Graben; URG, Upper Rhine Graben; OW, Odenwald; VG, Vosges (after Dèzes et al., 2004).

on the Massif Central and its eastern flank, respectively. These grabens are linked via the Burgundy transfer zone to the northerly striking Upper Rhine Graben which bifurcates northwards into the northwest trending Roer Valley Graben and the north-easterly trending Hessian Grabens, which transect the Rhenish Massif. The northeast striking Eger Graben, which transects the Bohemian Massif, forms an integral part of ECRIS (Ziegler, 1994). Localization of ECRIS involved the reactivation of Permo-Carboniferous shear systems. Although the on-shore parts of ECRIS are characterized by relatively low crustal stretching factors they associate with a distinct uplift of the crust-mantle boundary. To what extent this feature must be attributed to Cenozoic rifting or whether Permo-Carboniferous processes have contributed to it, remains an open question (Ziegler and Dèzes, 2006). The evolution of ECRIS was accompanied by the development of major volcanic centres in Iberia, on the Massif Central, the Rhenish Massif and the Bohemian Massif, particularly during Miocene and Plio-Pleistocene times. High resolution seismic tomography indicates that mantle plumes well up beneath the Massif Central and the Rhenish Massif (Granet et al., 1995; Ritter et al., 2001), but not beneath the Vosges–Black Forest arch. Similar data resolution capable to prove the presence or absence of mantle plumes is, however, not available for Iberia and the Bohemian Massif. Despite this, the evolution of ECRIS is considered to be a clear phase of passive rifting.

During the Late Eocene, the Limagne, Valence, Bresse, Upper Rhine and Hessian grabens began to subside in response to northerly-directed compressional stresses (Ziegler and Dèzes, 2006) that may be related to collisional interaction of the Pyrenees and the Alps with their foreland (Merle and Michon, 2001; Schumacher, 2002). During their Oligocene main extensional phase these originally separated rifted basins coalesced, and the Roer Valley and Eger graben came into evidence. During the Late Oligocene, rifting propagated southward across the Pyrenean orogen into the Gulf of Lions and along coastal Spain in response to back-arc extension that was controlled by eastward roll-back of the subducted Betic-Balearic slab. By Late Burdigalian times, crustal separation was achieved, the oceanic Provencal Basin began to open and the grabens of southern France became inactive (Roca, 2001). By contrast, the intra-continental parts of ECRIS remained tectonically active until the present, although their subsidence was repeatedly interrupted, possibly in conjunction with stresses controlling far-field inversion tectonics. By End Oligocene times, the area of the triple junction between the Upper Rhine, Roer Valley and Hessian grabens became uplifted, and magmatic activity on the Rhenish Shield increased. By middle-Late Miocene times, the Massif Central, the Vosges–Black Forest arch and slightly later also the Bohemian Massif were uplifted This was accompanied by increased mantle-derived volcanic activity. As

at the level of the Moho a broad anticlinal feature extends from the Massif Central via the Burgundy Transfer zone, the Vosges–Black Forest into the Bohemian Massif, uplift of these arches may have involved folding of the lithosphere in response to increased collisional coupling of the Alpine orogen with its foreland. Uplift of the Burgundy transfer zone entailed partial erosional isolation of the Paris Basin.

Under the present northwest directed stress regime, which built up during the Pliocene, the Upper Rhine Graben is subjected to sinistral shear, the Roer Valley Graben is under active extension, whereas the North Sea Basin experiences a late phase of accelerated subsidence that can be related to stress-induced deflection of the lithosphere (van Wees and Cloetingh, 1996). Similarly, the continued uplift of Fennoscandia is thought to be related to intraplate compressional deformation under the present stress field that reflects a combination of Atlantic ridge push and collisional coupling of the Alpine orogen with its foreland (Gölke and Coblentz, 1996).

In ECRIS, lithospheric thickness is similar to that of the adjacent Palaeozoic Variscan structures (80–120 km), although in some parts it can be as thin as 65–80 km, i.e. in the western Bohemian Massif (Heuer et al., 2006). In the Eifel region regional and large scale P-wave tomography models show a narrow low-velocity anomaly down to the bottom of the upper mantle (Ritter et al., 2001; Montelli et al., 2004) supporting diapiric upwelling of small scale, finger-like convective instabilities from the base of the upper mantle, which presumably act as the main source for Tertiary–Quaternary volcanism of Western and Central Europe. This volcanism and domal uplift of Variscan basement massifs is spatially and temporally linked to the development of ECRIS (Wilson and Patterson, 2001). Tomographic images for the Upper Rhine Graben (URG) portion of the ECRIS (Achauer and Masson, 2002) suggest that the URG originated as a passive rift, with complex regional stress fields associated with the convergence of the Eurasian and African plates and inherited structures playing a controlling role in its evolution (Dèzes et al., 2004).

Beneath the French Massif Central both local and global seismic tomographic studies (Granet et al., 1995) indicate the presence of an upper mantle anomaly with a diameter of 100–300 km that rises from the upper to lower mantle transition zone and involves material 100–200 °C hotter than the ambient mantle, similar to the Eifel area. Similarly to the Rhenish Massif, some authors explain the low-velocity zone in the upper mantle (60–100 km, Granet et al., 1995) and the Cenozoic volcanic activity in the Massif Central by a plume or mantle diapir (Lucazeau et al., 1984; Cebriá and Wilson, 1995; Sobolev et al., 1996). In addition, topography profiles over the Eifel and Massif Central areas contain distinct spectral signatures anywhere else in Europe, consistent with predictions from thermo-mechanical models of plume-head continental lithosphere interactions (Guillou-Frottier et al., 2007). Other authors propose asthenospheric flow related to west Mediterranean extension (Barruol and Granet, 2002).

3.2. Back-arc and post-orogenic collapse basins

The aftermath of the collision of the European and African lithospheric plates resulted in the opening of extensional basins in the Mediterranean region. From west to east, these basins are the Alboran, Ligurian, Tyrrhenian, Pannonian and Aegean basins. It is common in their formation and evolution that they were formed on former orogenic wedges by back-arc extension due to roll-back of subducted lithospheric fragments of the Tethys Ocean in the general frame of slow convergence between Africa and Europe (Fig. 13). Within this geodynamic framework, the western Mediterranean was initiated during the late Oligocene as the west-directed Apennines–Maghrebides subduction began to retreat towards southeast (Robertson and Grasso, 1995). At this time either the main east-directed Alpine subduction changed polarity to west-directed subduction, because the Alpine–Betic system had by then reached the continental collision stage making subduction more difficult (Doglioni et al., 1998; Gueguen et al., 1998), or the subduction was always going on slowly towards west since 80 Ma and by this time it reached a critical stage and began to accelerate (Faccenna et al., 2001). Roll-back of this west directed subduction then induced opening of the Ligurian–Valencia–Alboran basins. Extension advanced until oceanic crust has been formed in the eastern Alboran and Ligurian basins. In early-middle Miocene times as the subducted slab has reached the 660 km transition zone the roll-back and the extension slowed (Faccenna et al., 2003). Detachment of the subducted slab along northern Africa in Middle Miocene resulted in the shift and renewal of the active subduction zone east of Corsica and Sardinia and formation of the Tyrrhenian basin. Finally, a last slab detachment process along the Apennines (Pliocene to recent) led to a concentration of the active expansion in the southern Tyrrhenian basin.

Formation of the Carpathian arc and the Pannonian basin took place in a similar tectonic setting from Early Miocene (Fig. 14). In Late Oligocene the northward convergence of the Adriatic plate towards the European foreland led to eastward tectonic escape of the Pannonian terrain from the collisional zone (Kázmér and Kovács, 1985; Royden, 1988; Ratschbacher et al., 1991). In the eastern boundary Tethyan oceanic crust persisted, which was subducting below the Pannonian lithosphere. In Early Miocene the compressional deformation changed to extensional due to the roll-back of the subducted oceanic slab and collapse of the previously thickened crust (Csontos et al., 1992; Horváth, 1993). The main phase of extension was Middle Miocene when several troughs and grabens were opened and connected by strike-slip faults (Royden et al., 1983a). By the end of the period the subductable oceanic lithosphere was consumed and the buoyant European continental crust entering into the subduction zone has blocked the process. The subducted lithosphere detached along the Carpathian arc and sank into the asthenosphere (Wortel and Spakman, 2000). The last remnant of the subducted slab hangs vertically in the Vrancea zone, in the hinge zone of the Eastern and Southern Carpathians (Fig. 14), as shown in seismic tomographic images (Wenzel et al. 2002; Martin et al., 2005). Since Pliocene to recent the Pannonian basin is in an initial phase of positive structural inversion. It manifests itself in large scale lithospheric folding and inversion of former extensional faults as thrust faults (Horváth and Cloetingh, 1996). The present tectonic regime is strike-slip and transpressional (Horváth et al., 2006; Bada et al., 2007a,b).

The Aegean domain has undergone two successive stages of extension since Oligocene times. In late Oligocene the southward migration of the African slab triggered the gravitational collapse of the crust thickened by nappe stacking in Eocene. This extension has formed core complexes through uplift of the lower middle continental crust to the surface in the central Aegean (Cyclades) during the middle upper Miocene (Lister et al., 1984). Overall crustal extension occurred during the same period within the northern Aegean (Dinter and Royden, 1993) and in southwestern Turkey (Hetzel et al., 1995a,b). The second stage of Plio-Pleistocene extension is related to the combined effects of the still active retreat of the African slab and of the westward extrusion of Anatolia (4, 10–14, from Tirel). Brittle extension affected mainly the southern and northern Aegean. The Cretan Sea thinning is controlled by the back-arc extension, while the North Aegean extension is due to the combined effects of the extrusion of Anatolia and back-arc extension. Between these two regions, the Cyclades likely behave as a rigid plateau.

Formation of the Mediterranean back-arc basins was accompanied by subduction related calc-alkaline magmatism producing large volume of volcanic rocks mainly during the active subduction phase and sporadic alkaline magmatism in the post-collisional phase. In the Western Mediterranean region the calc-alkaline magmatism became progressively younger from west to east: Oligocene in Provence, Miocene in the Betics–Alboran–Valencia region and Sardinia–Corsica, and Plio-Pleistocene in the eastern coast of the Tyrrhenian basin. In the Pannonian region the main phase of calc-alkaline volcanism was coeval with the extension in middle Miocene. However, in the Eastern Carpathians volcanism lasted until recently, and it is interpreted as a consequence of gradual slab detachment. In the Aegean region the main calc-alkaline volcanic centres

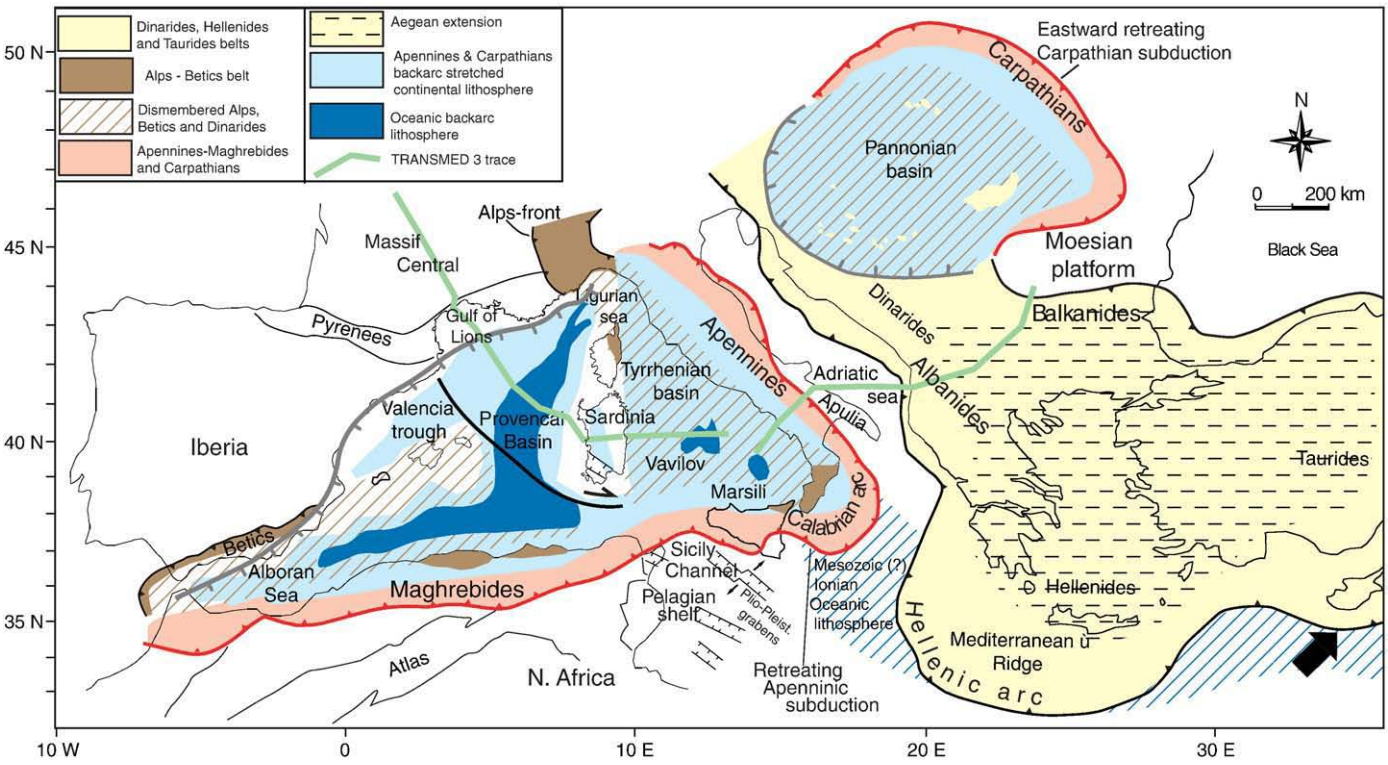

Fig. 13. Outline map of back-arc extensional basins in the Mediterranean and Carpathian system (after Cavazza et al., 2004).

of Oligocene–middle Miocene age are found interestingly in NE-Aegean and W-Anatolia. The volcanic activity shifted to Central Anatolia in middle Miocene and terminated only a few hundred thousand years ago. It was probably related to the subduction along the Cyprus arc. At the present day active subduction occurs only beneath Calabria and the Aegean arc resulting in volcanic activity in the Aeolian Islands, and in the volcanic islands of the Cretan Sea, respectively.

3.3. Quantitative assessment of basin temperatures beyond well control in extensional basins

Steady state models linking heat flow to lithosphere temperatures generally hold well for most of Europe. However in regions, marked by lithosphere scale (depth-dependent) kinematics over the last 50 million years, such as subduction in the Alps, subcrustal thermal attenuation by mantle plumes in the Eifel area or rapid erosion and/or sedimentation in the Alps and Rhine graben, respectively, the lithosphere scale temperature assessment need to take into account non steady state kinematic effects.

Kinematic effects are incorporated in numerical lithosphere models by calculating the transient thermal effects of perturbing the initial steady state geotherm of the lithosphere using the deformation history, constrained by the geological record (e.g. burial histories, apatite fission track data, etc.). Thermo-kinematic models have been widely adopted to take into account the formation of crustal and lithospheric root in the Alps (Willingshofer et al., 2001), extensional basins in the ECRIS and north-Sea (e.g. Kooi and Cloetingh, 1989; van Wees and Cloetingh, 1996; van Wees and Beekman, 2000; Ziegler et al., 2006) and the Mediterranean (back-arc) basins, including the Valencia Trough (Morgan and Fernàndez, 1992; Watts and Torné, 1992; Zeyen and Fernández, 1994), Gulf of Lion (Bessis, 1985; Burrus, 1989; Kooi et al., 1989), Tyrrhenian sea (Spadini et al., 1995), Pannonian basin (Royden et al., 1983b; Royden and Dövényi, 1988; Lenkey, 1999), Aegean sea (Le Pichon et al., 1988; Wijbrans et al., 1993).

The most widespread thermo-mechanical models of extensional basin formation are the various lithospheric stretching models. The concept of lithospheric stretching was introduced by McKenzie (1978). In the McKenzie model of homogeneous stretching it is assumed that the lithosphere is stretched instantaneously in pure shear mode by a certain amount. Due to conservation of mass the lithosphere is thinned by the same amount. During thinning each elementary volume of the lithosphere keeps its original temperature as it is rising to a higher position, resulting in higher geothermal gradient in the lithosphere, and thus, higher surface heat flow. The high temperature in the lithosphere is not stable, the lithosphere begins to cool by heat conduction. Since heat transfer by conduction is a very slow process it takes a few hundred million years for the temperature to reach its original steady state.

The McKenzie (1978) stretching model was widely accepted and used, because it explains the subsidence history of extensional basins. In passive margins and back-arc basins it was observed that during the active tectonic phase an initial, or syn-rift subsidence occurs, which is followed by a long term, exponentially decaying postrift subsidence. The syn-rift subsidence is an isostatic response to thinning of the crust, and the postrift subsidence is due to thermal contraction caused by the cooling of the lithosphere. In later modifications (Royden and Keen, 1980) the amount of stretching in the crust and mantle lithosphere can be different (Fig. 15), which changes the relative magnitudes of the syn-rift and postrift subsidence compared to the uniform stretching model. Also more realistic models, in which the synrift phase is not instantaneous, turned out to affect the relative magnitudes of syn- and postrift subsidence. Using these models, it was shown that the ratio between syn- and postrift subsidence depends on the stretching rate (e.g. ter Voorde and Cloetingh, 1996).

The evolution of the temperature in the lithosphere basically depends on the stretching (thinning) factors. In general, the stretching factors are accepted if the model is able to reproduce the subsidence history. If temperature measurements and hydrocarbon maturity indicators (e.g. vitrinite reflectance) are also available from boreholes, then the modelled present day temperature and vitrinite reflectances must also fit to the observed data. Vitrinite reflectance depends on the cumulated heat effected the organic material,

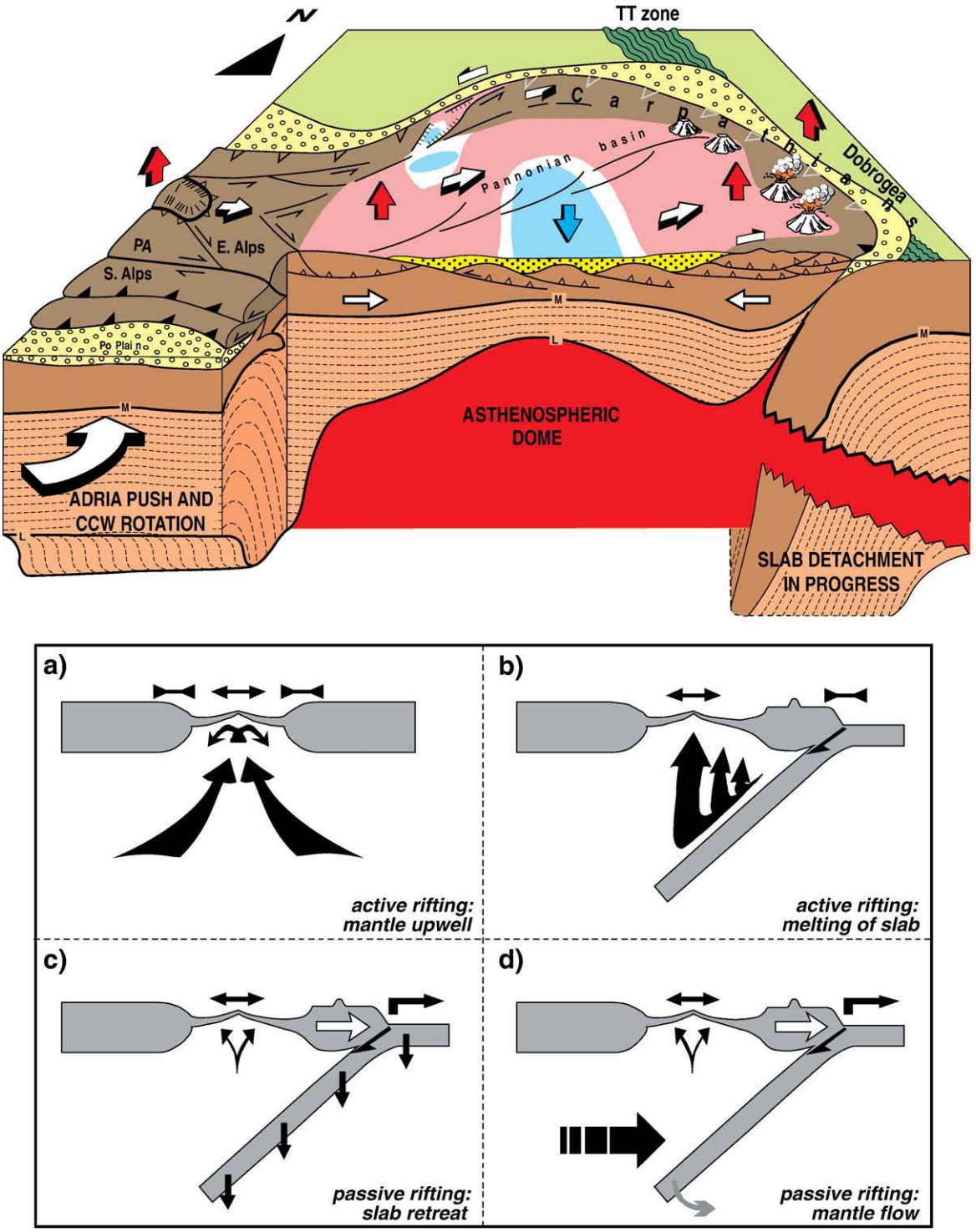

Fig. 14. (top) Cartoon of the Late-stage scenario of the Pannonian Basin–Carpathians system during the Late Cenozoic (after Horváth and Cloetingh, 1996), illustrating its back-arc setting, involving slab detachment and post-orogenic collapse. (bottom) Models proposed for the Miocene formation of the Pannonian Basin.

therefore it is an indicator of the thermal history. In the oil industry the vitrinite reflectance is modelled by varying the basement heat flow until the modelled vitrinite reflectance fits to the observed values (e.g. van Wees et al., 2009). However, in an extensional tectonic setting the stretching model predicts the evolution of the temperature in the lithosphere, thus also the basement heat flow. It, therefore, is evident to couple the two modelling procedures (Horváth et al., 1988, van Balen et al., 2000; van Wees et al., 2009). The fit to the thermal observations increases the reliability of the stretching model.

In the McKenzie (1978) stretching model high heat flows are associated to regions of ongoing lithosphere extension. However, it has been recently demonstrated that heat flows for sedimentary extensional basins should be considerably lower than predicted by this model, as it does not include the effects of sediment infill. Sediments damp the heat flow effect of extension by their low temperature, but may enhance temperature and heat flow by their insulating nature (e.g. ter Voorde and Bertotti, 1994; van Wees and Beekman, 2000; Sandiford et al., 2003). Furthermore, crustal

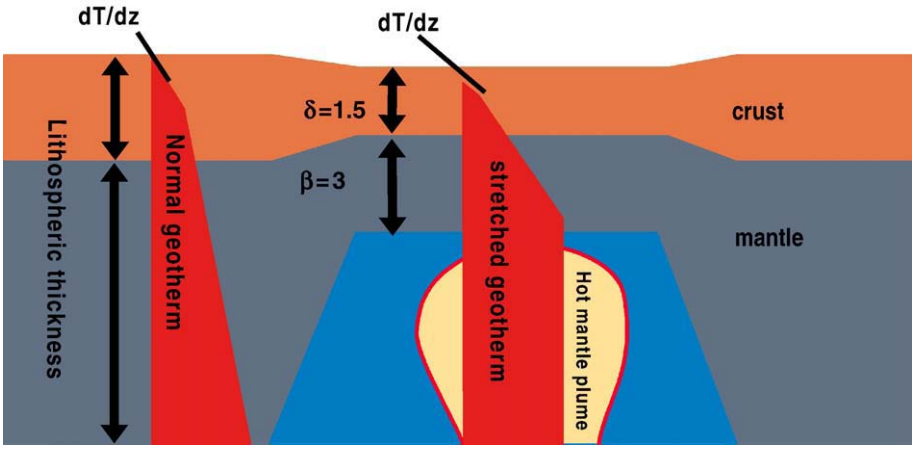

Fig. 15. Cartoon of two-layered stretching model, in which the kinematic stretching factor of the subcrustal mantle (β) is higher than the stretching factor in the overlying crust. The stretching factor of the crust (δ) is the ratio of initial and stretched crustal thickness whereas the subcrustal stretching factor is the ratio of the thermal thickness – defined by the 1300 °C isotherm – of the initial and an instantaneously stretched subcrustal lithosphere. Subcrustal mantle attenuation in excess of crustal stretching can either be related to mantle plumes as for the ECRIS system or slab detachment in back-arc basins.

extension results in a reduction of crustal heat production further, lowering the heat flow. The combined effect results in moderate extensional heat flow, which for onshore basins is generally less than the heat flow prior to extension (van Wees et al., 2009, see also Fig. 16). Such a prediction is clearly not in agreement with strongly elevated heat flows observed in onshore extensional basins in the ECRIS system, and back-arc basins such as the Pannonian Basin. Below we present a number of mechanisms which can cause elevated heat flow in extensional basins, incorporating basin evolution aspects beyond the McKenzie model.

3.3.1. Post-orogenic collapse

In the McKenzie (1978) model it is assumed that extension occurs on a lithospheric column with its top at sea level. In back-arc basins sedimentary basins developed on top of orogenic wedges, having the top of the thickened lithosphere column at elevated topography. During the (initial stages of) extension the basin is relatively sediment starved as it remains above sea level. Heat flow predicted for sediment starved basins (Fig. 15), lacking the damping effect of the sediments result in considerably higher heat flow than sediment filled basins developing on passive margins (e.g. North Sea, Beekman et al., 2000; van Balen et al., 2000; van Wees et al., 2009, Fig. 16). Consequently heat flows can be considerably enhanced in sediment-starved post-orogenic collapse settings.

3.3.2. Subcrustal mantle attenuation

In parts of the ECRIS, and back-arc basins a major contributing factor to elevated heat flow appears to be the fact that thermal attenuation is considerably larger in the mantle than in the crust. This effect can be adopted in the extension model by a kinematic stretching factor of the subcrustal mantle (β), in excess of stretching in the overlying crust (δ) ((Fig. 15). The predicted heat flow in this model (Fig. 16) becomes significantly elevated in an onshore setting (Fig. 16). Various explanations are possible for the subcrustal mantle attenuation, depending on the tectonic setting. In back-arc settings mantle lithosphere attenuation can take place faster than crustal stretching because of slab delamination (e.g. van Wees et al., 2000; Ziegler et al., 2006) or because of various models for mantle flow (Fig. 14, lower panel a–d). In the ECRIS impingement of mantle plumes as demonstrated for the URG and MC can cause thermal uplift and thermal alteration of the mantle lithosphere which can be modelled through applying $\beta>1$, $\delta=1$ (Cloetingh and van Wees, 2005). In case of subcrustal mantle attenuation the heat flow peak at the surface is delayed for millions of year relative to the timing of mantle attenuation (Fig. 16). The delay in heat flow is consistent with the observation that in areas such as the Eifel, surface heat flow is not yet at its peak, and transient effects may in this case result in over-optimistic exploration potential using deep lithosphere steady state approaches (Goes et al., 2000a,b).

3.3.3. Subduction and extension derived melts thickening the crust

Thermal attenuation in the mantle can cause pervasive magmatism as melt occurs when temperatures are in excess of the mantle solidus (McKenzie and Bickle, 1988). Melts accumulate as underplates at the base of the crust and can cause basalt extrusions at the surface (White and McKenzie, 1995). Modelling of detailed kinematic effects such as volcanism, which can make up to 10–50% of the crustal thickness and results in permanent uplift, is beyond the scope of this study. The uplift effect and large scale thermal attenuation can be taken into account using a crustal stretching value which is less than

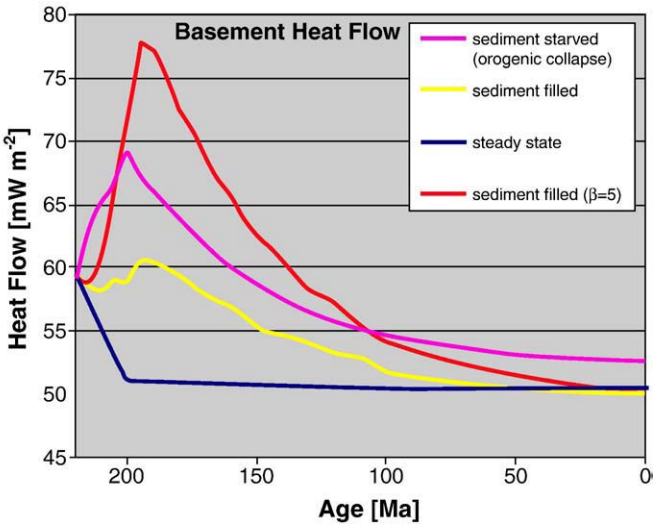

Fig. 16. Synthetic heat flow model results marked by crustal stretching of 1.44, with synrift phase from 220–200 Ma, followed by a post rift phase of 200 My duration, illustrating significant thermal effects of rifting up to 30 My after rifting. In uniform stretching, onshore basins are predicted to be marked by flat or decreasing heat flow (yellow curve), thermally elevated compared to the theoretical steady state heat flow for the lithosphere thickness (cf Fig. 7). However, back-arc basins developed on orogenic wedges these are marked by elevated heat flow because they can remain relatively sediment starved (pink curve). In addition parts of the ECRIS and most back-arc basins are marked by non-uniform extension ($\beta>\delta$) resulting in strong elevated heat flow (red curve). Please note that heat flow peak arrives later because of time delay in diffusion of heat through the crust.

subcrustal stretching ($\beta > \delta$), which is similar to the effect of subcrustal mantle attenuation. Subduction related magmatism can also result in apparent thickening of the crust ($\beta > \delta$), provided magmatic volumes correspond as reflected by large deep seated volcanic provinces such as in Tuscany. Local scale thermal attenuation, which can involve volcanism in the crust will result in much more elevated heat flow as tectonically predicted by lithosphere kinematics. These secondary effects may explain patterns of heat flow up to 400 mW m^{-2} in Larderello Tuscany (Ranalli and Rybach, 2005), related to volcanism at crustal levels.

3.3.4. Example from the Pannonian Basin

The subsidence, thermal and maturation history of the Jász-I well from the Pannonian basin is presented in Fig. 17 as an example of an orogenic collapse setting (Horváth et al., 1988). The temperature-depth and vitrinite reflectance-depth profiles calculated for the present are in good agreement with the observations. The best fit model of the Jász-I well is obtained assuming that the lithospheric extension started at 17 Ma and lasted till 11 Ma and it caused thinning of the crust and the mantle lithosphere by a factor of 1.8 (β_c) and 100 (β_m), respectively. The large mantle thinning factor means that the mantle was practically removed during stretching. Since 11 Ma cooling of the lithosphere causes thermal subsidence. As the model reproduces the subsidence history and fits to the thermal data, we assume that it predicts correctly the present day temperature distribution in the lithosphere (Fig. 17).

3.4. Orogenic belts and flank uplift: exhumation and surface heat flow

Collisional orogenic belts such as the European Alps portray a two-stage tectono-thermal evolution during which stacking of crustal units lead to burial of rocks (stage I) and subsequent denudation of the mountain belt by erosion and tectonics (stage II) results in exhumation of rocks back to the surface. Both, burial and exhumation of rock units perturb the thermal structure of the lithosphere transiently, but with opposite sign. While burial by for example thrust imbrication leads to downward deflection of isotherms, exhumation through normal faulting or erosion has the opposite affect and may result in up-warped isotherms (Fig. 18). Controlling parameter for the magnitude of the thermal perturbation is the velocity at which rocks are buried or exhumed (e.g. Mancktelow and Grasemann, 1997).

In the Eastern Alps post-collisional exhumation of the metamorphic core commenced during the Late Oligocene and resulted in the formation of fault-bound metamorphic domes, the Tauern and Rechnitz domes. A wealth of structural and stratigraphic data suggests that rock exhumation was driven by a combination of orogen-parallel extension and erosion (e.g. Frisch et al., 1998). Exhumation rates deduced for the western Tauern Window were high (~ 4 mm a^{-1}) during the Late Oligocene to early Miocene. Since the middle Miocene exhumation rates decreased rapidly to about 1 mm a^{-1} for the time period between 15 and 10 Ma and to ca. 0.2 mm a^{-1} for the last 10 Ma (Fügenschuh et al., 1997). Rapid exhumation of the Tauern Window occurred under isothermal conditions due to the upward advection of heat. The resulting thermal perturbation resembles that of a thermal dome with strong lateral gradients (Genser et al., 1996). In accord with the geochronological data, Sachsenhofer (2001) estimated the paleo-heat flow at the end of the rapid exhumation phase, based on vitrinite reflectance data from syn-orogenic strata, to be in the order of 175–210 mW m^{-2} for the Tauern Window region. The thermal anomaly associated with this exhumation decayed from the Middle

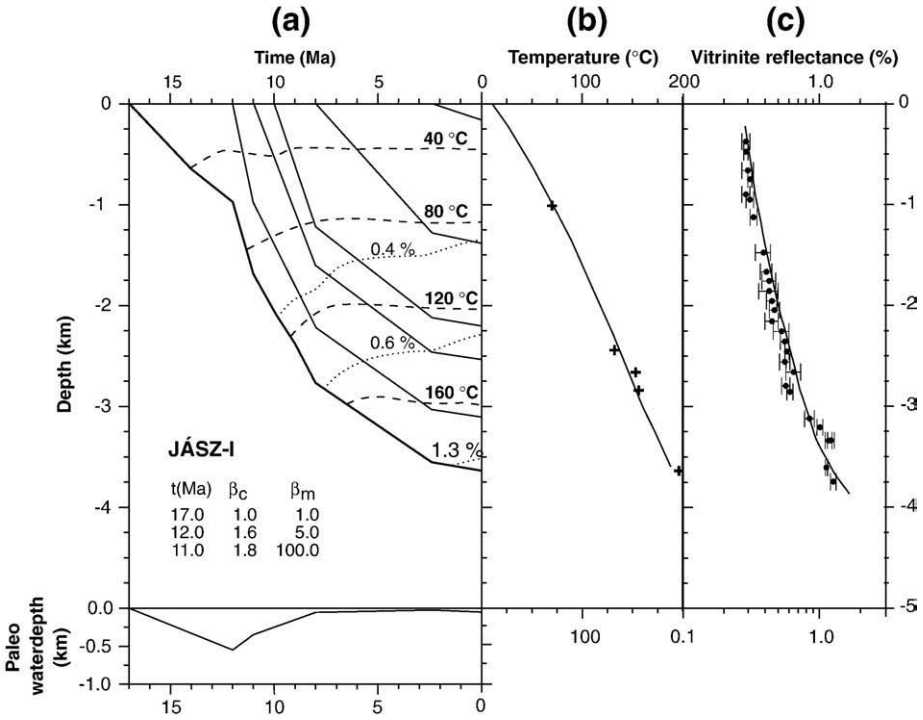

Fig. 17. Basin modelling results for the Pannonian Basin. Presented are (a) subsidence, (b) thermal history, and (c) the maturation history of the Jász-I well. The well penetrated the Paleozoic basement at a depth of 3637 m. High postrift subsidence and maturity and temperature data are explained through a two-layered model ($\beta > \delta$), in agreement with strong mantle upwelling. Thermal effects of the two-layered stretching have resulted in a marked elevated geotherm and surface heat flow compared to initial geothermal conditions; (a) burial curves with depth. The thick line on the left panel starting from the surface at 17 Ma and reaching 3637 m at the present shows the accumulation of the Neogene and Quaternary sediments. The other lines starting from the surface from left to right show the thicknesses of progressively younger sediments. The water depth was calculated as the difference between the predicted basement depth from the forward model and the thickness of sediments. The subsidence rate in the first 5 Ma was higher than the sediment accumulation rate resulting in relatively deep water of 500 m. This is in agreement with the sedimentological observations (Juhász, 1994) and interpretation of seismic sections (Vakarcs et al., 1994), which show that the basin was filled up by a delta system prograding into the basin from the peripheral areas. The dashed and dotted lines indicate the evolution of temperature and vitrinite reflectance through time, respectively; (b) Modelled geothermal gradient curve fitted with the temperatures data; (c) Modelled vitrinite reflectance curve with the vitrinite reflectance data.

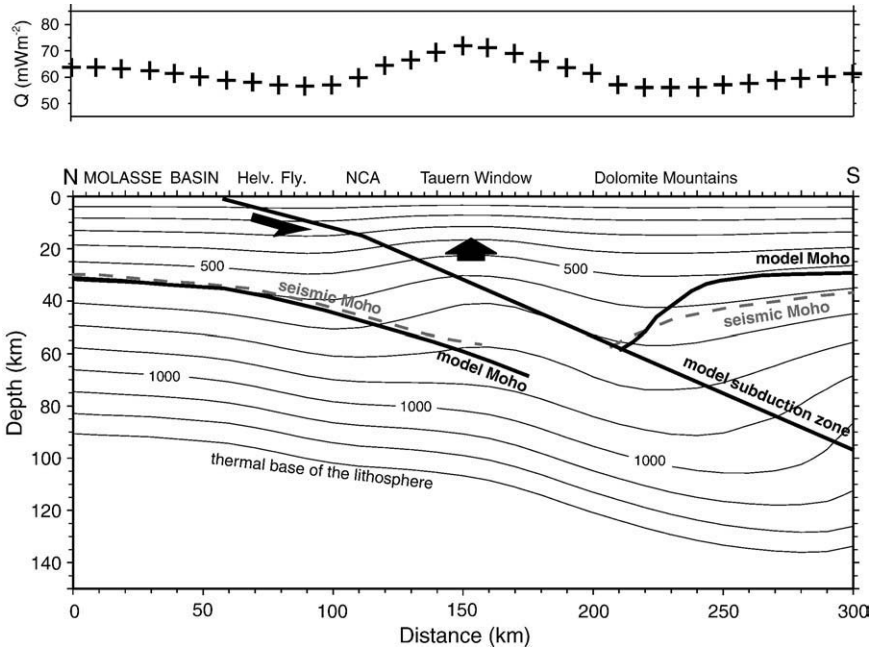

Fig. 18. Predicted thermal structure (bottom) and surface heat flow (top) of the Eastern Alps along the TRANSALP deep seismic line for the present-day crustal configuration (Modified from Willingshofer and Cloetingh, 2003).

Miocene onward resulting in a present-day heat flow in the order of 60–70 mW m^{-2} what is still higher when compared to the neighbouring regions in the north (<55 mW m^{-2}) (Sachsenhofer, 2001), and the south (<60 mW m^{-2}) though data coverage in the Southern Alps is poor (della Vedova et al., 2001). These findings have been supported by 2D thermal-modelling of Willingshofer and Cloetingh (2003) along the TRANSALP deep seismic line (TRANSALP Working Group, 2002), where the predicted present-day up-warping of the isotherms in lower and mid-crustal levels as well as the presence of condensed isotherms in upper crustal levels probably reflects the decay of a more pronounced early Miocene thermal perturbation (Fig. 18). This interpretation of the Tauern thermal anomaly is at variance with a more recent thermal modelling study along the same transect in which Vosteen et al. (2006) argue, based on 1d-thermal modelling, that the calculated deviation of the temperature from steady state (+3.5 K in 1 km and 15 K at 5 km depth, respectively) is merely the consequence of slow exhumation (0.3 mm a^{-1}) during the past 14 Ma.

As the example of the Eastern Alps illustrates, quantifying the rates of mass movement through the crust and lithosphere in terms of rock exhumation is essential for clarifying its influence on the thermal evolution of the lithosphere.

Subsidence of rocks by thrusting and denudation by erosion does not necessarily occur in different stages; simultaneous thrust faulting and exhumation is also possible. These two scenarios can be distinguished from temperature-time curves obtained from, for example, fission track thermochronology, as has been shown for the Sierra de Guadarrama in the Spanish Central System (SCS) (ter Voorde et al., 2004). The SCS were formed for a large part in the mid-Tertiary, as a consequence of stresses acting from the Pyrenean and Betic borders of Iberia. Nevertheless, fission track analysis by De Bruijne and Andriessen (2000, 2002) also revealed large amounts of cooling in the period from Pliocene to present day, which were suggested by ter Voorde et al. (2004) to be caused by a period of active compressional deformation coeval with erosion.

Exhumation of rocks takes place not only in compressional areas. When rifting occurs, the resulting basins may be filled with sediments, but the adjacent rift flanks are uplifted and subjected to erosion (e.g. van der Beek et al., 1994). In the case of the Catalan Coastal Ranges (NE Spain) the effects of rifting and compression interfere in the thermal signals derived from apatite fission track and (U–Th)/He analysis. These mountain ranges can be regarded as a region of faults that were active from the early Eocene to present day, on a scale of several tens of kilometres, but they also form a small part of a much larger system, as they are one of the flanks of the late Oligocene–Miocene Valencia Through rift basin (e.g. Roca et al., 1999; Roca, 2001; Gaspar-Escribano et al., 2001, 2004). Furthermore, it can be concluded from apatite fission track and (U–Th)/He analysis (Juez-Larré and Andriessen, 2006), numerical thermal modelling (ter Voorde et al., 2007) and earlier work of Fernández and Banda (1989, 1990) that the thermal effects of forced groundwater convection have also played a major role in the pattern of heat flow in this area.

3.5. Implications for geothermal exploration

Geothermal characterization of the lithosphere shows at large wavelength a clear relationship between proven favourable conditions for EGS and underlying tectonic processes. In Neogene times, for extensional areas heat advection by thermal attenuation of crust and lithosphere give rise to elevated heat flow, as observed for established r EGS sites, including Tuscany (central Italy) and the Upper Rhine Graben (URG). Quantitative models for lithosphere extension demonstrate that sedimentation can significantly damp the thermal attenuation effects. This quantitative approach also sheds light on observed large wavelength domains with elevated heat flows in continental areas favourable for EGS. According to the models, these should either be attributed to mantle plumes (e.g. URG) or extensional collapse of overthickened lithosphere which occurred over large regions in the Mediterranean (e.g. Spain, Italy, Greece, Turkey) and the Pannonian Basin. This concept is in agreement with geophysical observations of thermal anomalies at large lithospheric depth. Seimic tomography indicates that large areas of Europe are currently marked by anomalously thin lithosphere, indicating that prospective zones can occur also outside conventionally preferred extensional tectonic settings.

For compressional areas, modelling studies for the Alps show that heat flow is significantly increased, because of erosion. In other areas such as the Himalayas, marked by significantly higher Cenozoic erosion rates (Beaumont et al., 2001), this effect may significantly

contribute to their prospectivity for geothermal energy, hitherto attributed to deep seated radiogenic granites (Chandrasekhar and Chandrasekharam, 2009).

At local scales the tectonic heat flow can be strongly influenced by compositional differences such as granites, causing elevated heat flows as a consequence of radiogenic heat production. Predicted tectonic heat flows for continental areas, marked by moderate crustal extension ($\beta<2$), are relatively low not exceeding ca 100 mW m^{-2} (Figs. 2, 3). For EGS sites it is commonly observed that shallow heat flow and geothermal gradients have been strongly enhanced by magmatism and hydrothermal processes. These effects can result in shallow heat flows in excess of 400 mW m^{-2} (ca 150 °C/km) in Tuscany attributed to both magmatism and hydrothermal activity (Ranalli and Rybach, 2005) and 150 mWm^{-2} (ca 50 °C/km) in Soultz, solely related to hydrothermal activity. Prior to exploration drilling of Soultz it had been assumed that the shallow elevated temperature gradient would continue at larger depth (Kohl et al., 2000; Bächler et al., 2003). In hind sight, tectonic heat flow models would at pre-drilling stage have aided in demonstrating a hydrothermal cause for shallow elevation of the heat flow and a more conservative estimation of temperatures at reservoir depth.Through a positive relationship between back-arc and plume geodynamics setting (e.g. Burov et al., 2007; Burov and Cloetingh, 2009), elevated tectonic heat flow and likelihood for magmatism and hydrothermal activity, prospective EGS areas can be outlined more robustly at continental scale. For example south east Spain is lacking heat flow data in a large area, but its setting, marked by a thin lithosphere, orogenic collapse of the Betic orogen, active faulting, natural and Quaternary volcanism suggest good prospectivity (e.g. Van der Beek and Cloetingh, 1992).

4. Active intraplate deformation and thermo- mechanical structure of Europe's lithosphere

In this section we review the connection of the thermo-mechanical structure of the European lithosphere and active deformation. Adopting lithosphere scale tectonic models, allows to identify the extent of actively deforming regions in particular tectonics settings favourable for EGS. Furthermore, this approach yields in-depth insight in the relationship of stress–strain interactions on geological time-scales and spatial distribution of natural seismicity. During Mesozoic and Cenozoic times, the lithosphere of the Alpine foreland has undergone repeated tectonic reactivation (Ziegler, 1989a; Ziegler et al., 1995, 1998) and is still being deformed at present, as evidenced by significant intraplate seismicity and on-going differential vertical motions controlling the development of dynamic topography at large distances from plate boundaries (Cloetingh et al., 2003b, 2005) (Fig. 19). Increasing evidence is accumulating for widespread Neogene uplift and tectonics around the northern Atlantic (e.g. Japsen and Chalmers, 2000; Chalmers and Cloetingh, 2000, Cloetingh et al., 2007), that are accompanied by accelerations of subsidence and sedimentation rates. Over the last few years, seismicity studies and geomorphologic evidence demonstrate the important contribution of neotectonics to the topographic evolution of intraplate Europe including France, the Netherlands, Germany, Spain and Hungary and Romenia (Fig. 19).

The origin of intraplate stress fields in continental lithosphere and their relationship to plate-tectonic driving forces has been the subject of a large number of observational (e.g., van der Pluim et al., 1997; Marotta et al., 2001) and modelling studies (e.g. Bada et al., 1998; Gölke and Coblentz, 1996). These have revealed the existence of consistently oriented first-order patterns of intraplate stress in, for example, the Northwest European platform (Fig. 4) and the North American craton. The effect of these stresses on vertical motions of the lithosphere, expressed in terms of, for example, apparent sea-level fluctuations (Cloetingh et al., 1985), development of foreland bulges (Ziegler et al., 2002), basin inversion (Ziegler et al., 1995, 1998) and lithosphere folding (Martinod and Davy, 1994; Cloetingh et al., 1999), has been demonstrated to be an important element in the dynamics of continental interiors (Cloetingh, 1988; van der Pluim et al., 1997).

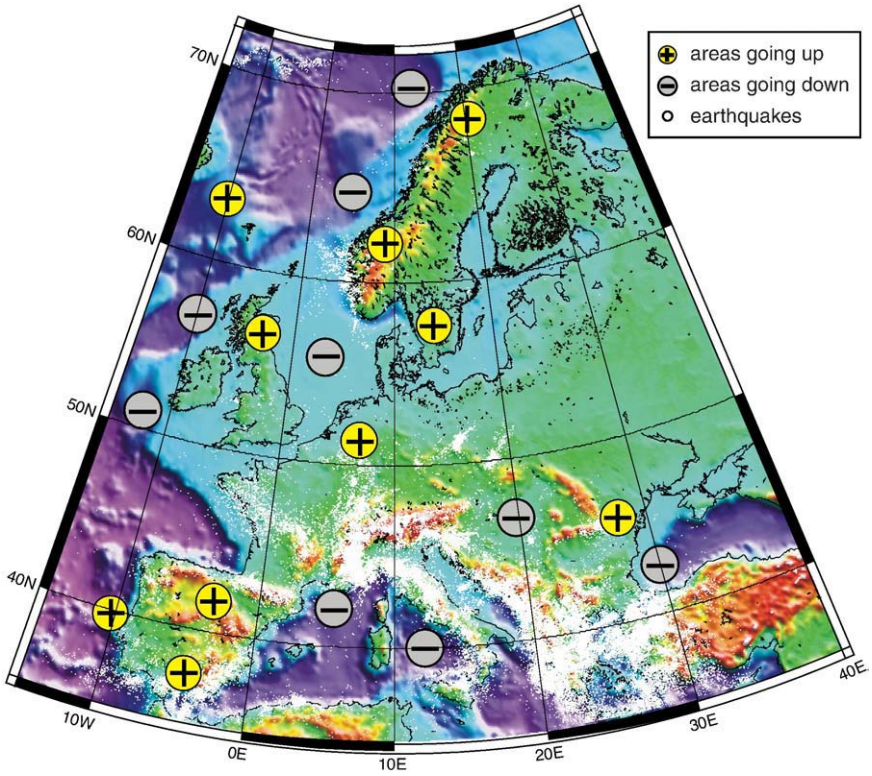

Fig. 19. Topographic map of Europe with superimposed distribution of seismicity (red dots), illustrating present-day active intraplate deformation. Also shown are intraplate areas of Late Neogene uplift (circles with plus symbols) and subsidence (circles with minus symbols). Background elevation image is extracted from the ETOPO2 data set (after Cloetingh et al., 2005).

Stress propagation occurs in a lithosphere that can be significantly weakened by inherited structural discontinuities, but also by upper mantle thermal perturbations (e.g. Goes et al., 2000a,b). Below we present first order scale thermo-mechanical models for large-scale intraplate deformation, and discuss constraints on these models inferred from recent studies on the rheology, mostly for the Northwest European foreland (Cloetingh et al., 2005, 2006, 2007; Tesauro et al., 2007).

4.1. Basic concepts of lithosphere strength

The strength of continental lithosphere is controlled by its depth-dependent rheological structure (Fig. 20) in which the thickness and composition of the crust, the thickness of the mantle–lithosphere, the potential temperature of the asthenosphere, the presence or absence of fluids, and strain rates play a dominant role (e.g. Carter and Tsenn, 1987; Kirby and Kronenberg, 1987). By contrast, the strength of oceanic lithosphere depends on its thermal regime, which controls it's essentially age dependent thickness (Panza et al., 1980; Kusznir and Park, 1987; Stephenson and Cloetingh, 1991; Cloetingh and Burov, 1996). Theoretical rheological models indicate that thermally stabilized continental lithosphere consists of the mechanically strong upper crust, which is separated by a weak lower crustal layer from the strong upper part of the mantle–lithosphere, which in turn overlies the weak lower mantle–lithosphere (e.g. Burov and Diament, 1995). By contrast, oceanic lithosphere has a more homogeneous composition and is characterized by a much simpler rheological structure. Rheologically speaking, thermally stabilized oceanic lithosphere is considerably stronger than all types of continental lithosphere. Atlantic-type continental margins are representative of the transition from oceanic to continental lithosphere, and are the sites of thinned continental lithosphere that was extended and heated during continental breakup. This has led to substantial lateral variations in the mechanical strength of the lithosphere that are controlled by complex variations in crustal thickness, composition of the lithospheric layers, and the thermal regime. The strength of continental crust depends largely on its composition, thermal regime and the presence of fluids, and also on the availability of pre-existing crustal discontinuities.

Deep-reaching crustal discontinuities, such as extensional, thrust- and wrench-faults, can cause significant weakening of the otherwise mechanically strong upper parts of the crust (van Wees and Stephenson, 1995, Ziegler et al., 1995; 1998; van Wees and Beekman, 2000). As such discontinuities are apparently characterized by a reduced frictional angle, particularly in the presence of fluids, and they are prone to reactivation at stress levels that are well below those required for the development of new faults. Extension of stabilized continental crustal segments precludes ductile flow of the lower crust and faults will be steep to listric and propagate towards the hanging wall, i.e. towards the basin centre (Bertotti et al., 2000). Under these conditions, the lower crust will deform by distributing ductile shear in the brittle–ductile transition domain. This is compatible with the occurrence of earthquakes within the lower crust and even close to the Moho (e.g. Upper Rhine Graben: Bonjer, 1997; East African rifts: Shudofsky et al., 1987). In young orogenic belts, which are characterized by a crustal thickness of up to 60 km and an elevated

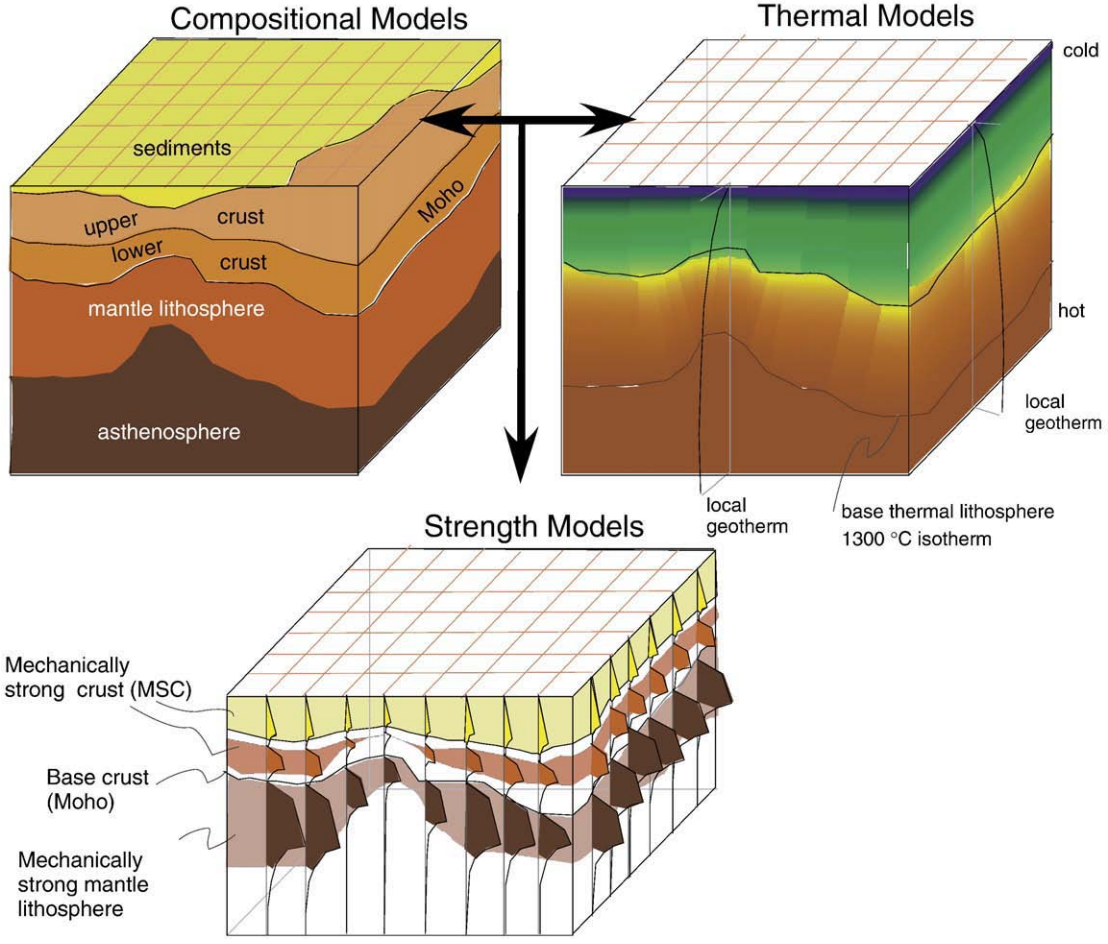

Fig. 20. From crustal thickness (top left) and thermal structure (top right) to lithospheric strength (bottom): conceptual configuration of the thermal structure and composition of the lithosphere, adopted for the calculation of 3D strength models (from Cloetingh et al., 2005).

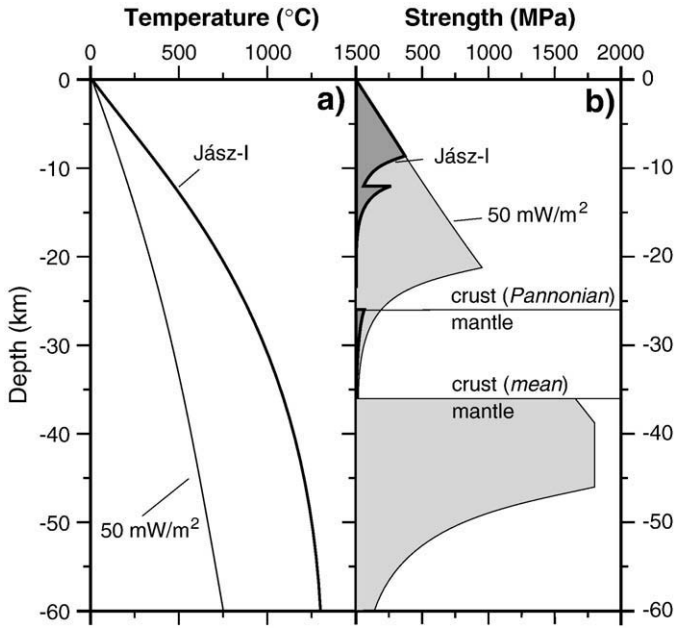

Fig. 21. Thermo-mechanical prediction of present day geotherm (left) and rheology (right) based on kinematic extension model presented in Fig. 15. Similar results were obtained by Sachsenhofer et al. (1997) and Lankreijer et al. (1997) for the Styrian basin and Danube basin, respectively, (sub basins in the Pannonian basin) assuming steady state temperature in the lithosphere, based on present day heat flows in the order of 100 mW/m^2. For comparison a rheological profile calculated with an unrealistically low surface heat flow of 50 mW/m^2 and assuming steady state temperature is also shown. The decrease of the lithospheric temperature and surface heat flow would result in considerable strengthening of the lithosphere, not compatible with earthquake depth distributions.

heat flow, the mechanically strong part of the crust is thin and the mantle–lithosphere is also weak. Extension of this type of lithosphere can involve ductile flow of the lower and middle crust along pressure gradients away from areas lacking upper crustal extension towards zone of major extensional unroofing of the upper crust, involving the development of core complexes (Bertotti et al., 2000).

The strength of the continental mantle–lithosphere depends to a large extent not only on the thickness of the crust but also on its age and thermal regime (Fig. 21). Generally, the upper mantle of thermally stabilized, old cratonic lithosphere is considerably stronger than the strong part of its upper crust (e.g. Moisio et al., 2000). However, the occurrence of upper mantle reflectors, which generally dip in the same direction as the crustal fabric and probably relate to subducted oceanic and/or continental crustal material, suggests that the continental mantle–lithosphere is not necessarily homogenous but can contain lithological discontinuities that enhance its mechanical anisotropy (Ziegler et al., 1995;Vauchez et al., 1998; Ziegler et al., 1998). Such discontinuities, consisting of eclogitized crustal material, can potentially weaken the strong upper part of the mantle–lithosphere. These factors contribute to weakening of former mobile zones to the end that they present rheologically weak zones within a craton, as evidenced by their preferential reactivation during the breakup of Pangea (Ziegler, 1989b; Janssen et al., 1995; Ziegler et al., 2001). From a rheological point of view, the thermally destabilized lithosphere of tectonically active rifts, as well as of rifts and passive margins that have undergone only a relatively short post-rift evolution (e.g. 25 Ma), is considerably weaker than that of thermally stabilized rifts and unstretched lithosphere (Ziegler et al., 1998; Ziegler and Cloetingh, 2004, Fig. 22). In this respect, it must be realized that during rifting, progressive mechanical and thermal thinning of the mantle–lithosphere and its substitution by the upwelling asthenosphere is accompanied by a rise of the geotherms, causing progressive weakening of the extended lithosphere. In addition, permeation of the lithosphere by fluids causes its further weakening. Upon decay of the rift-induced thermal anomaly (Fig. 22), rift zones become rheologically speaking considerably stronger than unstretched lithosphere. However, thermal blanketing through the accumulation of thick syn- and post-rift sedimentary sequences can cause a weakening of the strong parts of the upper crust and mantle–lithosphere of rifted basins (Stephenson, 1989). Moreover, as faults permanently weaken the crust of rifted basins, they are prone to tensional as well as compressional reactivation (Ziegler et al., 1995, 1998, 2001, 2002; Ziegler and Cloetingh, 2004). The reactivation potential of such discontinuities depends essentially on their orientation with respect to the prevailing stress field (Ziegler et al., 1995; Brun and Nalpas, 1996; Worum et al., 2004). In view of its rheological structure, the continental lithosphere can be regarded under certain conditions as a two-layered visco-elastic beam (Reston, 1990; Ter Voorde et al., 1998). The response of such a system to the build-up of extensional and compressional stresses depends on the thickness, strength and spacing of the two competent layers, on stress magnitudes and strain rates and the thermal regime (Zeyen et al., 1997). The heterogeneous nature of the lithosphere results in differential deformation depending on the distribution of intraplate stress levels that exceed the local strength (e.g., Brun, 2002; Handy and Brun, 2004). In this respect, the presence of crustal and mantle–lithospheric discontinuities, which can significantly reduce the strength of the lithosphere, play an important role. On the other hand, oceanic lithosphere behaves as a single-layer beam that is thinner than the competent parts of thick cratonic continental lithosphere. However, in view of the high strength of the mature oceanic lithosphere, its deformation requires considerably higher stress levels than the deformation of continental lithosphere (Cloetingh et al., 1989). This suggests a scenario whereby tectonic stresses responsible for deformation of continental lithosphere can be transmitted through the impervious oceanic lithosphere portions of the same plate (Ziegler et al., 1998, 2002). Regarding the localization of rift zones, the strength of the mechanically strong upper part of the mantle–lithosphere plays an important role (Ziegler and Cloetingh, 2004). Furthermore, lateral thickness heterogeneities of the lithosphere can play an important role in the localization of rifts (e.g. Oslo Graben: Pascal et al., 2002; Pascal and Cloetingh, 2009). At crustal scales , the width and deformation mode of evolving rifts depend on the thickness of the mechanically strong upper parts of the crust and on the availability of pre-existing crustal discontinuities, which can be tensionally reactivated under the prevailing stress field. Evidence for tensional reactivation of rifts, which have been abandoned millions of years ago, suggests that crustal-scale faults permanently weaken the lithosphere to the degree that rifts are prone to tensional and compressional reactivation (Ziegler et al., 1995, 2001, 2002). Rifted basins are marked by a relatively low crustal strength throughout their syn- and post-rift evolution.

By contrast, the strength of the mantle–lithosphere is strongly reduced during rifting, followed by a steady increase due to post-rift cooling, ultimately leading to a configuration in which a strong basin is flanked by weaker margins (see Cloetingh et al., 2003a). Models adopting zero strength for the continental mantle (e.g. Jackson, 2002; see also Watts and Burov, 2003) predict ongoing deformation in the central region of rifted basins, which in this case are the weakest part of the basin system. These findings are, however, incompatible with observations (see Cloetingh et al., 2003a; Cloetingh and van Wees, 2005). Intraplate stresses (Cloetingh and Burov, 1996), fluids and shear zones (Handy and Brun, 2004) may further reduce the actual strength of the lithosphere, but they do not affect the first order patterns of the inferred temporal and spatial evolution of lithospheric strength in the European foreland.

4.2. Model setup

Drawing on the Moho map of Europe of Dèzes and Ziegler (2004), on constraints on the thermal lithospheric structure from heat flow

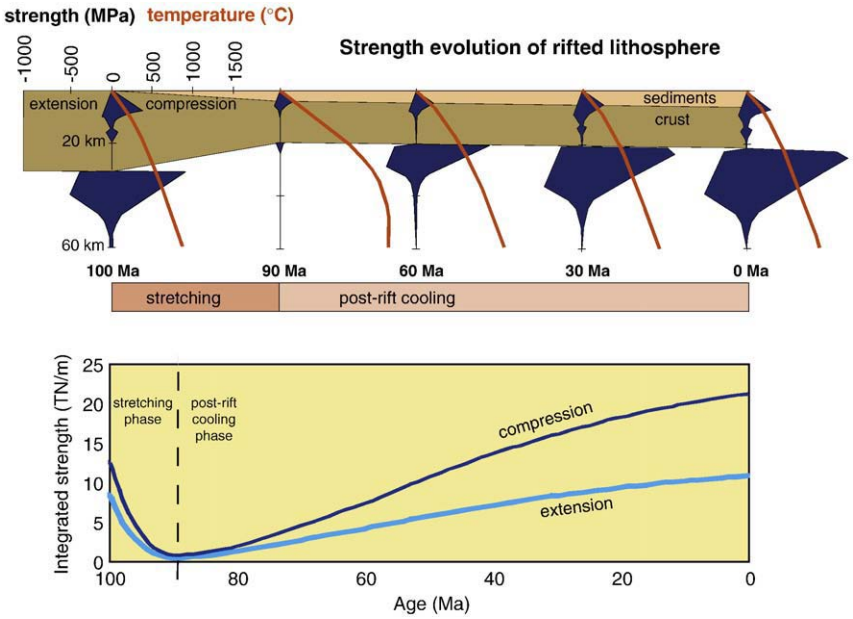

Fig. 22. Depth-dependent rheological model (upper panel) and integrated strength evolution (lower panel) for the evolution of a rifted upper plate passive margin (after Ziegler et al., 1998, their model). Area of the strength envelope (upper panel) gives intraplate force (Integrated strength, lower panel) necessary to obtain lithospheric deformation. Integrated strength values for extensional deformation are considerably less than for compression. Initially integrated strength decreases during stretching, but increases considerably ca. 50 Ma after stretching.

studies and estimates of the lithospheric thickness from seismological studies (Plomerová et al., 2002), Cloetingh et al. (2005) constructed a 3-dimensional strength cube for the lithosphere of a large part of Europe. The strength model is based on a 3D multi-layer compositional model (Table 1) including one upper mantle layer, two to three crustal layers and a sedimentary cover layer (Fig. 20) (Hardebol et al., 2003). The temperature structure of the lithosphere below Europe inferred from seismic tomography (Goes et al., 2000a,b) has only limited resolution in the mechanically strong part of the lithosphere. Therefore, in this study the temperatures in the lithosphere were calculated analytically, using Fourier's law for heat conduction, taking surface heat flow as boundary constraint (Fig. 2). Thermal rock properties (listed in Table 1) were taken from Cloetingh and Burov (1996), whereas the thermal boundary conditions were extracted from Babuška and Plomerová (1992) and Plomerová et al. (2002), or, where available, from higher quality regional or local studies. A comparison of the calculated thermal cube with temperature structures inferred from seismic tomography studies of upper mantle below Europe (Goes et al., 2000a,b) shows a first order overall agreement at depths corresponding to the lithosphere–asthenosphere boundary, as further discussed below.

We estimate the total lithospheric strength (σ_L) through a vertical integration of the yield strength envelope (YSEs):

$$\sigma_L = \int_0^h (\sigma_1 - \sigma_3) \cdot dz$$

where h is the thickness of the lithosphere. and σ_1 and σ_3 are the minimum and maximum principal stress, Either σ_1 (compression) or σ_3 (extension) is constrained by the overburden pressure whereas the other is determined from rheological models assessing the depth dependent stress difference required for brittle or ductile deformation, whichever is dominant. One of the major experimental rheology laws used for construction of YSEs is the Byerlee's law of brittle failure (Byerlee, 1978). The Byerlee's law demonstrates that the brittle strength is a function of pressure and depth independent of rock type. On the other hand, the ductile creep strength strongly depends on the rock type and temperature, as well as on the other specific conditions (e.g. grain size, macro and microstructure). In particular, the ductile behaviour non-linearly depends on strain rate and thus on the time scale of the deformation process. In this work we used a constant strain rate value of $10^{-16}\,s^{-1}$, which is a characteristic value for intraplate Europe.

In several areas of Europe the rheological structure of the lithosphere will deviate locally and/or regionally from our first order 3D model, and consequently will affect the estimated strength to some degree. For instance, local variations in crustal composition and crustal architecture (e.g. caused by faults offsetting parts of the crust) were not incorporated in our model. These features hardly affect the first order patterns of integrated strength, as crustal compositional differences have hardly any effect on frictional behaviour and mantle strength is generally far more dominant than crustal strength Furthermore, care should be taken not to over-interpret our modelling results in areas that have experienced rigorous crustal thickening or are characterized by complex crustal architecture (e.g. the orogenic zones of the Alps and Pyrenees and plate boundaries). Other second order regional/local processes may influence the strength estimates, such as the presence of water or serpentinite in the subcrustal lithosphere, both of which reduce the strength of the mantle (e.g. Bassi, 1995; Pérez-Gussinyé and Reston, 2001), or the removal of melts, which strengthens the mantle (van Wijk and Cloetingh, 2002). A depth-varying rheology such as employed in this study depends on several parameters, of which the most important are crustal thickness, composition and temperature. Spatial variations of these parameters across Europe are described by first order models, as explained above, thus neglecting local, second order scale deviations. In tectonically active areas, such as the Alps, the strain rate might be higher than the adopted default value of $10^{-16}\,s^{-1}$. Further it is likely that local deformation mechanisms are better described by higher strain rates, such as, for instance, in the ECRIS areas. In these tectonically active areas, our strength predictions may underestimate the true strength of the lithosphere. However, this assumption affects the results only marginally.

Summarizing, we want to emphasize that the 3D strength cube for the European intraplate lithosphere at its present state, as given in this paper, is based on large-scale variations in the geometry, composition and temperature of the lithosphere. Thus, interpretations and conclusions reflect only variations in bulk (integrated) strength across Europe.

Any interpretation of the estimated strength has to be first order and preferably qualitative — comparing different parts of intraplate Europe in terms of being relatively (much) stronger or weaker.

4.3. Lithospheric strength maps for intraplate Europe

Figs. 23 and 24 show the integrated compressional strength of the entire lithosphere of Western and Central Europe. As evident from Figs. 23 and 24, Europe's lithosphere is characterized by major lateral mechanical strength variations, with a pronounced contrast between the strong lithosphere of the East-European Platform east of the Teisseyre–Tornquist line and the relatively weak lithosphere of Western Europe. A clear strength contrast occurs also at the transition from strong oceanic lithosphere to the relatively weak continental lithosphere of Western Europe. Within the Alpine foreland, a pronounced northwest — southeast trending weak zone is evident, which coincides with the Mesozoic Sole Pit and West Netherlands Basins, the Cenozoic Rhine Rift System and the southwestern margin of the Bohemian Massif. Furthermore, a broad zone of weak lithosphere characterizes the Massif Central and surrounding areas, as well as the Alps. Higher-strength zones are associated with the central parts of the North German Basin, the British Isles and parts of the Armorican and Bohemian Massifs. The presence of thickened crust in the area of the Teisseyre–Tornquist suture zone gives rise to a pronounced mechanical weakening of the crustal parts of the lithosphere, whereas the mantle–lithosphere retains a moderate strength. Whereas the lithosphere of Fennoscandia is characterized by relatively high strengths, the North Sea rift system corresponds to a zone of weakened lithosphere. A pronounced strength contrast is evident between the strong Adriatic indenter and the weak Pannonian Basin, the Apennines and the Alps. The lateral strength variations of Europe's intraplate lithosphere are primarily caused by variations in the mechanical strength of the mantle–lithosphere (MSML) (Cloetingh et al., 2005). The variations in MSML are primarily related to variations in the thermal structure of the lithosphere, reflecting upper mantle thermal perturbations imaged by seismic tomography (e.g. Bijwaard and Spakman, 2000; Koulakov et al., 2009), with lateral changes in crustal thickness playing a secondary role, apart from Alpine domains that are characterized by deep crustal roots. For instance, the strong lithosphere of the East-European Platform, the Bohemian Massif, the London–Brabant Massif, and the Fennoscandian Shield can be explained by the presence of old, cold lithosphere, whereas the European Cenozoic Rift System coincides with a major axis of weakened lithosphere within the Northwest European Platform. Similarly, weakening of the lithosphere of southern France can be attributed to the presence of a tomographically imaged plume rising up under the Massif Central (Granet et al., 1995; Wilson and Patterson, 2001).

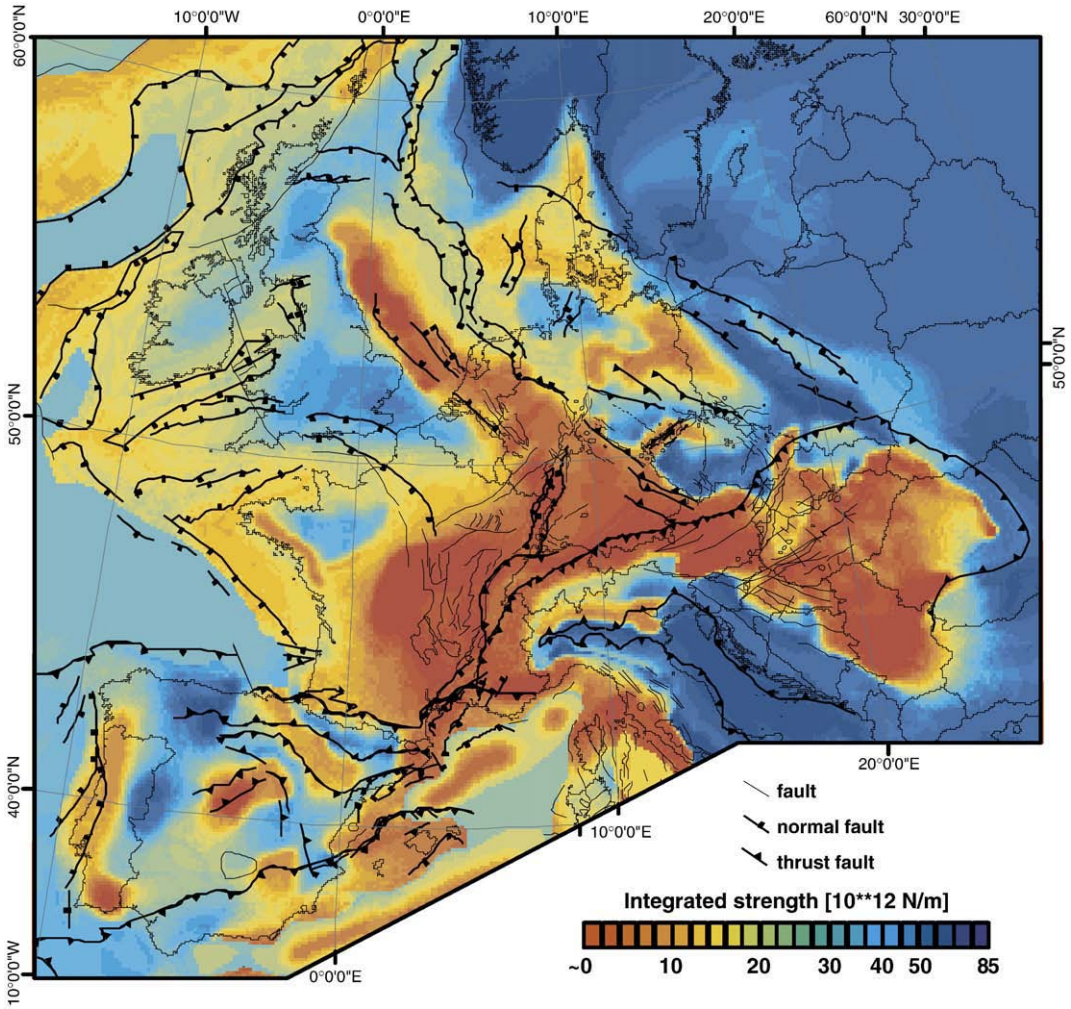

Fig. 23. Integrated lithosphere strength maps for intraplate Europe. Adopted composition for upper crust, lower crust and mantle is based on a wet quartzite, diorite and dry olivine composition, respectively. Rheological rock parameters are based on Carter and Tsenn (1987). The adopted bulk strain-rate is 10^{-16} s^{-1}, compatible with constraints from GPS measurements (see text). Contours represent integrated strength in compression for total lithosphere. The main structural features of Europe are superimposed on the strength maps (after Ziegler, 1988; Dèzes et al., 2004) (From Cloetingh et al., 2005).

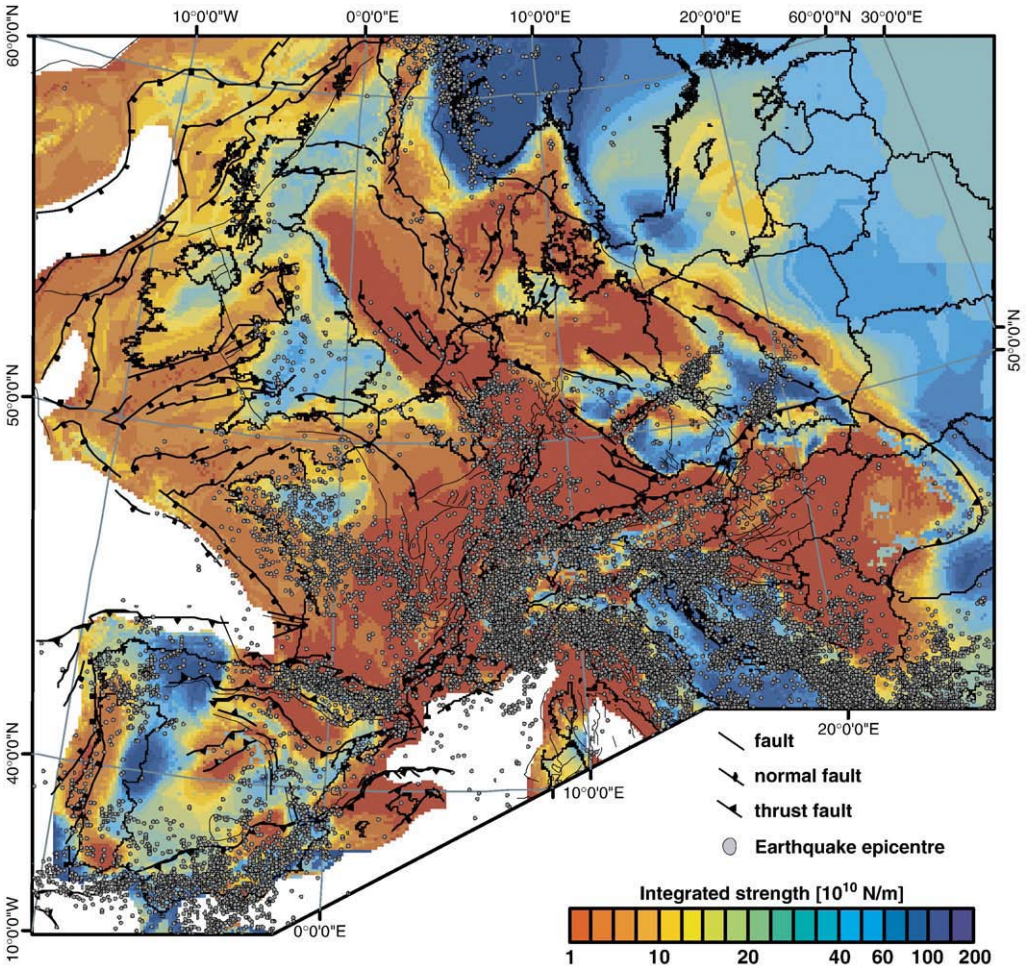

Fig. 24. Spatial comparison of crustal seismicity and integrated crustal strength. Earthquake epicentres from the NEIC data centre (NEIC, 2004), queried for magnitude >2 and focal depths <35 km (after Cloetingh et al., 2006).

Increased seismic activity is associated with the ECRIS (Fig. 24), the Armorican shear zone and the Massif Central, as well as with the Eger Graben. This cannot be directly attributed to the activity of mantle plumes impinging to the attenuated lithosphere of the Massif Central, the Rhenish Massif and the Bohemian Massif (Wilson and Patterson, 2001) but instead to the reactivation of Cenozoic and older crustal scale faults under the present compressional stress field of the Alpine foreland (Fig. 23). On a much broader scale, seismicity (Fig. 24; Grünthal et al., 1999) and stress indicator data (Müller et al., 1992; Tesauro et al., 2005, see also Gölke and Coblentz, 1996) demonstrate that active compressional deformation continues in the Alpine foreland, also outside the different segments of ECRIS. Zones of concentrated seismic activity correspond to areas of crustal contrast between the Cenozoic rifts and their surrounding platform areas, as well as to areas of crustal contrast in the rifted northeastern Atlantic margins. In general, earthquakes are associated with pre-existing faults, such as those bounding the Bohemian Massif and transecting the Armorican Massif. The simultaneous occurrence of thrust faulting, normal faulting and strike slip faulting mechanisms in the Alpine foreland supports a stress distribution dominated by heterogeneous crustal structures, including weak zones therein (Handy and Brun, 2004). For regions outside the ECRIS, Cloetingh and van Wees (2005) have shown that impingement of mantle plumes has caused a Late Cenozoic strength inversion facilitating intraplate reactivation of major fault zones bordering Paleozoic massif areas, instead of North Sea Basin inversion which abated in Miocene times.

4.4. Strength transects of the Rhine Rift System and adjacent segments of ECRIS

Examining the spatial lithospheric strength variations in the wider ECRIS area and its tectonic setting in the Alpine foreland in more detail, we examine below two regional rheological lithosphere-scale transects across the Massif Central and the Bresse graben, the Rhine Rift System and its flanks (Fig. 25). More sections are presented in Cloetingh et al. (2005).

4.4.1. Rheological transect along the Rhine Rift System (Amsterdam–Basel)

Fig. 25, section A, presents a NNW–SSE transect that extends from Amsterdam across the Ardennes, the Vosges–Black Forest Arch and ends at Basel. Along this transect important lateral variations in the strength of the crust but mainly at the level of the mantle–lithosphere, are evident. In the area of the Vosges–Black Forest Arch, the MSML is apparently rather thin (about 20 km). This arch, which involves a 25–28 km thick crust and about a 100 km thick lithosphere (Babuška and Plomerová, 1992), has an amplitude of 2.5 km and in a N–S direction, a wavelength of 200 km. Its Mio-Pliocene development is attributed to lithospheric folding (Dèzes et al., 2004) that was accompanied by partial melting of the lithospheric thermal boundary layer and the upper asthenosphere, as evidenced by volcanic activity within and outside the Upper Rhine Graben spanning 18–7 Ma (Jung, 1999). However, there is no evidence for thermal thinning of the

lithosphere (Achauer and Masson, 2002). Towards the Rhenish Massif the thickness of the MSML increases to about 40 km. Beneath the Ardennes, which flank the volcanic fields of the Eifel, plume-related thermal weakening of the MSML and the lower crust is evident (see also Fig. 12). Further northward, the thickness of MSML increases and reaches a maximum of 50 km at the transition to the North Sea Basin near Amsterdam where the thermal thickness of the lithosphere is of the order of 120–150 km (Goes et al., 2000a,b).

4.4.2. Rheological transect through the triple junction of the Upper and Lower Rhine and Hessian grabens

Fig. 25, section D, presents a transect that extends from the Paris Basin across the triple junction of the Upper and Lower Rhine and the Hessian grabens near Frankfurt into the area of the Eger Graben on the Bohemian Massif. The thermal thickness of the lithosphere decreases from 120 km to 150 km under the Paris Basin to 50–60 km beneath the Rhenish Massif (Babuška and Plomerová, 1992; Prodehl et al., 1995) and reaches about 80 km beneath the Eger Graben (Babuška and Plomerová, 2001). Thinning of the lithosphere beneath the area of the Rhenish triple junction is attributed to plume-related thermal thinning of the mantle lithosphere, with lithospheric extension playing a subordinate role (Dèzes et al., 2004). This transect displays very prominent lateral variations in the thickness of the MSML, but also in lower and upper crustal strength. The base of the MSML rises abruptly from about 60 km beneath the eastern part of the Paris Basin to about 30 km in the area of the Rhenish triple junction and gradually descends eastward towards the Bohemian Massif to about 70 km. In the area of the Eger Graben our model shows rapid and major lateral variations in MSML thickness. A strong reduction in strength of crustal and mantle–lithospheric layers in the area of the Rhenish triple junction is attributed to the presence of finger shaped upper mantle plumes rising up to the base of the lithosphere (Ritter et al., 2001). It should be noted that in this area the zones of upper mantle and lower and upper crustal weakening closely coincide, thus forming vertical cylindrical structures.

4.5. Effective elastic thickness (EET), regional gravity and seismic strain rates

The 3D strength distribution can be used to compute the effective elastic plate thickness (EET) of the European lithosphere. The EET, subsequently, can be compared with various independent parameters that characterize lithosphere deformation and rigidity, such as regional gravity anomalies and seismic and geodetic strain rates, to provide new insights into the localization of intraplate deformation in Europe (Tesauro et al., 2007).

4.5.1. Effective elastic thickness of the European lithosphere

The calculated 3D strength distribution can be used to quantify spatial variations in effective elastic plate thickness of the European lithosphere. Burov and Diament (1995) proposed a unified model of the lithosphere that relates EET with thermal age, crustal thickness and flexural curvature. EET of the lithosphere depends on three main parameters: (1) thermal state of the lithosphere; (2) thickness and proportions of the mechanically competent crust–mantle interface (decoupling crust and mantle); and (3) the local curvature of the plate, which depends on the rheological structure and distribution of the external load applied to the plate (Burov and Diament, 1995). Rheological properties of the continental upper crust are primarily controlled by content of quartz (Brace and Kohlstedt, 1980), while mechanical behaviour of the lower and middle crust may be conditioned by a variety of lithologies such as quartz, diorite, diabase or plagioclase. If the crust is thick (>35 km), the lower crustal temperatures could be high enough to reduce the creep strength of the rocks in the vicinity of the Moho (Burov and Diament, 1995). By contrast, when the stress is below the yield limits, the lower crust and mantle are mechanically coupled and the lithosphere behaves like a single plate. In this case the EET value gradually depends on temperature and should correspond to an isotherm of 700–750 °C. However, only few estimates for old and cold lithosphere plates satisfy this condition. On the other hand, the crust–mantle decoupling results in a drastic reduction of the total effective strength of the lithosphere and of the EET (Burov and Diament, 1995).

According to Burov and Diament (1995), the EET of the plate consisting of n detached layers is equal to:

$$EET^n = \left(\sum_{i=1}^{n} \Delta h_i^3\right)^{1/3} \tag{3}$$

where $\Delta h_i = y_i^+ - y_i^-$ is the effective elastic thickness of the layer i. For a coupled rheology, the crust and mantle are mechanically "welded" together, and the upper EET estimate is simply:

$$EET^n = \left(\sum_{i=1}^{n} \Delta h_i\right) \tag{4}$$

Local studies of EET in Europe (e.g. Poudjom Djomani et al., 1999) have demonstrated that the largest changes in EET occur at the sutures that separate different provinces, characterized by major changes in lithospheric strength. The EET values are generally consistent with other physical properties of the lithosphere: high EET regions correlate with areas of large thermal thickness (as derived from heat flow data) and fast seismic S-wave velocities and vice versa. In addition, a close correlation exists between EET and seismicity: high-and low-EET regions are characterized by sparse and abundant seismicity, respectively.

Eqs. (3) and (4) are used to calculate the EET distribution (Tesauro et al., 2007). When strength decreases below 20 MPa, which is the case at the transition zones from the upper to the lower crust and from the lower crust to the upper mantle, the layers are considered detached, while they are welded together in the opposite case. The results are displayed in Fig. 26a–c. Predominantly high EET values (up to 80 km) are found for the Eastern European Platform (EEP) where the upper and lower crustal layers are coupled. In the central part of Western Europe the lithosphere is more heterogeneous and characterized by a wide range of the EET values (5–80 km), with much lower average values for EET (<30 km) than in the EEP. The minimum values correspond to the Eifel, the Massif Central and the Balearic Rift, which are characterized by high thermal anomalies. Low EET values are also observed along the ECRIS, in the German Plain, in the Pannonian Basin, and in the basins of the Iberian Peninsula, where the upper and lower crust are decoupled (Fig. 26c) and the lithosphere mantle are weak. In contrast, high values of EET characterize the Iberian massif, the Apennines and the Bohemian Massif, where upper and lower crust are welded together (Fig. 26c). The EET distribution is generally in agreement with the results obtained by using cross-spectral analysis of gravity and topography data by Pérez-Gussinyé and Watts (2005). These authors have also shown that the strength of the old lithosphere in the EEP is much larger (usually with EET's>60 km) than that of much younger Central and Western Europe (EET<30 km).

The assumptions, which are used to calculate the strength distribution in the lithosphere, also affect the EET estimates. One of the main uncertainties could be due to not considering the effect of the horizontal regional stresses. It has been demonstrated that this parameter might have a strong effect on the EET (Cloetingh and Burov, 1996). Tectonic stresses of 200–500 MPa can decrease EET values of mid-age lithosphere (400 Ma) by 15–20% and of lithosphere younger than 200 Ma by 30%. Furthermore, horizontal stresses may facilitate weakening of the lower crust with subsequent crust–mantle decoupling.

4.5.2. Gravity model for the European lithosphere

Temperature variations within the lithosphere and upper mantle produce density variations reflected in the observed gravity field.

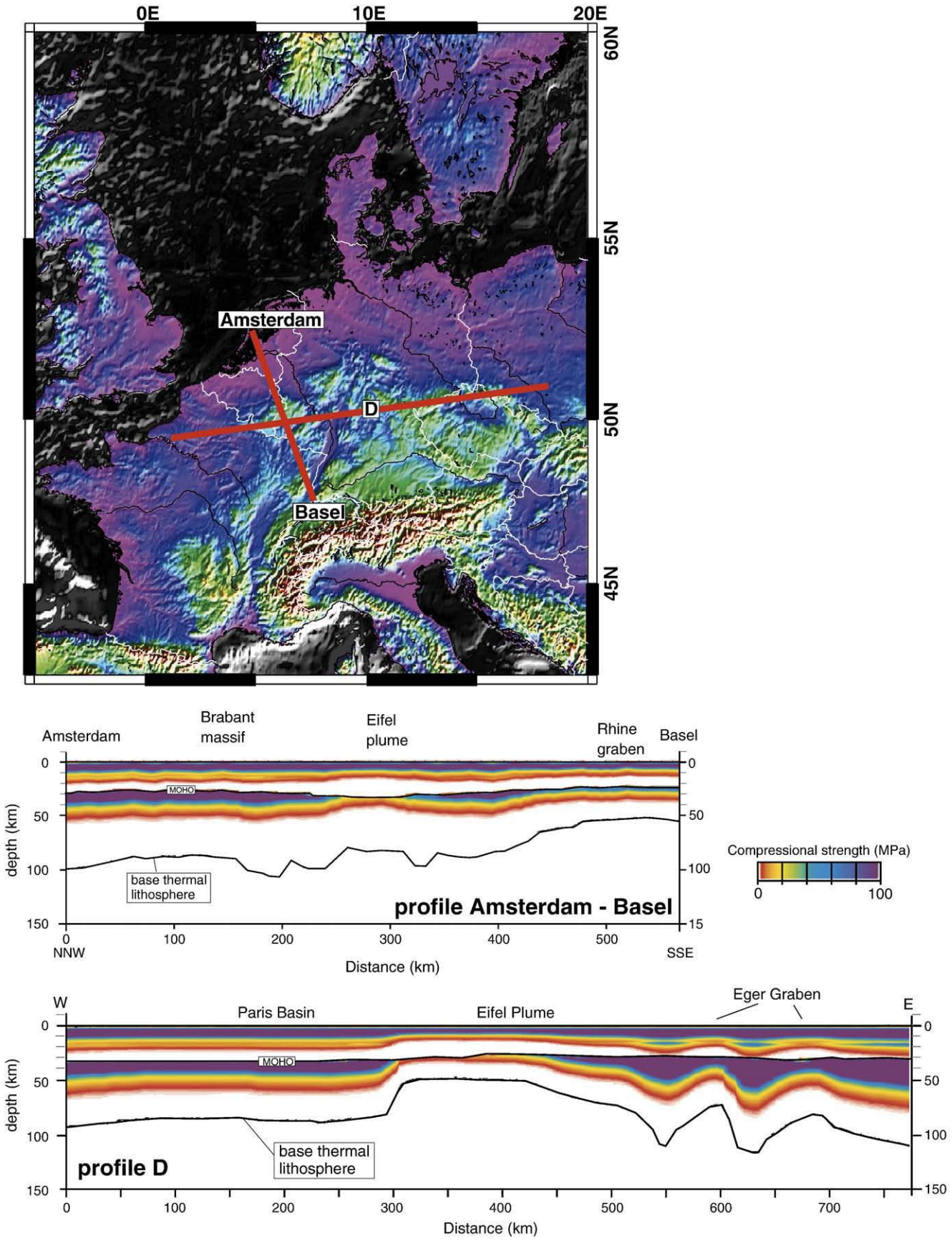

Fig. 25. Topographic map of the Alpine foreland, extracted from ETOPO-2. The red lines denote the location of the rheological cross sections. (bottom) Rheological cross-sections along the Rhine graben segments of ECRIS (Amsterdam-Basel) and east-west oriented along the Eifel and Rhine graben (section D). The lower boundary of the mechanically strong part of each intra-lithospheric layer is taken at 2 MPa, and coincides in the colour contouring with the transition from red to white. The base of the thermal lithosphere is taken at 1300 °C and is indicated by the solid black line (after Cloetingh et al., 2006).

Therefore, gravity modelling provides independent information for comparison with the strength maps presented in this paper. The main problem is that the observed field contains signatures of nearly all heterogeneities within a broad zone from each point. In order to extract the mantle component, the effect of crustal heterogeneities should be eliminated based on existing a-priori information. The residual gravity anomalies will then reflect the effect of mantle density variations including temperature anomalies and variations of the lithosphere thickness (e.g. Tesauro et al., 2007, 2008).

Despite the large body of gravity observations existing in Europe, a significant problem so far has been the creation of a homogeneous gravity model for this region. Existing national gravity surveys have often been performed based on different principles and with different corrections (e.g. terrain correction), which are not always specified. The new gravity model EIGEN-GL04C, which is based on CHAMP, GRACE and terrestrial data, has been recently constructed at GFZ Potsdam. The model is complete to degree/order 360 in terms of spherical harmonic coefficients and resolves features of about 55 km width in the geoid and gravity anomaly fields. A special band-limited combination method has been applied in order to preserve the high accuracy from the satellite data in the lower frequency band of the geopotential and to form a smooth transition to the high frequency information coming from the surface data. The difference with the old EGM96 model is up to about 30 mGal in Europe and it reaches values of 50 mGal in the southern margins of the Alpine fold belt (Reigber et al., 2006).

In order to derive residual mantle anomalies we have used as reference crustal models presented in previous studies (Kaban, 2001; Artemieva et al., 2006). Density inhomogeneities within the sedimentary layer and solid crust are estimated in different ways. For sediments we use generalized density–depth relationships based on geological data, well logs, seismic velocities and borehole-determined density-compaction relations. This approach has been successfully used in previous gravity modelling of sedimentary basins (e.g. Artemjev et al., 1994; Kaban, 2004). The density–depth relationships reflect specific characteristics of major sedimentary basins in Europe (Kaban, 2001).

To calculate the gravity effect of the solid crust we use data for Moho depth and crustal densities converted from seismic velocities. To this purpose, we have employed the Moho map from Kaban (2004), which is based on seismic data. The resolution is about $1^\circ \times 1^\circ$ for most of Europe, which is sufficient for gravity modelling since smaller features are not reflected in the surface gravity. Density variations within the solid crust have been computed from the same seismic data. The gravity field of the crust is calculated relative to an applying experimental velocity-to-density scaling factors horizontally homogeneous reference model. In this study, (Christensen and Mooney, 1995) a two-layer reference model with densities of 2.7 g cm^{-3} in the upper crust, 2.9 g cm^{-3} in the lower crust, and 3.35 g cm^{-3} in the mantle are used. The depth to the lower boundary is 35 km, coinciding with the average Moho depth within the region studied. The depth to the crustal density discontinuity (2.7/2.9 g cm^{-3}) is 14 km, giving an average crust density of 2.84 g cm^{-3}, which is consistent with worldwide data (Mooney et al., 1998). It is important to note that a choice of the reference model may affect only a constant level of the resulting gravity anomalies, which is not considered in this study. The calculation technique is described in detail in Kaban and Mooney (2001) and Kaban et al. (2004).

Residual mantle anomalies obtained after removing the crustal effect from the observed gravity field (Tesauro et al., 2007) are shown in Fig. 27a. Their variations are large and range from approximately −283 to +261 mGal. The amplitudes of the most prominent anomalies significantly exceed possible determination errors, which are conservatively estimated to be of the order of 25–50 mGal for most of intraplate Europe where coverage by seismic profiles is dense (Kaban and Schwintzer, 2001; Kaban et al., 2003). A pronounced large-scale difference (200 mGal on the average) is found between Eastern and Western Europe separated by the Teisseyre–Tornquist Zone (TTZ) (Fig. 27a). Western Europe is mainly characterized by pronounced negative anomalies, whereas generally positive anomalies are found all over Eastern Europe. Strong negative residual mantle anomalies suggest a presence of low-density masses within the upper mantle and provide an indirect evidence for high mantle temperatures in Western Europe. The transition from positive to negative residual gravity anomalies coincides with the TTZ, where an abrupt change of all geophysical parameters of the European lithosphere, in particularly of the thermal regime, is observed (Kaban, 2001; Artemieva et al., 2006).

Obtained differences between Eastern and Western Europe are generally in agreement with previous results (e.g. Kaban, 2001; Yegorova and Starostenko, 2002). In addition, distinct characteristics of smaller scale tectonic units obtained in the present study are resolved due to higher resolution of the initial crustal data. To emphasize these differences we have subtracted a long-wavelength component from the total mantle gravity field. In continental-wide and global studies, the mantle gravity anomalies can be clearly separated into two components depending on wavelength (e.g. Kaban, 2001). The long-wavelength component reflects large-scale structural heterogeneities of the lithosphere, probably related to its thermal regime. For a reliable estimation of the long-wavelength component we also incorporated data outside the region under study, from the most complete global database (Kaban et al., 2004). By subtracting the large-scale component from the total mantle field we obtain the "regional" field representing wavelengths less than 2000 km (Fig. 27b).

The regional mantle gravity anomalies correlate well with specific tectonic structures (Fig. 27b). A chain of the negative mantle anomalies depicts the areas of active neotectonics and recent back-arc extension in the Western Mediterranean (Tyrrhenian Sea and Valencia Trough–Balearic Basin the Gibraltar arc–Alboran Sea), the Pannonian basin, the German–Polish Basins, the North Sea, the Bay of Biscay and the Rhine Graben. Negative anomalies of smaller amplitude are found over the ECRIS and the Massif Central. These negative anomalies are likely of thermal origin. The high-temperature regime in these areas is possible controlled by upwelling of hot asthenosphere up to a depth of 30 km (Western Mediterranean Basin) to 60–80 km (North Sea, Rhine Graben, Pannonian Basin) (Babuška and Plomerová, 1993), which is confirmed by high values of the surface heat flow [up to 120 mW m^{-2} in the Pannonian Basin, (Lenkey, 1999)] and low P-and S-wave velocities (Spakman et al., 1993; Bijwaard et al., 1998; Piromallo and Morelli, 2003).

A very distinctive positive anomaly is located over the Adriatic Sea, extending with smaller amplitudes toward the Apennines and the Dinarides, as well as over the Calabrian Arc and the Ionian Sea (Fig. 27b). These positive anomalies support the notion of a cold and high velocity domain in the uppermost mantle. More specifically, the anomalies over the Adriatic plate and the adjoining parts of the Apennines and Dinarides probably reveal an increase of lithosphere thickness. At the same time, the anomalies over the Calabrian Arc and the Ionian Sea are related to the presence of a cold African slab subducting under the European plate, as imaged by tomography data (Piromallo and Morelli, 2003). A weaker positive anomaly is observed over the Carpathians, possibly related to the presence of thick lithosphere in this area. Two other smaller positive anomalies are found over the Aquitaine Basin, extending over the Pyrenees and over the western part of the Bay of Biscay. The last one could be related to an old and cold lithosphere block in the upper mantle down to a depth of 140 km (Yegorova and Starostenko, 2002). A gradual change from positive to negative anomalies is observed from the centre of the Baltic Shield to the south and to the western coast of Norway (Fig. 27b), possibly related to a decrease in lithospheric thickness. However, the amplitude of these anomalies is small (less than ±50 mGal), demonstrating compensation of the effects of temperature and

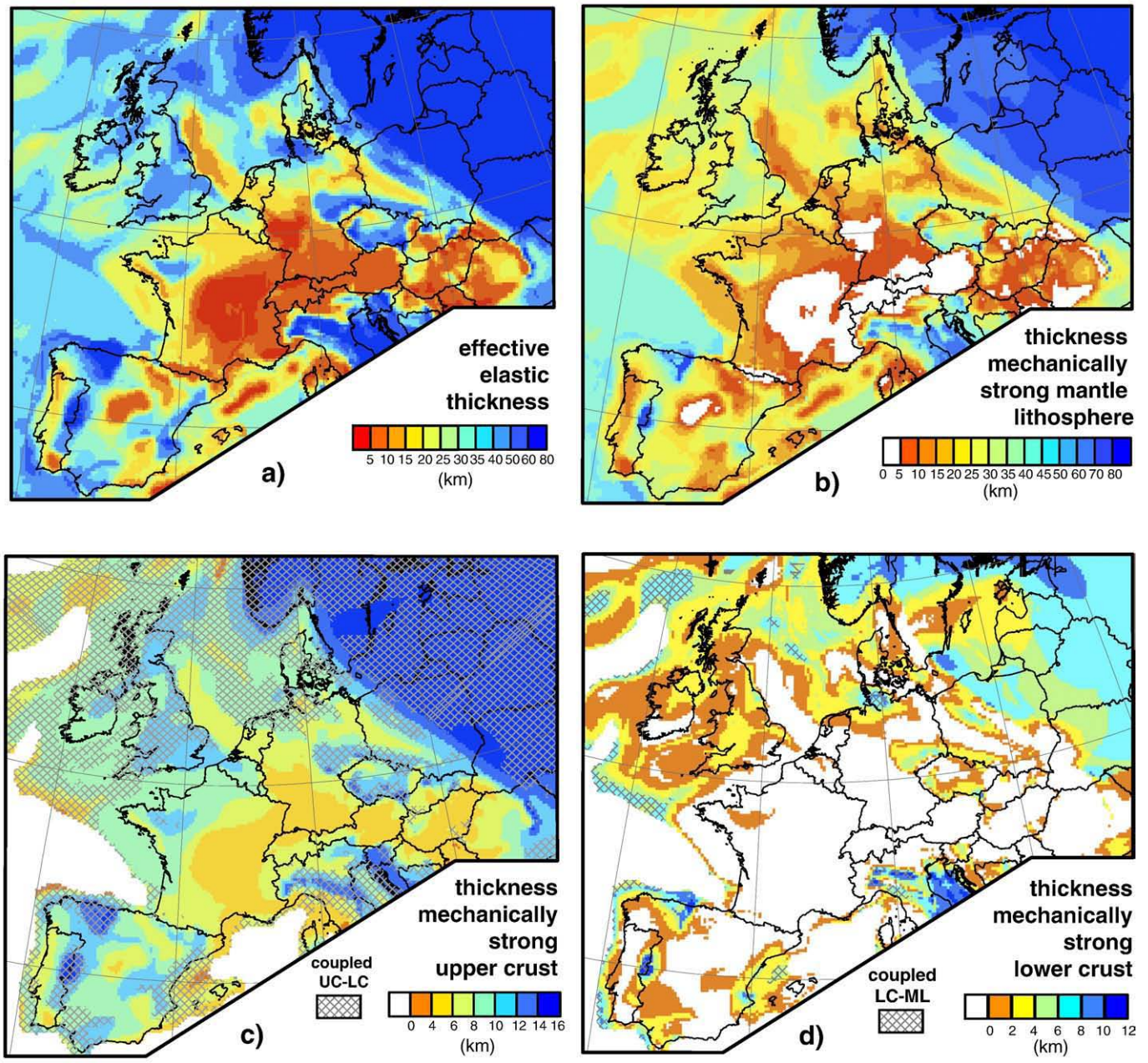

Fig. 26. (a) EET of the European lithosphere calculated using the Burov and Diament (1995) approach; (b) thickness of the mechanically strong part of the mantle lithosphere; (c) thickness of the mechanically strong part of the upper crust; (d) thickness of the mechanically strong lower crust. Hatching indicates the areas where upper and lower crusts are mechanically coupled. See text for further explanations (after Hardebol, 2010).

compositional anomalies (Kaban et al., 2003). We observe a gradual change of the mantle gravity anomalies in the centre of the Tyrrhenian Basin: from negative (in the Provençal Basin) to positive (in the Algerian Basin) values (Fig. 27b). A strong negative anomaly up to −250 mGal is inferred in the same area in previous studies (e.g. Yegorova and Starostenko, 2002). The origin of this discrepancy warrants further investigations.

4.5.3. Seismic and geodetic strain rate distribution

Most of the earthquake activity in Central and Western Europe (Fig. 24) is localized in the Alpine chain, the ECRIS and the zone between the Armorican Massif and the Massif Central (Fig. 24). Zones of concentrated seismic activity correspond to areas of strong differences in crustal properties between Cenozoic rifts and the surrounding platforms, as well as to rifted Atlantic margins. In general, earthquakes are associated with pre-existing faults, such as those bounding the Bohemian Massif and crossing the Armorican Massif, which are reactivated by present compressional stress in the Alpine foreland. The highest seismicity is observed at the Alps–Dinarides transition in North Italy and Slovenia, indicating significant present-day deformations in the vicinity of the margins of Adria. At the same time, seismic activity is moderate and diffuse in the Pannonian basin compared to the peripheral areas (e.g. Bada et al., 2007a,b).

Tesauro et al. (2007) used seismic data to evaluate the amplitude of the seismic strain rates in the central part of Western Europe applying the following equation (Kostrov, 1974):

$$\dot{\varepsilon} = \frac{1}{2\mu VT}\sum M_0 \tag{5}$$

where μ is the shear modulus of the brittle crust, V the cell volume elastically deformed, T the time period of the earthquake record and

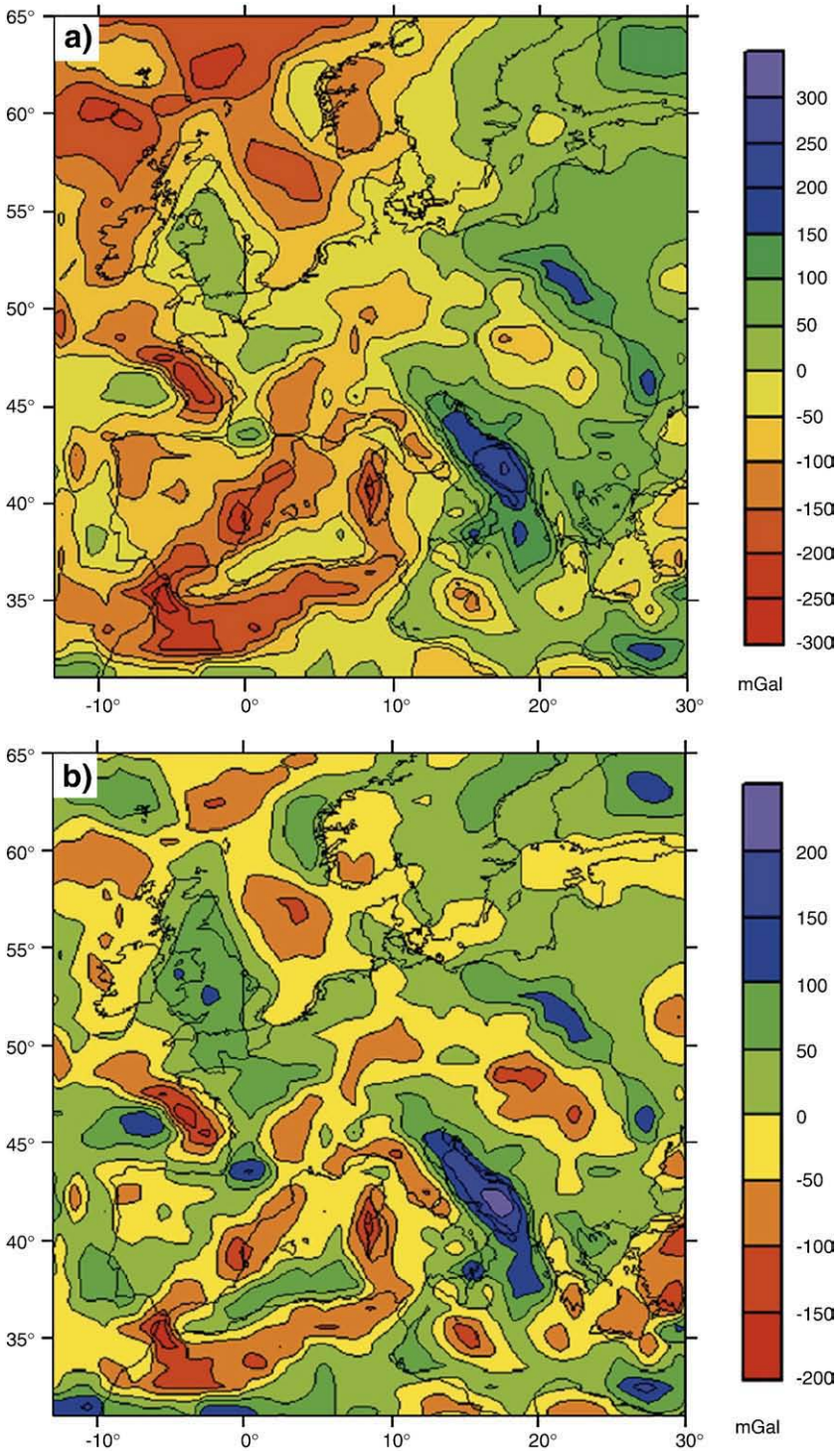

Fig. 27. Residual mantle anomalies of the gravity field obtained after removal of the crustal effect from the observed field. (a) Total anomaly; (b) Regional component ($\lambda < 2000$ km) of the residual mantle anomalies correlating with specific tectonic structures. See text for further details (after Tesauro et al., 2007).

M_0 the seismic moment. For more details on the parameters and basic assumptions required for Eq. (5) see Tesauro et al. (2006).

The estimated strain rates for the central part of Western Europe (43° N–54° N and 5° W–15° E) are displayed in Fig. 28. They show that about half of the central part of Western Europe is not seismically active, being characterized by strain rates less than 10^{-3} nstrain[1]/yr. These regions correspond mainly to the Aquitaine Basin, the Paris Basin and the North German Plain. Relatively low deformation rates, up to 1 nstrain/yr, are determined for the Massif Central, the Armorican Massif, the Lower Rhine Graben (LRG) and the North Sea. The highest values of seismic strain rates (up to 10 nstrain/yr) are detected in the central and northeastern part of Italy along the Slovenian border and in the convergence zone of the Adria block. The Alps are characterized by relatively high strain rates, up to 10 nstrain/yr, especially in the northern part of Italy and in Western Switzerland. Relatively high values of strain rates (up to 10 nstrain/yr) are detected also in the southern part of the Upper Rhine Graben (URG), in the

[1] "nstrain" = nano-strain. 1 nstrain/yr corresponds to a change of distance of 1 mm per 1000 km and year and is equivalent to 3.17×10^{-17}/s.

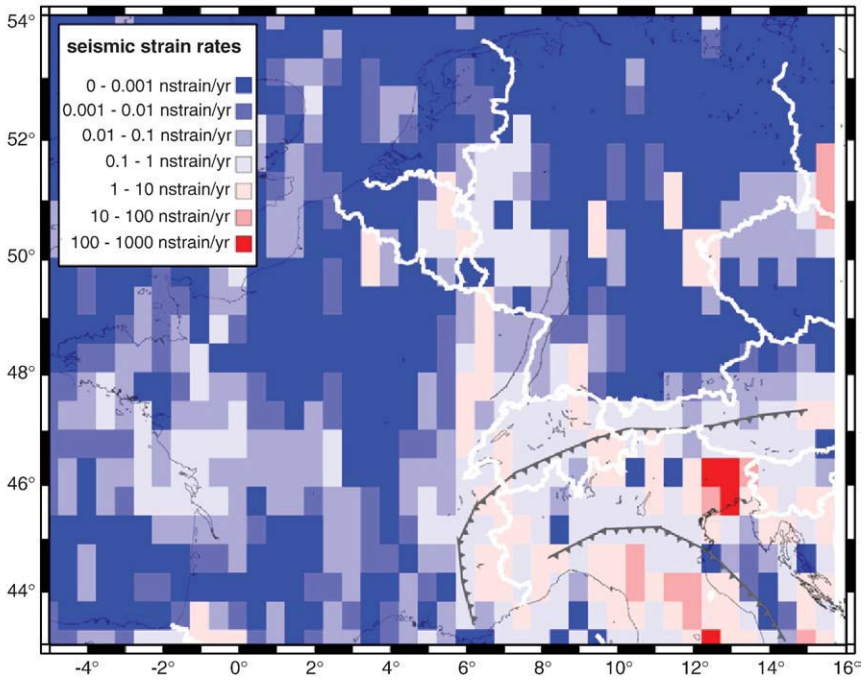

Fig. 28. Horizontal strain-rate distribution in Central Europe from GPS measurements Highest strain-rates occur in the Alps and Apennines. A N–S oriented corridor of elevated strain-rate clearly demonstrates ongoing tectonics in the European Cenozoic Rift System (ECRIS). The orientation and magnitude of GPS derived motions reveals that to the east of the corridor movement is relatively to the north, whereas to the west relatively to the west (after Tesauro et al., 2007).

Vosges, in the Jura Mountains, in the Rhenish Massif, and in the Bohemian Massif.

Furthermore, GPS results (Tesauro et al., 2005, 2006) have shown that central western Europe is characterized by small movements, with 2.4 mm/year relative to Eurasia, with a concentration of strain in the central part of the Alps and the Molasse Basin (up to 6.5 ± 2 nstrain/year). In general, we obtained a good agreement between the distribution of seismic and geodetic strain rates, despite the poorly constrained parameter value of the Kostrov estimate and the inhomogeneous distribution of GPS stations.

To conclude, significant spatial variations in lithospheric strength exist within the Central and Western European lithosphere, in contrast to a more uniform strong lithosphere of the East European Platform. These variations are consistent with differences in the density structure of the mantle lithosphere reflected in mantle gravity anomalies (Tesauro et al., 2007). Western Europe is mostly characterized by negative mantle gravity anomalies and thinning of the effective elastic thickness of the lithosphere (generally $\leq$20 km), whereas the opposite is true for Eastern Europe. Large differences exist also for specific tectonic units: e.g. a pronounced contrast in lithosphere properties is found between the strong Adriatic plate and the weak Pannonian Basin area, as well as between the Baltic Shield and the North Sea rift system. Tesauro et al. (2007) show that the European Cenozoic Rift System (ECRIS), which is characterized by low EET values and negative mantle gravity anomalies, localizes neotectonic deformation manifested by relatively high geodetic and seismic strain rates.

4.6. Implications for geothermal exploration

Lithosphere strength maps show a first order correspondence to active intraplate deformation and provides a framework to understand the distribution and localization of stress as a function of spatial and vertical variation in lithospheric strength. The lithosphere strength displays considerable spatial variations, within many areas marked by a mechanical decoupling of crust and subcrustal lithosphere. In a regime of fairly uniform intraplate stresses resulting from plate boundary forces, relatively weak areas in this framework, are expected to lead to stress concentration towards critical stress levels. Actually zones with a weak crustal rheology appear to correspond to areas of elevated natural seismicity. Consequently, identification of weak crustal rheology aids to identify the extend of critically stressed regions, complementary to stress and natural seismicity data.

This appears to be particularly relevant for tectonic settings such as the European Cenozoic rift system (ECRIS) and the Pannonian basin, marked by relatively low crustal strength in an area with a much larger extent than its individual sub basins.

5. Crustal stress and strain controls in Neotectonic extension in the ECRIS: natural laboratory studies

In the previous sections we have shown that large parts of the ECRIS and back-arc basins such as the Pannonian Basin are characterized by mechanical decoupling of the crust and underlying mantle lithosphere, at large scales. Consequently, for regional and site scale assessment of the interaction of stress and basement rheology for EGS exploration it suffices assessing this interaction in the upper crust, using appropriate thermo-mechanical boundary conditions from deeper parts of the lithosphere (cf section 3).

Following this approach, neotectonically active structures in the ECRIS have been intensively studied in the last decade by various European (e.g. ENTEC) and national research initiatives focused on geohazard assessment (e.g. Cloetingh et al., 2005; Cloetingh et al., 2006).

Multidisciplinary research on selected natural laboratories in the ECRIS have provided key insights in the relative importance of deep crustal scale faults (>5 km) controlling neotectonic deformation, stress orientation and magnitude, and showing a close relationship with deformation partitioning in basins and seismicity. These controls are relevant for geothermal exploration of active tectonic fabric at intermediate depth ($\leq$5 km), to identify which fault or fracture zones, as function of fault/fracture rheology and stress, are proximal to (shear) failure stresses, facilitating hydraulic fracturing (e.g. Zoback,

2007). Furthermore active fault zones appear to be marked by natural permeability on geological timescales (e.g. Gartrell et al., 2006), which may retain permeable on timescales of geothermal production. Below we demonstrate key insights for two subareas in the ECRIS system located in the Lower Rhine Graben (LRG) and Upper Rhine Graben (URG) (Fig. 12).

5.1. Lower Rhine Graben

The Lower Rhine Graben (LRG), which forms the northwestern segment of the European Cenozoic Rift System, extends from the margins of the Rhenish Massif to the Dutch North Sea coast (Fig. 29). Its main structural elements are the Erft half graben in the German Lower Rhine Embayment and the Roer Valley Rift System (RVRS) of the Netherlands (Fig. 30).

The late Oligocene RVRS is superimposed on the older West Netherlands basin that is characterized by a complex evolution involving several Mesozoic and Paleogene extensional and inversion phases (Zijerveld et al., 1992; Geluk et al., 1994; Dirkzwager et al., 2000; van Balen et al., 2005). During these phases, late Palaeozoic faults were repeatedly reactivated (Ziegler, 1990, 1992; Dirkzwager et al., 2000; Houtgast et al., 2002).

As shown in Fig. 30a, the RVRS structurally consists from SW to NE of the Campine Block, the Roer Valley Graben (RVG) and the Peel Block (Dirkzwager et al., 2000). Subsidence of the RVG was controlled by multi-stage evolution of the main bounding fault zones, including the Peel Boundary fault zone (PBFZ), the Feldbiss Fault Zone (FFZ), the Veldhoven Fault and the Rijen Fault. Remarkably, the subsidence of the basin is almost balanced by the offsets along these fault zones (Houtgast and van Balen 2000; Michon et al., 2003). The Oligocene and younger syn-rift sediments attain a thickness of 1700 m. In its central, deepest parts, the RVG has the geometry of a half-graben that is bounded in the NE by the Peel Boundary fault zone (Fig. 30b). Towards the NW and SE the RVG shallows progressively. In its SE parts, the RVG has the geometry of a symmetric graben, with the bounding fault zones having about equal throws. In the southeastern continuation of the RVRS, the main extension is accommodated in the asymmetric Erft Graben that is, however, not the direct continuation of the RVG but corresponds to a separate structural element (Geluk et al., 1994; Klett et al., 2002; Michon et al., 2003).

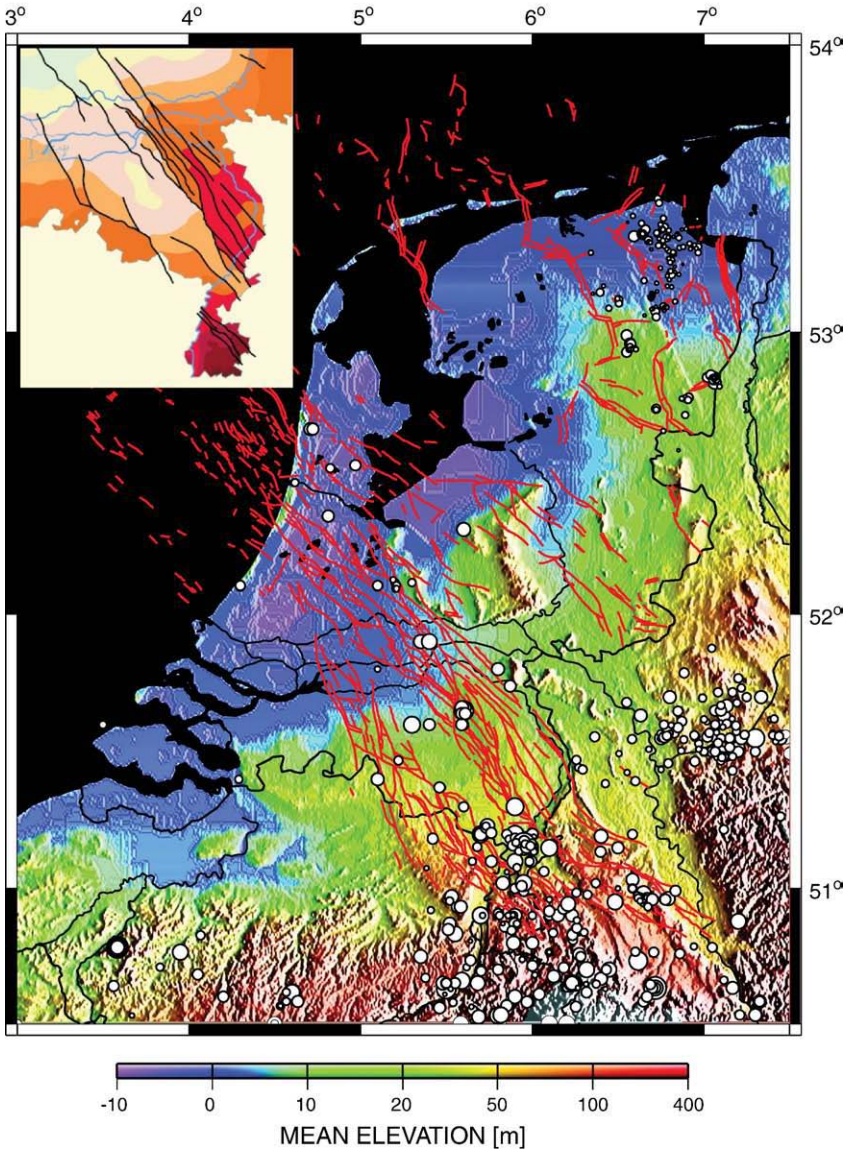

Fig. 29. Topography of the Netherlands in a colour contoured relief map. Earthquakes epicentres, from the ORFEUS data centre, are shown in white, size indicates magnitude. Red lines are reactivated Mesozoic faults in the subsurface. Inset shows Quaternary thickness map (range 0–400 m) and active faults in the south-eastern part of Netherlands (De Mulder et al., 2003).

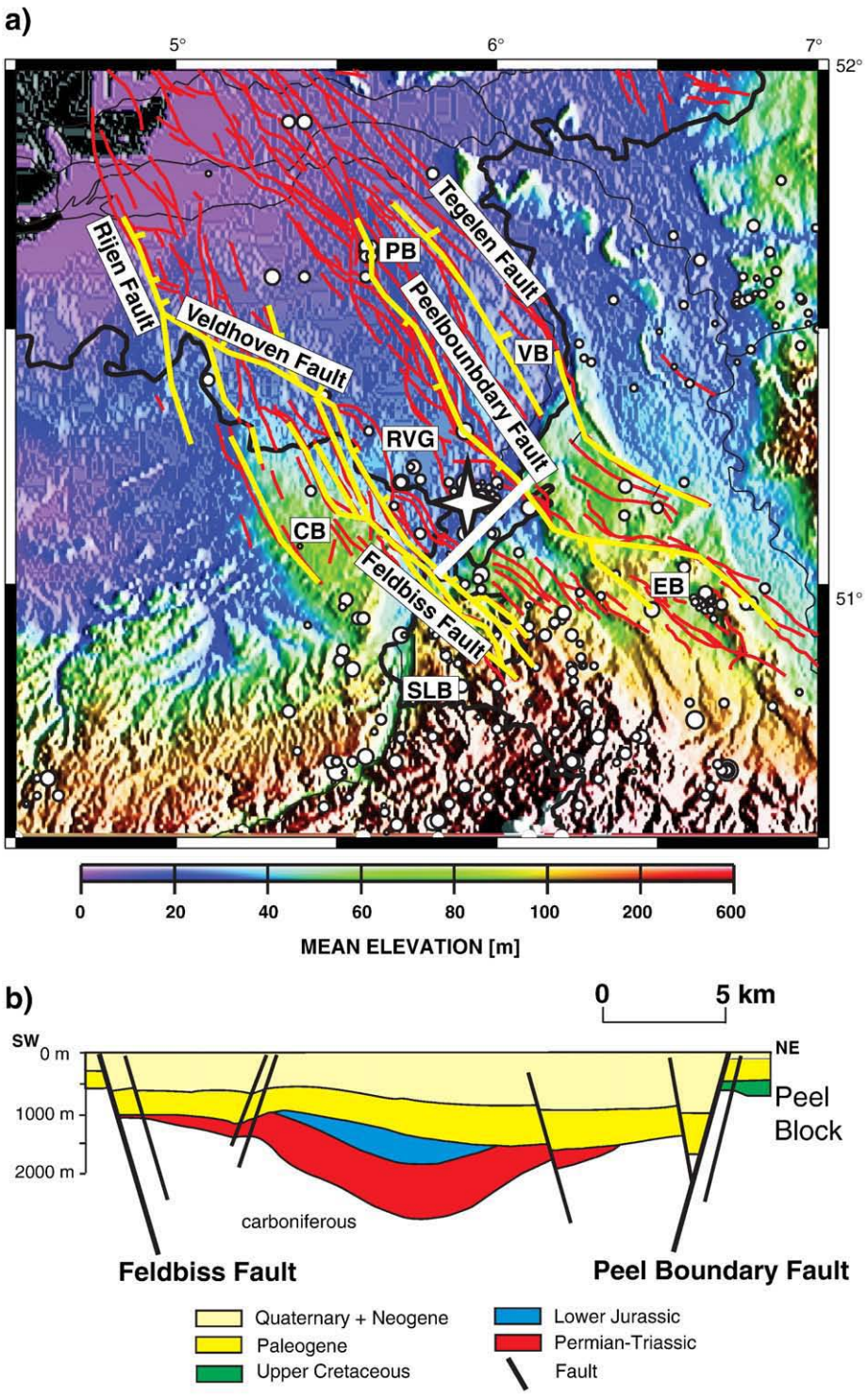

Fig. 30. (a). Topography of the Roer Valley Rift System (RVRS) area in colour contoured relief map. Data are from the GTOPO30 global data set. Earthquake epicentres are from the ORFEUS data centre, and are shown as white dots, with dot size indicating magnitude. White star gives the location of the 1992 $M_L = 5.8$ Roermond earthquake. Red lines depict Base Tertiary faults, yellow lines depict Base Miocene faults. Faults are digitized from Geluk et al. (1994) and De Mulder et al. (2003). Main tectonic structures: RVG = Roer Valley Graben; PB = Peel Block; VB = Venlo Block; CB = Campine Block; EB = Erft Block; SLB = South Limburg Block; PBF = Peel Boundary Fault; FF = Feldbiss Fault; (b) Cross section through the Roer Valley Rift System (after Geluk et al., 1994). Location of profile is indicated by the white line in Fig. 30a.

The RVRS started to subside during the late Oligocene under a northerly-directed compressional stress regime, controlling WNW–ESE directed oblique extension across the evolving graben at the transition to the Miocene, the compressional stress regime permutated to a NW-directed one, causing nearly orthogonal NE–SW extension across the RVRS). This stress regime persisted until the present, although its magnitude apparently increased during the Pliocene, as evidenced by a subsidence acceleration of the RVRS. In the recent past, fault movements, some of which may have been accompanied by earthquakes, gave rise to the development of distinct fault-scarps. Some of these have been investigated in the framework of paleoseismologic research (Camelbeeck and Meghraoui, 1998; Camelbeeck et al., 2001; Houtgast et al., 2002, 2003, 2005). At present, the RVRS is seismotectonically active, and thus presents a zone of

increased seismic hazard, as highlighted by the 1992 Roermond earthquake ($M_L = 5.8$) (Fig. 30a, Plenefisch and Bonjer, 1997; van Eck and Davenport, 1994; Hinzen, 2003).

5.1.1. Earthquake activity and fault rheology in the LRG

Since the early studies of Ahorner (1983) on seismicity and faulting in the LRG much progress has been made owing to a multidisciplinary approach that integrates German, Belgian and Dutch studies on seismicity (EUCOR-URGENT; Dost and Haak, 2007; Camelbeeck et al., 1994) and high resolution digital elevation models (Cloetingh and Cornu, 2005) with the results of trenching (Meghraoui et al., 2000; Houtgast et al., 2003), high-resolution reflection-seismic data recorded on rivers (e.g. Cloetingh, 2000; Dèzes et al., 2004) and detailed analyses of industrial reflection-seismic and well data (Geluk et al., 1994; De Mulder et al., 2003), as well as geomechanical modelling of fault reactivation (e.g. Dirkzwager et al., 2000; Worum et al., 2004). Geomechanical modelling results (Fig. 31) demonstrate that (border) faults are characterized by a relative mechanical weakness compared to the default rheology of the basin, thus facilitating localization of strain and seismicity on the major faults. These results support inferences of tectonic studies demonstrating that pre-existing fault or fracture zones are marked–on geological timescales over 100 My–by reduced strength relative to intact rock (e.g. Van Wees and Stephenson, 1995; Ziegler et al., 1995; Van Wees and Beekman, 2000).

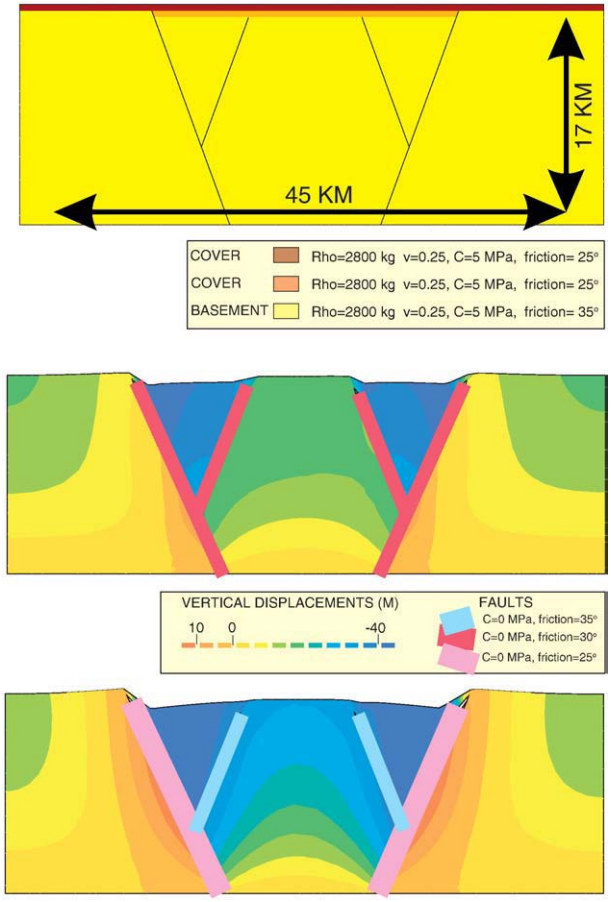

Fig. 31. Finite element modelling of the upper crustal and basin architecture of the Roer Valley Graben, illustrating the effects of planar faults with varying extent and properties in the upper crust (after Dirkzwager et al., 2000). (a) Model setup, yellow = crust-Mesozoic sediments, orange = Oligocene cover sediments, lines denote pre-existing faults. b) and c) deformed mesh after 200 m of extension, assuming different values for friction coefficient of the faults indicated by fault colour. Uniform properties of faults (b) show less concentration of fault motion on the larger border faults than for strongly reduced friction on the border faults (c). The latter is better in agreement with strain portioning in the graben (cf. Fig. 31b).

These studies, which are based on subsurface data that were not yet available at the time Ahorner (1983) carried out his initial studies, reveal the prolongation of neotectonically active faults into the vulnerable coastal lowlands of the Netherlands (Figs. 29, 30). These active faults largely coincide with Base Miocene faults. (Fig. 30 inset) (Geluk et al., 1994; De Mulder et al., 2003; Worum et al., 2004; Cloetingh and Cornu, 2005).

5.1.2. Stress tensor calibration using tectonic models

In tectonically active regions, the ratio of effective shear stress and normal stress on active faults–defined as slip tendency (cf Worum et al., 2004, Fig. 32)–is expected to be close to the critical value to generate slip. Under Mohr–Coulomb failure this critical value corresponds to the coefficient of friction. For intact rock the coefficient of friction is typically around 0.6 (e.g. Zoback, 2007) and for pre-existing faults in the range of 0.3–0.6 (Ziegler et al., 1995; Worum et al., 2004).

Slip tendency (ST) can be calculated for each segment of a pre-existing fault as a function of the effective principal stress magnitudes and the normal of the fault segment :

$$ST = \sqrt{\frac{n_x^2 + \left(\frac{\sigma_h}{\sigma_H}\right)^2 \cdot n_y^2 + \left(\frac{\sigma_v}{\sigma_H}\right)^2 \cdot n_z^2 - \left(n_x^2 + \left(\frac{\sigma_h}{\sigma_H}\right) \cdot n_y^2 + \left(\frac{\sigma_v}{\sigma_H}\right) \cdot n_z^2\right)^2}{n_x^2 + \left(\frac{\sigma_h}{\sigma_H}\right) \cdot n_y^2 + \left(\frac{\sigma_v}{\sigma_H}\right) \cdot n_z^2}}$$

where n_x, n_y and n_z denote the x, y and z components respectively of the normal vector of the surface element described in the eigensystem of the stress tensor, marked by effective principal vertical stress σ_v, minimum effective horizontal stress σ_h, and maximum effective horizontal stress σ_H (Worum et al., 2004).

In a uniform intraplate stress field the slip tendency is strongly sensitive to the orientation of faults in the stress field and the relative magnitudes of the principal stresses. Theoretically, a valid stress field is marked by ST values on active faults which are sufficiently high to generate slip on active faults ($ST > 0.3$) and sufficiently low to prevent failure of intact rock inside the graben area and. ($ST < 0.6$).

Using this modelling approach the estimation of the stress tensor using data from independent sources such as focal mechanisms and borehole breakout data can be validated and translated into valid stress tensor scenarios.

In the LGR (Fig. 33) we have to rely upon regional stress indicators, since local data with high spatial density is not available. By inverting the focal mechanism data of the 1992 Roermond earthquake and its aftershocks Camelbeeck et al. (1994) and Camelbeeck and van Eck (1994) found that the direction of the maximum horizontal (σ_H) principal stress was N139 degrees. At the same time, the confidence interval of the stress inversion suggests that N135–165_directions are also possible. Borehole breakout analysis carried out in the NE Netherlands indicated a N160_$\pm$5 σ_H orientation (Rondeel and Everaars, 1993). These observations are in agreement with intraplate stress orientations found in Western Europe (e.g., Ahorner, 1975; Klein and Barr, 1987; Müller et al., 1992; Plenefisch and Bonjer, 1997). The published stress inversion data constrain also the principal stress magnitudes in the area. The R-value range ($R = (\sigma_2 - \sigma_1)/(\sigma_3 - \sigma_1)$)[2] of 0.25–0.45, found by Camelbeeck et al. (1994) using the 1992 Roermond earthquake sequence is in agreement with that of Plenefisch and Bonjer (1997) ($R = 0.4$) who used focal mechanism data from a much larger area (Upper Rhine Graben–Roer Valley Rift System). Both of these authors emphasised that the confidence regions of the stress inversion do not make possible an unequivocal distinction between normal faulting and strike-slip faulting stress regimes.

[2] σ_1, σ_2 and σ_3 are maximum intermediate and minimum principal stress respectively.

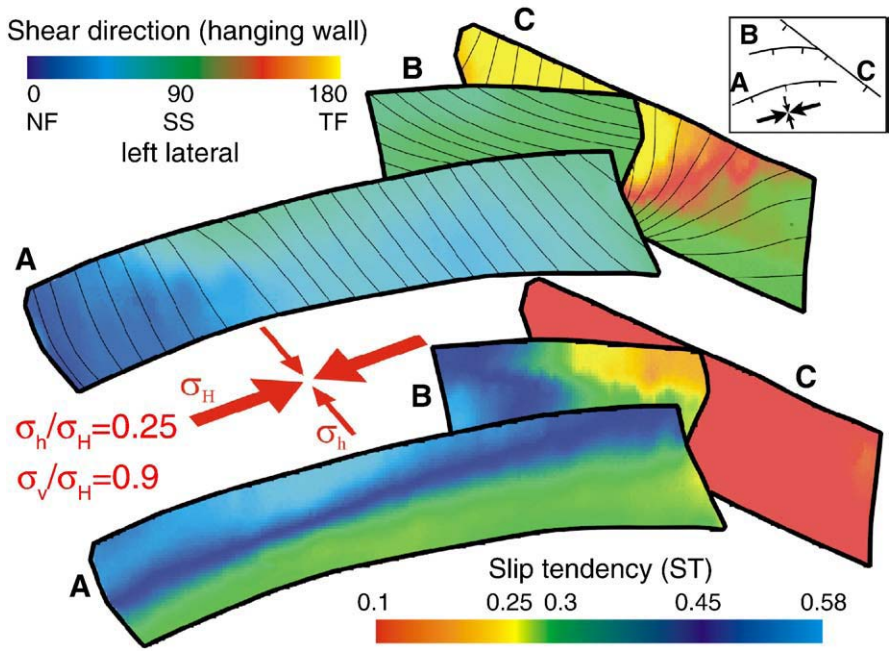

Fig. 32. Reactivation analysis of a fictional fault system in a synthetic strike slip stress scenario. Inset shows the map view of the modelled faults. Lower and upper panels show, respectively, the calculated slip tendency and shear directions. Shear trajectories are also shown (thin lines). NF, SS and TF denote normal faulting, strike slip faulting and thrust faulting respectively. See text for further discussion (from Worum et al., 2004).

Based on the aforementioned observations, the following assumptions were made regarding the recent stress field in the study area: (1) due to the lack of available stress indicator data with high spatial density the stress field is assumed to be laterally homogeneous within the study area; (2) σ_H direction is between N145 and N160; (3) the R-value of the stress tensor is between 0.25 and 0.45; and (4) the maximum principal

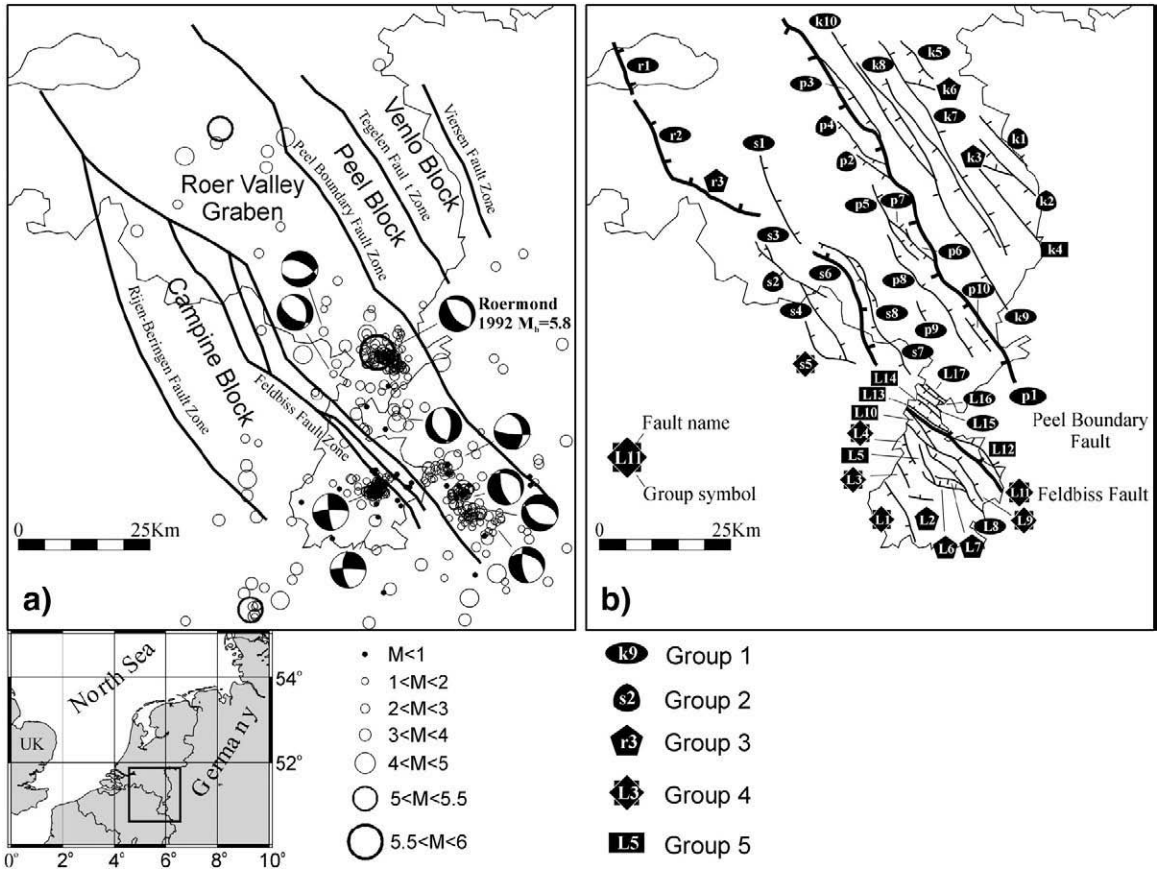

Fig. 33. (a) Location and main structural elements of the Roer Valley Rift System. Earthquakes that occurred in the last century are shown by circles. Focal mechanisms are after Camelbeeck and van Eck (1994). (b) Map view of the three-dimensional 3-D fault models implemented in the analysis (from Worum et al., 2004).

stress is either vertical (normal faulting regime) or horizontal (strike-slip faulting regime).

As input we applied depth-dependent stress fields, in which s_v corresponds to the burial stress minus hydrostatic pressure, and the other stresses are determined through the R-value and varying the σ_h/σ_H ratio. The orientation and magnitude of the input stress tensors were in agreement with the observed end-members of the σ_H direction and the R-value range. Thus, slip tendency and slip direction were calculated for stress tensors having 0.25 and 0.45 R-value as well as N145 and N160 σ_H direction. Every possible R-value-σ_H orientation combination was modelled both in normal faulting and in strike-slip faulting stress regimes. Since stress tensors with different principal stress ratios can have the same R-value, we modelled the σ_h/σ_H ratio between 0.2 and 0.9 with 0.1 steps for both R-value end-members. Although there are published data sets available constraining the σ_h/σ_H ratio (σ_h/σ_H 0.6 (Grünthal and Stromeyer, 1994)) our prime objective was to study the resolved stresses caused by stress fields having also lower σ_h/σ_H ratios. This altogether resulted in 32 different input stress tensors.

Due to the large number of input stress tensors, not all of the results are presented in the form of a 3-D perspective view. Instead, for every fault the minimum and maximum of the average slip tendency and slip direction values were calculated. The minimum and maximum values correspond to the two end-members of the modelled R-value range (0.25 and 0.45). The range of average slip tendencies is displayed as the function of the σ_h/σ_H ratio (Fig. 34). In Fig. 35 the 3-D pattern of slip tendencies are shown for a single stress scenario. Only a _1500 m high strip in the centre of the faults is visualised, to prevent the view of the faults from being obstructed by other faults. In reality the depth range of the faults are much larger.

For the sake of clarity the faults were clustered into five groups based on the characteristics of the ST–σ_h/σ_H curves (Figs. 33, 34). In the case of group 1–3, the faults belonging to the same group have similar orientations. Group 1 is the most packed group (25 faults) containing faults having _N145–150 orientation (see Fig. 34). Group 2 and 3 contain faults with N130–140 and N120 orientations, respectively. Group 4 contains faults mainly from the southernmost Limburg area having less consistent orientations and therefore less consistent ST–σ_h/σ_H curve shape than faults in the previous groups. Group 5 is the "group of outliers" (6 faults also mainly from Limburg) which contain faults with ST–σ_h/σ_H curve characteristics not fitting into any of the previous groups. This group is not represented on Fig. 34.

The average slip tendency (Fig. 34) and the 3-D patterns (Fig. 35) indicate that the slip tendency is a decreasing function of the σ_h/σ_H ratio both for normal faulting and for strike-slip faulting stress regimes. However, to prevent failure of intact rock a minimum value of σ_h/σ_H of approximately 0.2–0.4 is required, depending on R-value and faulting regime. It is also evident that the slip tendency of the modelled faults is always lower for strike slip faulting stress tensors than for normal faulting ones, indicating that reactivation would be more difficult if the σ_2 were vertical. Neither of the faults are likely to reactivate if the σ_h/σ_H ratio is larger than 0.65 for normal faulting and 0.5 for strike-slip faulting regimes, since is these cases the calculated slip tendency is lower than 0.3.

From the analysis of the stress tensors we conclude that the maximum principal stress of the stress field in the area is more likely vertical (normal faulting regime) than horizontal. This conclusion is built upon the following: (1) if the stress tensor describes a strike-slip faulting regime then a much lower s_h/s_H ratio is required to overcome a given slip threshold; (2) very low s_h/s_H ratios would be in disagreement with s_h/s_H predictions based on finite element modelling (Grünthal and Stromeyer, 1994); (3) in case of a stress tensor having a vertical σ_2, a very low slip threshold (0.1–0.2) would be required to reactivate the faults within a reasonable range of σ_h/σ_H ratios, which would suggest very low frictional coefficients or high pore fluid pressures, which are not observed in the area.

In terms of stress orientation the N145E orientation of σ_H results in slightly higher slip tendency values than the N160E results, favouring the first scenario.

5.2. Upper Rhine Graben

Studies carried out in the framework of ENTEC (e.g. Cloetingh et al., 2006) addressed particularly the southern parts of URG (Fig. 36), an area of increased seismic hazard (Figs. 5, 24), as for instance evidenced by the 1356 earthquake that severely damaged the city of Basel. Despite dedicated research, the seismic source of this historical earthquake (strike slip, thrust or normal faulting, reactivation of Oligocene or Permo-Carboniferous faults) has not yet be unequivocally identified (Meyer et al., 1994; Nivière and Winter, 2000; Meghraoui et al., 2001; Müller et al., 2002; Lambert et al., 2005). Furthermore, it is not clear whether on-going deformation of the North-Alpine foreland at convergence rates of about 1 mm/y or less (Müller et al., 2002; Ustaszewski et al., 2005) is partitioned between the crystalline basement (including Permo-Carboniferous troughs) and its sedimentary cover along rheologically weak Middle and Upper Triassic evaporite layers (Müller et al., 1987). During the Pliocene, shortening in the Jura Mountains propagated north-westward and northward and encroached during Late Pliocene times on the southern margin of the URG (Nivière and Winter, 2000; Giamboni et al., 2004). This late phase of Jura Mountain folding was accompanied by a change from previously "thin-" to "thick-skinned" deformation (Philippe et al., 1996; Becker, 2000; Dèzes et al., 2004). Solving these problems is a key issue in assessing the seismic hazard potential of the southern URG area that requires knowledge on fault kinematics during the geological past.

ENTEC research in the southernmost URG concentrated on detailed mapping of basement faults and kinematic reconstructions throughout time, integrating available geophysical data with results of structural field studies and geomorphologic observations.

Crustal extension across the southern URG accounts for a net stretching factor of 1.2 (Villemin et al., 1986), corresponding to a total extensional strain of 6–7 km (Brun et al., 1992). During the late Eocene and Oligocene, deformation was concentrated on the NNE-striking main border faults, which obliquely cross-cut Palaeozoic structures (Sittler, 1969). During the early Miocene, deformation progressively migrated towards the interior of the evolving graben as initial E–W directed extension rotated counter-clockwise to a nearly NE–SW directed one (Behrmann et al., 2003; Bertrand et al., 2005). The modelling study discussed below covers parts of the southern URG and its shoulders in the Colmar and Freiburg–Offenburg area (Fig. 36).

The rifting history of the southern URG was analyzed by applying numerical modelling techniques, based on finite element methods and contact mechanics (Cloetingh et al., 2006). Both forward and backward models were carried out to address two major aspects of rifting processes, namely the kinematics of extension and fault propagation. The forward model, running forwards in time starting from a assumed initial structural setting, aimed at defining the evolution of faulting during the rifting phase, and at analyzing the relationship between the strike of faults and the extension direction (orthogonal versus oblique extension) (Fig. 36). The backward model focused on reconstructing the kinematics of rifting backwards in time in the southern parts of the URG. Retro-deformation of this graben segment helped to define the finite amount of extension that occurred across it, the potential contribution of strike-slip deformation to observed displacements, and the cumulate amount of subsidence and possible post-rift uplift (Fig. 26).

5.2.1. Discussion of forward model

Qualitative results show that deformation is mainly concentrated on contact zones, the border faults, while the central part of the graben remains less deformed. However, in case of oblique extension, deformation is not necessarily restricted to the border faults: a narrow band of high strain and brittle behaviour develops in the centre of the graben along its axis (Fig. 36) (Cornu and Bertrand, 2005a). This zone

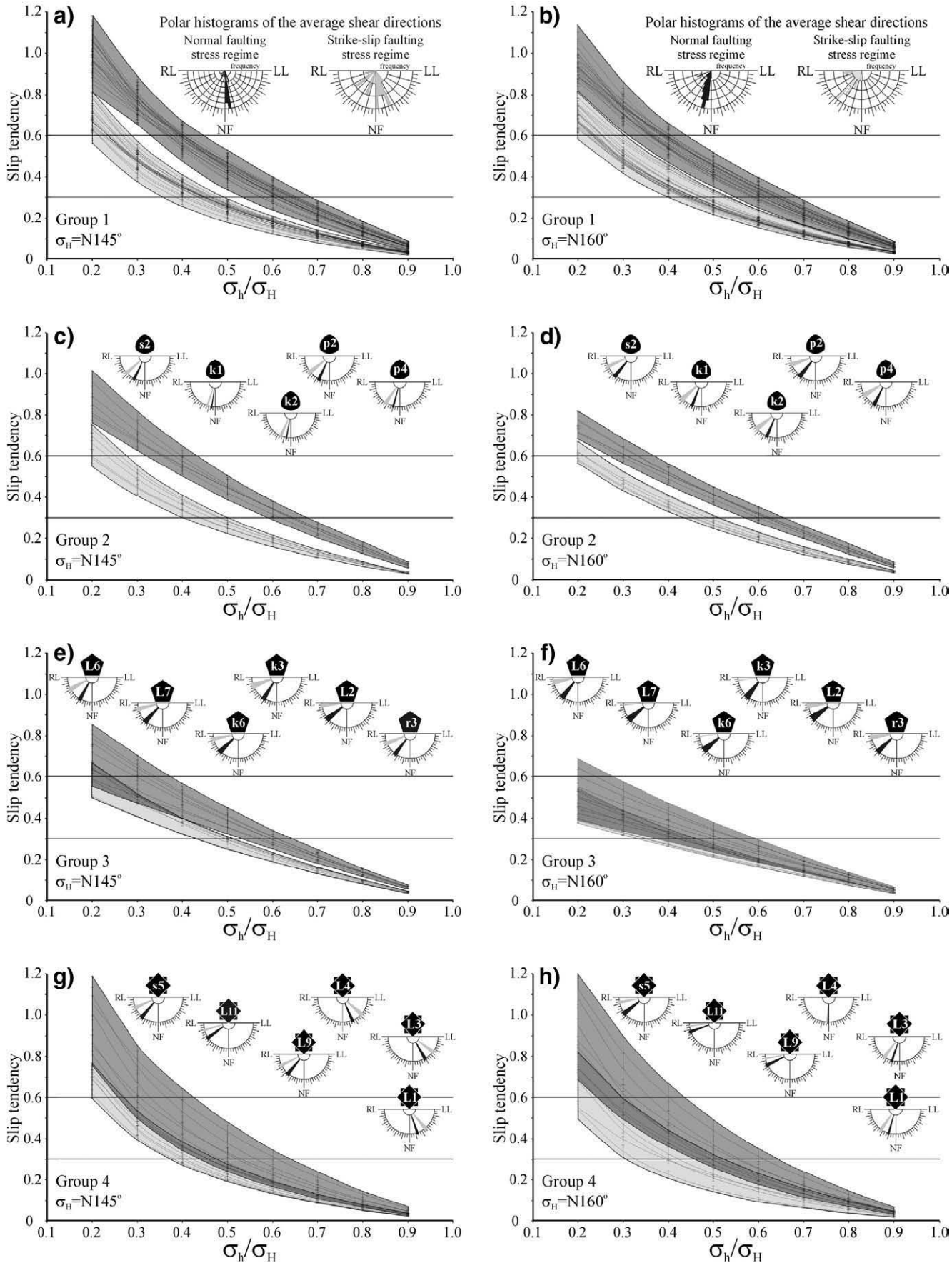
a)
Polar histograms of the average shear directions
Normal faulting stress regime
Strike-slip faulting stress regime
RL
LL
NF
frequency
Slip tendency
Group 1
σH=N145°
σh/σH
b)
Group 1
σH=N160°
c)
s2
k1
p2
p4
k2
Group 2
σH=N145°
d)
Group 2
σH=N160°
e)
L6
L7
k3
L2
k6
r3
Group 3
σH=N145°
f)
Group 3
σH=N160°
g)
s5
L11
L4
L3
L9
L1
Group 4
σH=N145°
h)
Group 4
σH=N160°

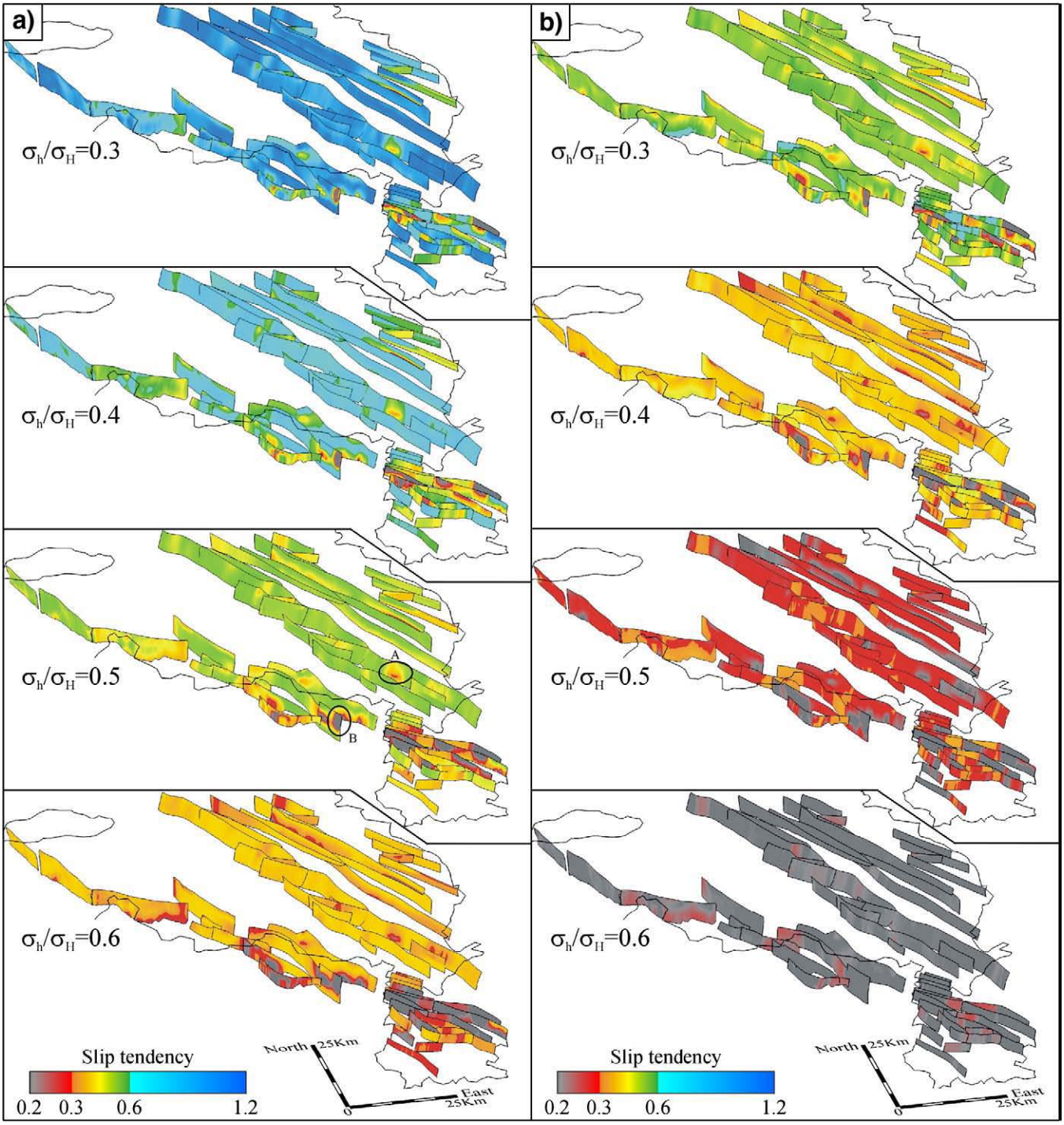

Fig. 35. Perspective view of the 3-D faults with slip tendency patterns calculated for input stress tensors having different σ_h/σ_H ratios and σ_H directions of N145 degrees. Vertical scale is four times exaggerated. (a) Stress tensors describing a normal faulting regime; (b) Strike-slip-faulting stress tensors. The R-value of the stress tensor was modelled as 0.45 for Figure 35a and as 0.25 for Figure 35b representing the maximum slip tendencies within the modelled R-value range.

is the likely location of subsequent faults that develop during oblique rifting. For this segment of the URG, the narrow zone of high strain and brittle behaviour closely fits the surface trace of the Rhine River Fault (Fig. 37).

It, however, is not possible to extract from this model the sense of displacement on a newly formed fault along the graben axis, as most of the vertical displacement is accommodated along the border faults. Moreover, as the zone of high brittle behaviour is rather vertical, one

Fig. 34. Average calculated slip tendency of faults as a function of the σ_h/σ_H ratio. The shaded areas indicate the total range of possible slip tendencies within the given group of faults. Light shading is for strike-slip-faulting stress tensors, and dark shading is for stress tensors describing a normal faulting stress regime. Insets for Figures 34a and 34b show the polar histograms of the average shear directions for group 1. Other insets (c–h) show the average shear direction range for the given fault representing the two end-members of the R-value range (0.25–0.45). Black indicates normal-faulting stress tensors, and light shading is for strike slip faulting stress tensors. The left and right panels of Figure 34 correspond to stress tensors with sH orientation being N145_and N160.

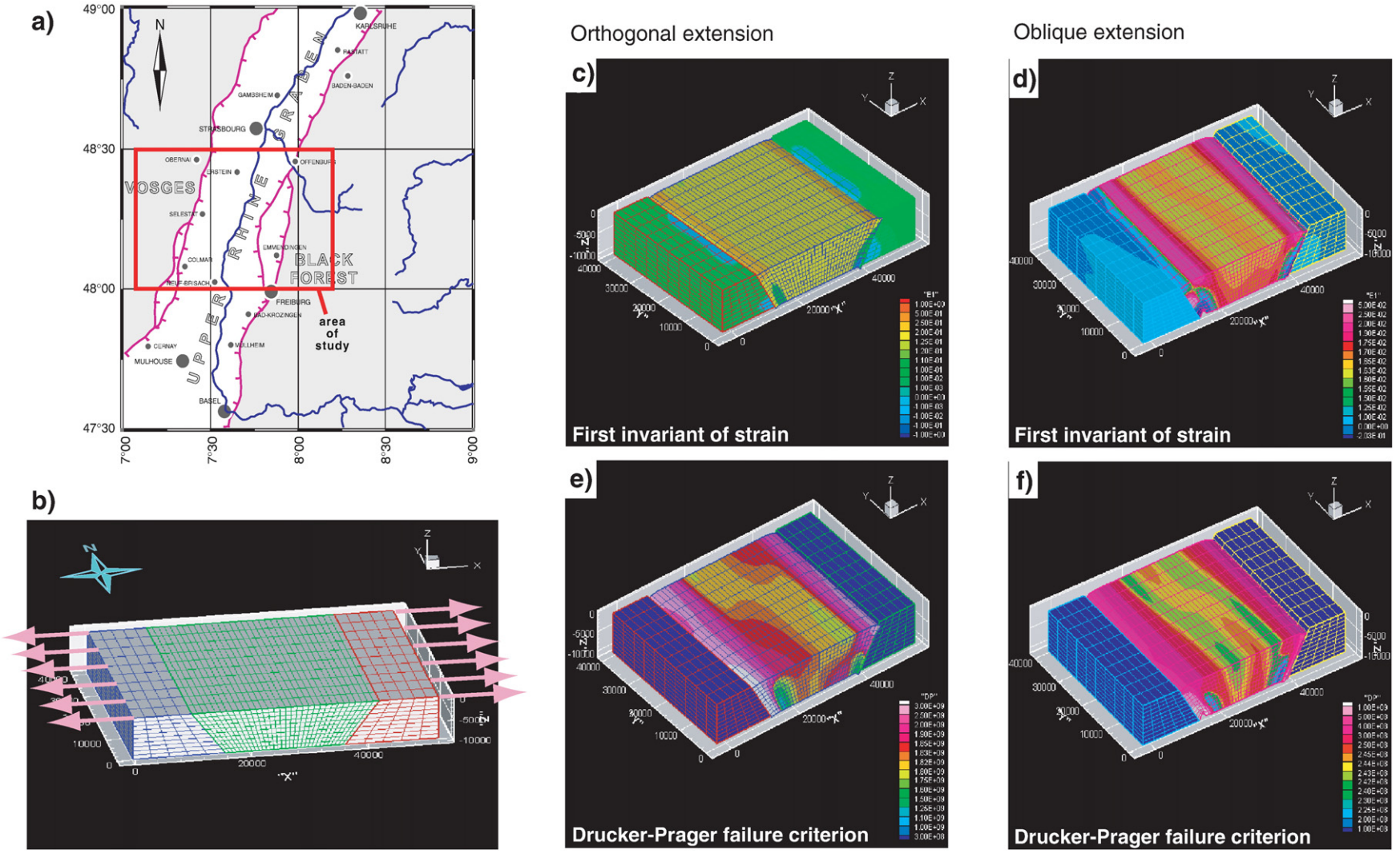

Fig. 36. (a). Sketch map of the southern part of the Upper Rhine Graben, showing the western and eastern main border faults. Red rectangle indicates the area for which the numerically modelling results are shown in panels b–f); (b) Initial (i.e. pre-rift) geometry of the studied graben segment, used for the forward model. The two lateral blocks correspond to the future graben shoulders (i.e. Vosges and Black Forest Mountains to the west and the east, respectively). Their contact zones with the central block correspond to the border faults delimiting the Upper Rhine Graben. Right Panel: Results of the forward model. Both purely orthogonal and partly oblique extension scenarios were tested. Results are presented in terms of the first invariant of strain E1 (sum of the diagonal terms of the strain tensor); (c) orthogonal and (d) oblique extension. And in terms of the Drucker-Prager (DP) failure criterion (numerical equivalent of a Mohr–Coulomb criterion; (e) orthogonal and (f) oblique extension. Cartesian coordinates are in meters (after Cloetingh et al., 2006).

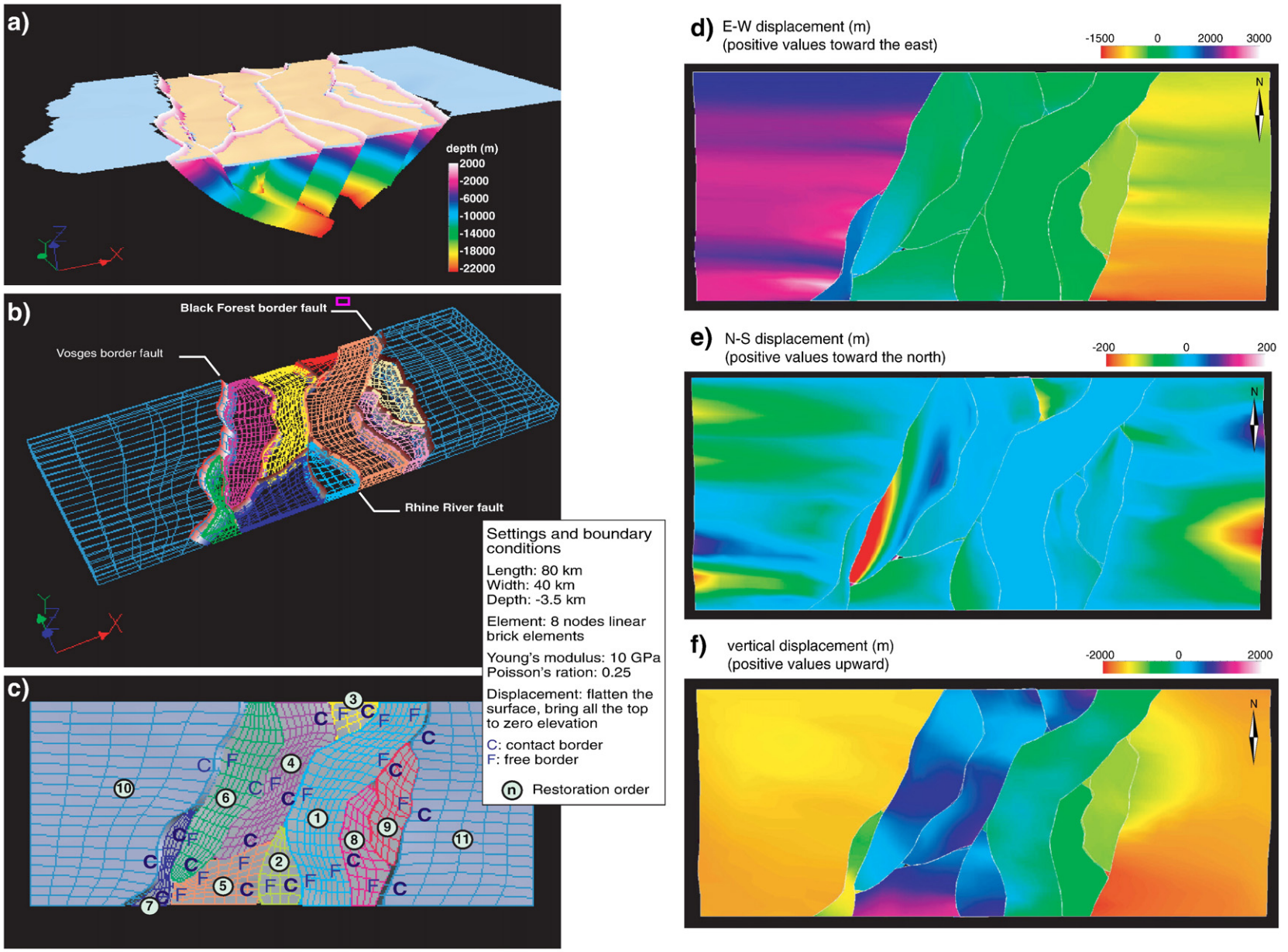

Fig. 37. Left panel: Construction of initial multi-block domain used for backward modelling (for location see Fig. 36a). (a) Present-day geometry of the geological domain; (b) Finite elements domain built from this geological domain; (c) Contact sequence of movement used for backward modelling, the contact borders, (C) are borders containing the "slave" nodes and free borders, (F) those containing "target" nodes (after Cloetingh et al., 2006). Right panel: Results of backward model, presented in terms of displacement (m), showing the top surface of all blocks, (a) displacement along the E–W x-axis, (b) displacement along the N–S y-axis, (c) displacement along the vertical z-axis (after Cloetingh et al., 2006).

would expect strike-slip motion combined with a normal component. A plausible rifting scenario for the URG could be, as proposed by Bertrand et al. (2005), that initially the border faults accommodated nearly orthogonal extension, and that, as the extension axis rotated counter-clockwise, new faults developed inside the graben. The models suggest that one of the most important features is the Rhine River fault that probably accommodated a significant amount of strike-slip movement whilst most of the normal displacement was taken up by the Main Border and associated faults.

5.2.2. Discussion of backward model

Displacement components along the 3 axes provide information on rifting processes in the URG. As previously suggested by forward modelling (Cornu and Bertrand, 2005b), the majority of deformation is initially accommodated along the border faults (Fig. 37a for heave and c for throw) with only a minor part being distributed within the graben itself. This confirms the model of Behrmann et al. (2003) and Bertrand et al. (2005) which suggests that deformation first concentrates on the main border faults whereas during later rifting stages localized deformation occurs within the graben.

Despite strict boundary conditions and a purely orthogonal rifting scenario, components of strike-slip motion have been identified along all faults. Strike-slip components range from a few tens to about 100 meters, as in the previous simple backward model (Cornu and Bertrand, 2005b). In case of partly oblique rifting, it is likely that the URG accommodated a significant component of strike-slip motion. At this point we are unable to quantify the cumulate strike-slip deformation component as no trace of strike-slip deformation has yet been identified in the field.

Although the main border faults accommodated the bulk of deformation, the Rhine River fault played an important role in the evolution of the URG. This fault, despite having a relatively low heave owing to its steep dip, accommodated a significant throw, and marks the boundary between the shallow eastern and the deep western part of the southern URG. Each fault block, although cut by secondary faults that accommodate smaller displacements, behaves more or less as a single block.

Summarizing, the forward model provides new insight into the possible faulting history of the URG. It clearly shows that 1) whatever the extension direction, deformation is mainly accommodated along the border faults, and 2) the observed fault pattern can only be reproduced under conditions of oblique extension.

The backward model is in good agreement with the results of previous studies (Behrmann et al., 2003; Cornu and Bertrand, 2005b; Bertrand et al., 2005) which show that 1) the maximum deformation occurs along the border faults, and 2) maximum subsidence is centred on the south-western part of the graben. In addition, the direction and magnitude of observed strike-slip values are compatible with those of a simple 4 blocks model (Cornu and Bertrand, 2005b). Although these lateral motions are mainly a function of fault orientation, an oblique extension component is required for the development of the observed fault pattern.

From the backward and forward models it appears that opening of the URG involved a component of oblique extension, and that the central Rhine River fault played a major role during the rifting history. Therefore, the Rhine River fault deserves further attention in future seismotectonic studies as it cuts densely populated and industrialized areas.

5.3. Implications for geothermal exploration

Tectonic models for fault rheology and stress field interactions in the upper crust assist in constraining the stress field, For the LRG we showed that slip tendency analysis allows to improve the robustness of the stress field determination, complementary to independent stress field data.

A heterogeneous rheology, and in particular the presence of faults, appears to be key to stress–strain interactions in the upper crust. The slip tendency approach combined with geomechanical modelling, supports the concept of reduced friction of pre-existing faults. These faults tend to be marked by large neo-tectonic displacements, when oriented favourably to the stress field, and are characterized by low absolute values of normal stress.

At production timescales, pre-existing faults and fractures appear to provide preferential pathways of hydraulic stimulation as documented by patterns of induced seismicity in the EGS project in Basel (Häring et al., 2008). This is in agreement with reduced friction for the pre-existing fabric inferred from the neotectonic analysis presented above. In the Gros-Schönebeck (eastern Germany) EGS project induced seismicity is largely distributed along a pre-existing fault orientation (Moeck et al., 2009). Using the slip tendency modelling approach, the latter authors demonstrate that the stimulated pre-existing fault is marked by relatively low strength, whereas its orientation aids in constraining the in-situ tectonic stress field. Moeck et al. (2009) also show through a slip tendency analysis that shear failure is more likely for pre-existing weak faults as high normal stresses prevent tensional failure. These examples illustrate the added value of the slip tendency approach for geothermal exploration and production both in terms of constraining the stress field, as well as assessing the importance of relatively weak pre-existing fault and fractures and the mode of fracturing.

Structural analysis for geothermal exploration indicates that in many areas faults can accommodate deep circulation of geothermal fluids (e.g. Fernández et al., 1990; Faulds et al., 2006). Structural analysis show that high temperature fluid pathways do not coincide with the positions of maximum slip but appear to be located at terminating, overlapping and intersecting fault zones (e.g. Faulds et al., 2009). At these locations, distributed damage or concentrated dilatation zones occur which are marked by a higher up-dip permeability than other parts of the fault network (cf Gartrell et al., 2006). Forward and backward modelling as presented for the URG sheds light on neotectonic strain partitioning, in particular in terms of assessing and validating the setting of oblique extension in which the basin evolved. Such a tectonic concept, supported by modelling, enhances the robustness of interpreting dilatational and shear mode fractured zones which form preferential pathways (cf. Faulds et al., 2009), through constraints on stress and strain portioning.

6. Conclusions and geothermal prospectivity

In this paper we have given an overview of how first order thermal constraints from surface heat flow and deep subsurface geophysical data sets can be used jointly to build and constrain thermal models of the lithosphere outside the coverage of well control. We demonstrated through integrated solid system earth models that the predicted first order patterns in thermal and rheological structure fit very well with earthquake distribution, and partitioning of deformation in Europe derived from geodetic measurements. The combined interpretation of the thermal and rheological state of the lithosphere is in close agreement with independent other geophysical data such as the gravity field.

In more detail, lithosphere and crustal scale weak zones which are inherited from previous deformation play an important role in distributing stress and strain in the upper crust representing the top 10 km in the Earth. Detailed geomechanical models incorporating weak zones, linking far field stress state to sub basin fault fabrics allow a validation of stress distributions in basins and aids in predicting critically stressed faults. Active faults that most likely represent active hydrothermal zones enhance the probability of conditions favourable for Enhanced Geothermal Systems (EGS), and pose opportunities and potential risk for fracturing and induced seismicity respectively.

The thermo-mechanical state that is observed for Europe relates to a complex evolution through geological times, involving pervasive extensional and compressional deformation. First order heat flow in onshore areas shows in particular a close relation to Cenozoic tectonics

at various depth levels in the lithosphere and crust. Numerical kinematic thermal models allow quantifying the effect of these tectonic processes, demonstrating the key role of subcrustal mantle processes in heat flow elevation over broad areas. In part these elevations are related to *plume impingement* such as observed in Central Europe in the Massif Central. On the other hand, *back-arc extension related mantle processes and volcanism* relate to broad zones of strong heat flow elevation, in particular in the Pannonian Basin, the western coast of Italy and the Aegean and parts of the western coast of Turkey.

This relationship allows to approach in a rational fashion continent-scale exploration for geothermal resources and to build hypotheses for both thermal and mechanical characterization at depth. The most favourable conditions for geothermal systems prevail in the active volcanic areas related to the deep lithosphere processes. Proven high enthalpy geothermal systems exist along the western coast of Italy, in the Tuscan region related to Late Quaternary volcanism, and in the Aegean region in Milos and Nikonos islands related to recent volcanism. Extensive high and medium enthalpy reservoirs can be found in Western Turkey (Akkus et al., 2005). The southernmost segment of the volcanic arc in the Eastern Carpathians also has some geothermal potential as the last eruption occurred 20 ka ago, though the existence of any reservoir is not proven.

EGS with expected production temperatures in excess of 150 °C can be developed in many places in Europe. Active fault zones, in particular, are known to provide permeable pathways for groundwater flow to penetrate to large depth (e.g. Fernández et al., 1990; Gartrell et al., 2006). Large fault zones located in relatively hot areas (Fig. 2) with ongoing–preferably extensional–deformation (Figs. 3–5, 19) are the most prospective places. The circum-Mediterranean region tectonically is the most active area in Europe as shown by numerous earthquakes (Fig. 5), marked by pronounced horizontal and vertical movements of smaller lithospheric blocks relative to each other (e.g. Cloetingh et al., 2005). Preferable areas for exploration include the (south-) east coast of Iberia, the North-Italian peninsula, the Aegean region including western Anatolia. Under extensional stress the cracks and fractures are more likely to be open than in case of compressional stress (Zoback, 2007). Faults in strike-slip tectonic regime may be also prospective as the termination of strike-slip faults, crossing of faults may result in local extension and open fractures.

Unconventional high enthalpy geothermal systems could be developed in deeply buried fractured, karstified carbonate rocks in the Pannonian basin. Such rocks are found in 4–5 km depth overlain by Neogene sediments. The buried carbonate reservoirs comprise closed systems with water temperature of 200 °C, and overpressure higher than 30 MPa.

Medium to low enthalpy systems, such as successfully developed in Unterhaching (Schoenwiesner-Bozkurt, 2006), could be developed in the highly permeable karstified sediments buried in other sections of the foreland of the Alps and Carpathians. Subduction of the European lithosphere beneath the Alps and Carpathians during the Tertiary and Neogene, respectively, resulted in 5–10 km deep foreland basins filled with clastic sediments. Though the porosity of the sediments decreases with depth due to compaction, applying hydraulic fracturing may increase the porosity and permeability to create EGS. Furthermore Medium enthalpy EGS systems can be developed in deep sedimentary strata of extensional basins in depth explored by hydrocarbon industry. These include the Rotliegend, well known from the Gross Schonebeck site.

In detail heat flow can show strong spatial variation, closely related to compositional variations such as for granites (cf. Fig. 7). Furthermore the temperature gradient can be strongly enhanced for relatively low conductivity rocks, such as shales and overpressured sediments, marked by high porosity. Secondary effects such as convective groundwater systems and fault conduits can be locally have a strong control on heat flow elevation. Integrated system earth process modelling allows understanding in detail temperature and heat flow variations and aid in targeting geothermal systems.

EGS exploration in the Upper Rhine Graben in Europe is marked by induced earthquakes varying considerably in magnitude up to 2.5 in Soultz (Gérard et al., 2006) up to 3.4 in Basel, involving reactivation of pre-existing crustal weak zones and faults. Neotectonic geomechanical modelling studies indeed demonstrate the key role of weak crustal faults in partitioning earth deformation. Such studies, linking subsurface rheology to natural seismicity, can provide key insights in potential earthquake magnitudes of induced seismicity.

Acknowledgements

This research was funded through the European Union (project Enhanced Geothermal Innovative Network for Europe, ENGINE, contract SES6-019760), TNO and the Netherlands Research Centre for Integrated Solid Earth Sciences (ISES). This paper benefitted from constructive comments by Dr. D. Coblenz and an anonymous reviewer.

References

Achauer, U., Masson, F., 2002. Seismic tomography on continental rifts revisited: from relative to absolute heterogeneities. Tectonophysics 358, 17–37.
Ádám, A., Vanyan, L.L., Varlamov, D.A., Yegorov, I.V., Shilovski, A.P., Shilovski, P.P., 1982. Depth of crustal conducting layer and asthenosphere in the Pannonian basin determined by magnetotellurics. Physics of the Earth and Planetary Interiors 28, 251–260.
Ahorner, L., 1975. Present-day stress field and seismotectonics block movements along major fault zones in Western Europe. Tectonophysics 29, 233–249.
Ahorner, L., 1983. Historical seismicity and present-day microearthquake activity of the Rhenish massif, central Europe. In: Fuchs, K., von Gehlen, K., Mälzer, H., Murawski, H., Semmel, A. (Eds.), Plateau Uplift. The Rhenish Shield. A Case History. Springer, Berlin, pp. 198–221.
Akkus, I., Aydogdu, O., Akilli, H., Gokmenoglu, O., Sarp, S., 2005. Geothermal Energy and Its Economic Dimension in Turkey. Proceedings World Geothermal Congress 2005, Antalya, Turkey.
Ansorge, J., Blundell, D., Mueller, S., 1992. Europe's Lithosphere—Seismic Structure. In: Blundell, D., Freeman, R., Mueller, S. (Eds.), A continent revealed, The European Geotraverse. University Press, Cambridge, pp. 33–69.
Artemieva, I., 2003. Lithospheric structure, composition, and thermal regime of the East European Craton: implications for the subsidence of the Russian platform. Earth and Planetary Science Letters 213, 431–446.
Artemieva, I., Thybo, H. and Kaban, M., 2006. Deep Europe today: geophysical synthesis of the upper mantle structure and lithospheric processes over 3.5 Ga. In: D. Gee and R. Stephenson (Editors), European Lithosphere Dynamics. Geological Society, London, Memoir, 32 pp. 662.
Artemjev, M.E., Kaban, M.K., Kucherinenko, V.A., Demyanov, G.V., Taranov, V.A., 1994. Subcrustal density inhomogeneities of Northern Eurasia as derived from the gravity data and isostatic models of the lithosphere. Tectonophysics 240, 249–280.
Babuška, V., Plomerová, J., 1992. The lithosphere in central Europe—seismological and petrological aspects. Tectonophysics 207, 141–163.
Babuška, V., Plomerová, J., 1993. Lithosphere thickness and velocity anisotropy—seismological and geothermal aspects. Tectonophysics 225, 79–89.
Babuška, V., Plomerová, J., 2001. Subcrustal Lithosphere around the Saxothuringian–Moldanubian Suture Zone—a model derived from anisotropy of seismic wave velocities. Tectonophysics 332, 185–199.
Bächler, D., Kohl, T., Rybach, L., 2003. Impact of graben parallel faults on hydrothermal convection—Rhine Graben case study. Physics and Chemistry of the Earth 28, 431–441.
Bada, G., Cloetingh, S.A.P.L., Gerner, P., Horvath, F., 1998. Sources of recent tectonic stress in the Pannonian region: inferences from finite element modelling. Geophysical Journal International 134, 87–101.
Bada, G., Grenerczy, G., Toth, L., Horváth, F., Stein, S., Cloetingh, S.A.P.L., Windhoffer, G., Fodor, L., Pinter, N., Fejes, I., 2007a. Motion of Adria and Ongoing Inversion of the Pannonian basin: Seismicity, GPS Velocities and Stress Transfer. In: Stein, S., Mazzotti, S. (Eds.), Geological Society of America, Book series 'Continental Intraplate Earthquakes: Science, Hazard and Policy Issues': Special Paper, 425, pp. 243–262.
Bada, G., Horváth, F., Dövényi, P., Szafián, P., Windhoffer, G., Cloetingh, S.A.P.L., 2007b. Present-day stress field and tectonic inversion in the Pannonian basin. Global and Planetary Change 58, 165–180.
Balling, N., 1995. Heat flow and thermal structure of the lithosphere across the Baltic Shield and northern Tornquist Zone. Tectonophysics 244, 13–50.
Barruol, G., Granet, M., 2002. A Tertiary asthenospheric flow beneath the southern French Massif Central related to the west Mediterranean extension evidenced by upper mantle seismic anisotropy. Earth and Planetary Science Letters 202, 31–47.
Bassi, G., 1995. Relative importance of strain rate and rheology for the mode of continental extension. Geophysical Journal International 122, 195–210.

Beaumont, C., Jamieson, R.A., Nguyen, M.H., Lee, B., 2001. Himalayan tectonics explained by extrusion of a low-viscosity crustal channel coupled to focused surface denudation. Nature 11, 738–742.
Becker, A., 2000. The Jura Mountains—an active foreland fold-and-thrust belt? Tectonophysics 321, 381–406.
Beekman, F., Badsi, M., van Wees, J.D., 2000. Faulting, fracturing and in-situ stress prediction in the Ahnet Basin, Algeria—A finite element approach. Tectonophysics 320, 311–329.
Behrmann, J., Hermann, O., Horstmann, M., Tanner, D., Bertrand, G., 2003. Anatomy and kinematics of oblique continental rifting revealed a 3D case study of the SE Upper Rhine Graben (Germany). American Association of Petroleum Geologists Bulletin 87, 1105–1121.
Bertotti, G., Podlachikov, Y., Daehler, A., 2000. Dynamic link between the level of ductile crustal flow and style of normal faulting of brittle crust. Tectonophysics 320, 195–218.
Bertrand, G., Horstmann, M., Hermann, O., Behrmann, J.H., 2005. Retrodeformation of the southern Upper Rhine Graben: new insights on continental oblique rifting. Quaternary Science Reviews 24, 345–352.
Bessis, F., 1985. Some remarks on the study of subsidence of sedimentary basins. Application to the Gulf of Lions margin (Western Mediterranean). Marine and Petroleum Geology 3, 37–63.
Bijwaard, H., Spakman, W., 1999a. Fast kinematic ray tracing of first- and later-arriving global seismic phases. Geophysical Journal International 139, 359–369.
Bijwaard, H., Spakman, W., 1999b. Tomographic evidence for a narrow whole mantle plume below Iceland. Earth and Planetary Science Letters 166, 121–126.
Bijwaard, H., Spakman, W., 2000. Nonlinear global P-wave tomography by iterated linearized inversion. Geophysical Journal International 141, 71–82.
Bijwaard, H., Spakman, W., Engdahl, E.R., 1998. Closing the gap between regional and global travel time tomography. Journal of Geophysical Research 103, 30055–30078.
Birch, F., Roy, R.F., Decker, E.R., 1968. Heat Flow and Thermal History of New England and New York. In: Zen, E., White, W.S., Hadley, J.B., Thompson, J.B. (Eds.), Studies of Appalachian Geology: Northern and Maritime. Wiley, New York, pp. 437–451.
Bonjer, K.-P., 1997. Seismicity pattern and style of seismic faulting at the eastern border fault of the southern Rhinegraben. Tectonophysics 275, 41–69.
Boschi, L., Ekström, G., Kustowski, B., 2004. Multiple resolution surface wave tomography: the Mediterranean basin. Geophysical Journal International 157, 293–304.
Brace, W.F., Kohlstedt, D.L., 1980. Limits on lithospheric stresses imposed by laboratory experiments. Journal of Geophysical Research 85, 6248–6252.
Brun, J.-P., 2002. Deformation of the Continental Lithosphere: Insights from Brittle-Ductile Models. In: De Meer, S., Drury, S.R., de Bresser, J.H.P., Pennock, G.M. (Eds.), Deformation Mechanisma. Current Status and Future Perspectives. Geological Society Special Publication, Rheology and Tectonics, pp. 355–370.
Brun, J.-P., Nalpas, T., 1996. Graben inversion in nature and experiments. Tectonics 15, 677–687.
Brun, J.P., Gutscher, M.A., Dekorp-Ecors team, 1992. Deep crustal structure of the Rhine Graben from DEKORP-ECORS seismic reflection data a summary. Tectonophysics 208, 203–210.
Burov, E.B., 2007. Plate rheology and mechanics. Treatise on Geophysics 6, 99–151.
Burov, E.B., Diament, M., 1995. The effective elastic thickness (Te) of continental lithosphere : what does it really mean? Journal of Geophysical Research 100, 3905–3927.
Burov, E.B., Cloetingh, S., 2009. Controls of mantle plumes and lithospheric folding on modes of intraplate continental tectonics: differences and similarities. Geophysical Journal International 178, 1691–1722.
Burov, E.B., Guillou-Frottier, L., d'Acredmont, E., Le Pourhiet, L., Cloetingh, S., 2007. Plume head-lithosphere interactions near intra-continental plate boundaries. Trectonophysics 434, 15–38.
Burrus, J., 1989. Review of geodynamic models for extensional basins: the paradox of stretching in the Gulf of Lions (Northwest Mediterranean). Bulletin de la Société Géologique de France 8, 377–393.
Byerlee, J.D., 1978. Friction of rocks. Pure and Applied Geophysics 116, 615–626.
Calcagnile, G., 1991. Deep structure of Fennoscandia from fundamental and higher mode dispersion of Rayleigh waves. Tectonophysics 195, 139–149.
Camelbeeck, T., van Eck, T., 1994. The Roer Valley Graben earthquake of 13 April 1992 and its seismotectonic setting. Terra Nova 6, 291–300.
Camelbeeck, T., Meghraoui, M., 1998. Geological and geophysical evidence for large paleoearthquakes with surface faulting in the Roer Graben (northwest Europe). Geophysical Journal International 132, 347–362.
Camelbeeck, T., van Eck, T., Pelzing, R., Ahorner, L., Loohuis, J., Haak, H.W., Hoang-Trong, P., Hollnack, D., 1994. The 1992 Roermond earthquake, the Netherlands, and its aftershocks. Geologie en Mijnbouw 73, 181–197.
Camelbeeck, T., Vanneste, K., Verbeeck, K., Meghraoui, M., Pelzing, R., Hinzen, K., Dost, B., van den Berg, M., 2001. Long-term seismic activity in the Lower Rhine Embayment. Cahiers du Centre Européen de Géodynamique et de Séismologie 18, 35–38.
Carter, N.L., Tsenn, M.C., 1987. Flow properties of continental lithosphere. Tectonophysics 136, 27–63.
Cavazza, W.M., Roure, F.M., Spakman, W., Stampfli, G.M., Ziegler, P.A. (Eds.), 2004. The Transmed Atlas. Springer, Berlin.
Cebriá, J.M., Wilson, M., 1995. Cenozoic mafic magmatism in western/central Europe: a common European asthenospheric reservoir? Terra Nova 7, 162.
Cermak, V., 1993. Lithospheric thermal regimes in Europe. Physical of the Earth and Planetary Interiors 79, 179193.
Cermak, V., Bodri, L., 1995. Three-dimensional deep temperature modelling along the European geotraverse. Tectonophysics 244, 1–11.
Chalmers, J.A., Cloetingh, S.A.P.L. (Eds.), 2000. Neogene Uplift and Tectonics around the North Atlantic: Global and Planetary Change, 27, pp. 1–173.
Charléty, J., Cuenot, N., Dorbath, L., Dorbath, C., Haessler, H., Frogneux, M., 2007. Large earthquakes during hydraulic stimulations at the geothermal site of Soultz-sous-Forets. International Journal of Rock Mechanics & Mining Sciences 44, 1091–1105.
Chandrasekhar, V., Chandrasekharam, D., 2009. Geothermal systems in India. Geothermal Resource Council Transactions 33, 607–610.
Christensen, N.I., Mooney, W.D., 1995. Seismic velocity structure and composition of the continental crust: a global view. Journal of Geophysical Research 100, 9761–9788.
Cloetingh, S.A.P.L., 1988. Intraplate stress: new element in Basin Analysis. In: Kleinspehn, K.L., Paola, C. (Eds.), New Perspectives in Basin Analysis. Springer, New York, pp. 205–230.
Cloetingh, S.A.P.L., 2000. Perspectives on environmental earth system dynamics. Global and Planetary Change 27, 1–21.
Cloetingh, S.A.P.L., Burov, E.B., 1996. Thermomechanical structure of European continental lithosphere: constraints from rheological profiles and EET estimates. Geophysical Journal International 124, 695–723.
Cloetingh, S.A.P.L., van Wees, J.D., 2005. Strength reversal in Europe's intraplate lithosphere: transition from basin inversion to lithospheric folding. Geology 33, 285–288.
Cloetingh, S.A.P.L., Cornu, T. (Eds.), 2005. Neotectonics and Quaternary Fault-reactivation in Europe's Intraplate Lithosphere: Quaternary Science Reviews, 24, pp. 236–508.
Cloetingh, S.A.P.L., McQueen, H., Lambeck, K., 1985. On a tectonic mechanism for regional sea-level variations. Earth and Planetary Science Letters 75, 157–166.
Cloetingh, S.A.P.L., Kooi, H., Groenewoud, W., 1989. Intraplate Stress and Sedimentary Basin Evolution. In: Price, R.A. (Ed.), Origin and Evolution of Sedimentary Basins and Their Energy and Mineral Resources: American Geophysical Union, Geophysical Monograph, 48, pp. 1–16.
Cloetingh, S.A.P.L., Burov, E., Poliakov, A., 1999. Lithospheric folding: primary response to compression, from Central Asia to the Paris Basin. Tectonics 18, 1064–1083.
Cloetingh, S.A.P.L., Spadini, G., van Wees, J.D., Beekman, F., 2003a. Thermo-mechanical modelling of Black Sea Basin (de)formation. Sedimentary Geology 156, 169–184.
Cloetingh, S.A.P.L., Horváth, F., Dinu, C., Stephenson, R.A., Bertotti, G., Bada, G., Matenco, L., Garcia-Castellanos, D., TECTOP Working Group, 2003b. Probing tectonic topography in the aftermath of continental convergence in Central Europe. EOS, Transactions, American Geophysical Union 84, 89–93.
Cloetingh, S.A.P.L., Ziegler, P.A., Beekman, F., Andriessen, P.A.M., Matenco, L., Bada, G., Garcia-Castellanos, D., Hardebol, N., Dèzes, P., Sokoutis, D., 2005. Lithospheric memory, state of stress and rheology: neotectonic controls on Europe's intraplate continental topography. Quaternary Science Reviews 24, 241–304.
Cloetingh, S.A.P.L., Cornu, T., Ziegler, P.A., Beekman, F., ENTEC Working Group1, 2006. Neotectonics and intraplate continental topography of the northern Alpine Foreland. Earth Science Reviews 74, 127–196.
Cloetingh, S.A.P.L., Ziegler, P.A., Bogaard, P.J.F., Andriessen, P.A.M., Artemieva, I.M., Bada, G., van Balen, R.T., Beekman, F., Ben-Avraham, Z., Brun, J.-P., Bunge, H.P., Burov, E.B., Carbonell, R., Facenna, C., Friedrich, A., Gallart, J., Green, A.G., Heidbach, O., Jones, A.G., Matenco, L., Mosar, J., Oncken, O., Pascal, C., Peters, G., Sliaupa, S., Soesoo, A., Spakman, W., Stephenson, R.A., Thybo, H., Torsvik, T., de Vicente, G., Wenzel, F., Wortel, M.J.R., TOPO-EUROPE Working Group, 2007. TOPO-EUROPE: the geoscience of coupled deep Earth-surface processes. Global and Planetary Change 58, 1–118.
Coisy, P., Nicolas, A., 1978. Structure et géodynamique du manteau supérieur sous le Massif Central (France) d'après l'étude des enclaves des basaltes. Bulletin de Minéralogie 101, 424–436.
Cornu, T., Bertrand, G., 2005a. Backward modelling of the rifting kinematics in the Upper Rhine Graben: insights from an elastic-perfect contact law on the restoration of a multi-bloc domain. International Journal of Earth Sciences 94, 751–757.
Cornu, T., Bertrand, G., 2005b. Numerical backward and forward modelling of the southern Upper Rhine Graben (France–Germany border): new insights on tectonic evolution of intracontinental rifts. Quaternary Science Reviews 24, 235–508.
Csontos, L., Nagymarosy, A., Horváth, F., Kovác, M., 1992. Tertiary evolution of the Intra-Carpathian area: a model. Tectonophysics 208, 221–241.
de Bruijne, C.H., Andriessen, P.A.M., 2000. Interplay of intraplate tectonics and surface processes in the Sierra de Guadarrama (central Spain), assessed by apatite fission track analysis. Physics and Chemistry Earth (A) 25, 555–563.
de Bruijne, C.H., Andriessen, P.A.M., 2002. Far field effects of Alpine plate tectonism in the Iberian microplate recorded by fault-related denudation in the Spanish Central System. Tectonophysics 349, 161–184.
de Mulder, E.F.J., Geluk, M.C., Ritsema, I., Westerhoff, W.E., Wong, T.E., 2003. De ondergrond van Nederland, The subsurface of the Netherlands. Netherlands Institute of Applied Geoscience TNO, p. 379.
Della Vedova, B., Bellani, S., Pellis, G., Squarci, P., 2001. Deep Temperatures and Surface Heat Flow Distribution. In: Vai, G.B., Martini, I.P. (Eds.), Anatomy of an Orogen: The Apennines and Adjacent Mediterranean Basins. Kluwer Academic Publishers, Amsterdam, pp. 65–76.
Dewey, J.F., 1969. Evolution of the Appalachian–Caledonian orogen. Nature 222, 124–129.
Dèzes, P., Schmid, S.M., Ziegler, P.A., 2004. Evolution of the European Cenozoic Rift System: interaction of the Alpine and Pyrenean orogens with their foreland lithosphere. Tectonophysics 389, 1–33.
Dèzes, P. and Ziegler, P.A., 2004. Moho depth map of Western and Central Europe. EUCOR-URGENT home page: http://www.unibas.ch/.
Dinter, D., Royden, L., 1993. Late Cenozoic extension in north-eastern Greece: Strymon valley detachment system and Rhodope metamorphic core complex. Geology 21, 45–48.
DiPippo, R., 2007. Ideal thermal efficiency for geothermal binary plants. Geothermics 36, 276–285.

Dirkzwager, J.B., van Wees, J.D., Cloetingh, S.A.P.L., Geluk, M.C., Dost, B., Beekman, F., 2000. Geo-mechanical and rheological modelling of upper crustal faults and their near-surface expression in the Netherlands. Global and Planetary Change 27, 67–88.
Doglioni, C., Dagostino, N., Mariotti, G., 1998. Normal faulting vs regional subsidence and sedimentation rate. Marine and Petroleum Geology 15, 737–750.
Dost, B., Haak, H.W., 2007. Natural and Induced Seismicity. In: Wong, T.E., Batjes, D.A.J., de Jager, J. (Eds.), Geology of the Netherlands: Royal Netherlands Academy of Arts and Sciences, pp. 223–239.
Du, Z.J., Michelini, A., Panza, G.F., 1998. EurID, a regionalized 3-D seismological model of Europe. Physical of the Earth and Planetary Interiors 105, 31–62.
Dunai, T.J., Baur, H., 1995. Helium, neon and argon systematics of the European subcontinental mantle: Implications for its geochemical evolution. Geochimica et Cosmochimica Acta 59, 2767–2783.
Faccenna, C., Becker, T., Pio Lucente, F., Jolivet, L., Rossetti, F., 2001. History of subduction and back-arc extension in the Central Mediterranean. Geophysical Journal International 145, 809–820.
Faccenna, C., Jolivet, L., Piromallo, C., Morelli, A., 2003. Subduction and the depth of convection in the Mediterranean mantle. Journal of Geophysical Research 108, 2099.
Faulds, J.E., Coolbauch, M.F., Vice, G.S., Edwards, M.L., 2006. Characterizing structural controls of geothermal fields in the north western Great Basin: a progress report. Geothermal Resources Council Transactions 30, 69–76.
Faulds, J.E., Bouchon, V., Moeck, I., Oguz, K., 2009. Structural controls on Geothermal Systems in Western Turkey: a preliminiary report. Geothermal Resources Council Transactions 33, 375–382.
Fernández, M., Banda, E., 1989. An approach to the thermal field in northeastern Spain. Tectonophysics 164, 259–266.
Fernández, M., Banda, E., 1990. Geothermal anomalies in the Vallés-Penedés master fault. Journal of Geophysical Research. Convection through the horst as a possible mechanism 95, 4887–4894.
Fernández, M., Torné, M., Zeyen, H., 1990. Modelling of thermal anomalies in the NW border of the Valencia Trough by groundwater convection. Geophysical Research Letters 17, 105–108.
Förster, A., Förster, H.-J., 2000. Crustal composition and mantle heat flow: implications from surface heat flow and radiogenic heat production in the Variscan Erzgebirge (Germany). Journal of Geophysical Research 105, 27917–27938.
Frisch, W., Kuhlemann, J., Dunkl, I., Brügel, A., 1998. Palinspastic reconstruction and topographic evolution of the Eastern Alps during late Tertiary tectonic extrusion. Tectonophysics 297, 1–15.
Fügenschuh, B., Seward, D., Mancktelow, N.S., 1997. Exhumation in a convergent orogen: the western Tauern window. Terra Nova 9, 213–217.
Gartrell, A., Bailey, W.R., Brincat, M., 2006. A new model for assessing trap integrity and oil preservation risks associated with postrift fault reactivation in the Timor Sea. AAPG Bulletin 90, 1921–1944.
Gaspar-Escribano, J.M., van Wees, J.D., ter Voorde, M., Cloetingh, S.A.P.L., Roca, E., Cabrera, L., Munoz, J.A., Ziegler, P.A., Garcia-Castellanos, D., 2001. 3D flexural modeling of the Ebro Basin (NE Iberia). Geophysical Journal International 145, 349–367.
Gaspar-Escribano, J.M., Garcia-Castellanos, D., Roca, E., Cloetingh, S.A.P.L., 2004. Cenozoic vertical motions of the Catalan Coastal Ranges (NE Spain): the role of tectonics, isostasy, and surface transport. Tectonics 23, TC1004.
Geluk, M.C., Duin, E.J., Dusar, M., Rijkers, R., van den Berg, M.W., van Rooijen, P., 1994. Stratigraphy and tectonics of the Roer Valley Graben. Geologie en Mijnbouw 73, 129–141.
Genser, J., van Wees, J.D., Cloetingh, S.A.P.L., Neubauer, F., 1996. Eastern Alpine tectono-metamorphic evolution: constraints from two-dimensional P–T–t modeling. Tectonics 15, 584–604.
Genter, A., Guillou-Frottier, L., Feybesse, L., Nicol, N., Dezayes, Ch., Schwartz, S., 2003. Typology of potential hot fractured rock resources in Europe. Geothermics 32, 701–710.
Gérard, A., Genter, A., Kohl, T., Lutz, P., Rose, P., 2006. The deep EGS (Enhanced Geothermal System) project at Soultz-sous-Forêts, Alsace, France. Geothermics 35, 473–714.
Giamboni, M., Ustaszewski, K., Schmid, S.M., Schumacher, M.E., Wetzel, A., 2004. Plio-Pleistocene transpressional reactivation of Paleozoic and Paleogene structures in the Rhine-Bresse transform zone (northern Switzerland and eastern France). International Journal of Earth Sciences 93, 207–223.
Goes, S., Spakman, W., Bijwaard, H., 1999. A lower mantle source for European volcanism. Science 286, 1928–1931.
Goes, S., Govers, R., Vachez, P., 2000a. Shallow upper mantle temperatures under Europe from P- and S-wave tomography. Journal of Geophysical Research 105, 11153–11169.
Goes, S., Loohuis, J.J.P., Wortel, M.J.R., Govers, R., 2000b. The effect of plate stresses and shallow mantle temperatures on tectonics of northwestern Europe. Global and Planetary Change 27, 23–38.
Gölke, M., Coblentz, D., 1996. Origins of the European regional stress field. Tectonophysics 266, 11–24.
Granet, M., Wilson, M., Achauer, U., 1995. Imaging a mantle plume beneath the Massif Central (France). Earth and Planetary Science Letters 17, 1109–1112.
Group, T.W., 2002. First deep seismic reflection images of the Eastern Alps reveal giant crustal wedges and transcrustal ramps. Geophysical Research Letters 29, 92.1–92.4.
Grünthal, G., Stromeyer, D., 1994. The recent crustal stress field in Central Europe sensu lato and its quantitative modeling. Geologie en Mijnbouw 73, 173–180.
Grünthal, G., the GHSAP Region 3 Working Group, 1999. Seismic hazard assessment for Central, Northern and Northwestern Europe: GSHAP Region 3. Annali di Geofisica 42, 999–1011.
Gueguen, E., Doglioni, C., Fernandez, M., 1998. On the post-25 Ma geodynamic evolution of the western Mediterranean. Tectonophysics 298, 259–269.
Guillou-Frottier, L., Burov, E., Neylig, P., Wyns, R., 2007. Deciphering plume-lithosphere interactions beneath Europe from tomographic signatures. Global and Planetary Change 58, 119–140.
Haenel, R., Rybach, L., Stegena, L. (Eds.), 1988. Handbook of Terrestrial Heat-Flow Determination. 486 pp., Solid Earth Science library. Kluwer Academic publishers, Dordrecht.
Handy, M.R., Brun, J.-P., 2004. Seismicity, structure and strength of the continental lithosphere. Earth and Planetary Science Letters 223, 427–441.
Hardebol, N., 2010. Strength patterns of intraplate lithosphere. in: the Foreland Belt of the SE Canadian Cordillera: from thrust-sheet to lithosphere controls on the burial and thermal evolution, PhD Thesis, VU university Amsterdam, pp.179.
Hardebol, N., Cloetingh, S.A.P.L., Beekman, F., 2003. Lithospheric strength of large-scale intraplate deformed NW Europe: constrained from interpretations of geophysical and geological datasets. EUCOR-URGENT Workshop 2003—Poster with Abstract. http://comp1.geol.unibas.ch.
Häring, M., Schanz, U., Ladner, F., Dyer, B., 2008. Characterisation of the Basel 1 enhanced geothermal system. Geothermics 37, 469–495.
Heidbach, O., Tingay, M., Barth, A., Reinecker, J., Kurfeß, D., Müller, B., 2008. The World Stress Map database release 2008. doi:10.1594/GFZ.WSM.Rel2008.
Hetzel, R., Passchier, C.W., Ring, U., Dora, 1995a. Bivergent extension in orogenic belts: the Menderes massif, southwestern Turkey. Geology 23, 455–458.
Hetzel, R., Ring, U., Akal, C., Troesch, M., 1995b. Miocene NNE-directed extensional unroofing in the Menderes massif, southwestern Turkey. Journal of the Geological Society of London 152, 639–654.
Heuer, B., Geissler, W.H., Kind, R., Kämpf, H., 2006. Seismic evidence for asthenosphere updoming beneath the western Bohemian Massif, central Europe. Geophysical Journal International 33, L05311.
Heuer, B., Kämpf, H., Kind, R., Geissler, W.H., 2007. Seismic evidence for whole lithosphere separation between Saxothuringian and Moldanubian tectonic units in central Europe. Geophysical Research Letters 34, L09304.
Hinzen, K.-G., 2003. Stress field in the Northern Rhine area, Central Europe, from earthquake fault plain solutions. Tectonophysics 377, 325–356.
Horváth, F., 1993. Towards a mechanical model for the formation of the Pannonian basin. Tectonophysics 226, 333–357.
Horváth, F., Cloetingh, S.A.P.L., 1996. Stress-induced late-stage subsidence anomalies in the Pannonian basin. Tectonophysics 266, 287–300.
Horváth, F., Dövényi, P., Szalay, Á., Royden, L.H., 1988. Subsidence, thermal and maturation history of the Great Hungarian Plain. In: Royden, L.H., Horváth, F. (Eds.), The Pannonian Basin, a Study in Basin Evolution: Amer. Assoc. Petr. Geol. Mem., 45, pp. 355–372.
Horváth, F., Bada, G., Szafián, P., Tari, G., Ádám, A., Cloetingh, S.A.P.L., 2006. Formation and Deformation of the Pannonian Basin: Constraints from Observational Data. In: Gee, D.G., Stephenson, R.A. (Eds.), European Lithosphere Dynamics: Geological Society, London, Memoirs, 32, pp. 191–206.
Houtgast, R.F., van Balen, R.T., 2000. Neotectonics of the Roer Valley Rift System, the Netherlands. Global and Planetary Change 27, 131–146.
Houtgast, R.F., van Balen, R.T., Bouwer, L.M., Brand, G.B.M., Brijker, J.M., 2002. Late Quaternary activity of the Feldbiss Fault Zone, Roer Valley Rift System, the Netherlands, based on displaced fluvial terrace fragments. Tectonophysics 352, 295–315.
Houtgast, R.F., van Balen, R.T., Kasse, C., Vandenberghe, J., 2003. Late Quaternary tectonic evolution and postseismic near surface fault displacements along the Geleen Fault (Feldbiss Fault Zone–Roer Valley Rift System, the Netherlands), based on trenching. Geologie en Mijnbouw 82, 177–196.
Houtgast, R.F., van Balen, R.T., Kasse, C., 2005. Late Quaternary tectonic evolution of the Feldbiss Fault (Feldbiss Fault Zone-Roer Valley Rift System, the Netherlands). Evidence for a Late Weichselian increase in fault activity due to glacial unloading in the Netherlands? Quaternary Science Reviews 24, 489–508.
Hurter, S., Haenel, R., 2002. Atlas of Geothermal Resources in Europe. Commission of the European Communities, EC Publication Nr. 1781 1.
Hurtig, E., Čermák, V., Haenel, R., Zui, V. (Eds.), 1992. Geothermal Atlas of Europe, International Association for Seismology and Physics of the Earth's Interior, 156 pp. Hermann Haack GmbH, Gotha.
Jackson, J.A., 2002. Strength of the continental lithosphere: time to abandon the jelly sandwich? GSA Today 12, 4–10.
Janssen, M., Stephenson, R.A., Cloetingh, S.A.P.L., 1995. Temporal and spatial correlations between changes in plate motions and the evolution of rifted basins in Africa. Geological Society of America Bulletin 107, 1317–1332.
Japsen, P., Chalmers, J.A., 2000. Neogene uplift and tectonics around the North Atlantic: overview. Global and Planetary Change 24, 165–173.
Jaupart, C., Mareschal, J.C., 1999. The thermal structure and thickness of continental roots. Lithos 48, 93–114.
Jaupart, C., Mareschal, J.-C., 2007a. Heat flow and thermal structure of the lithosphere. Treatise on Geophysics 6, 217–251.
Jaupart, C., Mareschal, J.-C., 2007b. Constraints on crustal heat production from heat flow data. Treatise on Geochemistry 3, 65–84.
Jaupart, C., Labrosse, S., Mareschal, J.-C., 2007. Temperatures, Heat and Energy in the Mantle of the Earth. Treatise on Geophysics 7, 253–303.
Jones, A.G., 1984. Electromagnetic Investigations in Eastern Canada — a Concise Review. In: Hjelt, S.-E. (Ed.), The Development of the Deep Geoelectric Model of the Baltic Shield. Dept. of Geophysics, Oulu University, pp. 166–178.
Juez-Larré, J., Andriessen, P.A.M., 2006. Tectonothermal evolution of the northeastern margin of Iberia since the break-up of Pangea to present, revealed by low-temperature fission-track and (U–Th)/He thermochronology. A case history of the Catalan Coastal Ranges. Earth and Planetary Science Letters 243, 159–180.
Juhász, G., 1994. Sedimentological and stratigraphical evidences of water-level fluctuations in the Pannonian Lake. Földtani Közlöny Budapest 123, 379–398.

Jung, S., 1999. The role of crustal contamination during evolution of continental rift-related basalts, a case study from the Vogelsberg area, Central Germany. Geolines 9, 48–58.
Kaban, M., 2001. A Gravity Model of the North Eurasia Crust and Upper Mantle: 1. Mantle and Isostatic Residual Gravity Anomalies. Russian Journal of Earth Sciences 3, 143–163.
Kaban, M.K., 2004. A gravity model of the North Eurasia crust and upper mantle. 3. Stress sate of the lithosphere induced by density inhomogeneities. Russian Journal of Earth Sciences 6 (2), 1–9.
Kaban, M.K., Mooney, W.D., 2001. Density structure of the lithosphere in the southwestern United States and its tectonic significance. Journal of Geophysical Research 106, 721–740.
Kaban, M.K., Schwintzer, P., 2001. Oceanic upper mantle structure from experimental scaling of Vs and density at different depths. Geophysical Journal International 147, 199–214.
Kaban, M.K., Schwintzer, P., Artemieva, I.M., Mooney, W.D., 2003. Density of the continental roots: compositional and thermal contributions. Earth and Planetary Science Letters 209, 53–69.
Kaban, M.K., Schwintzer, P., Reigber, C., 2004. A new isostatic model of the lithosphere and gravity field. Journal of Geodesy 78, 368–385.
Kázmér, M., Kovács, S., 1985. Permian–Paleogene paleogeography along the eastern part of the Insubric–Periadriatic lineament system: evidence for continental escape of the Bakony–Drauzug unit. Acta Geologica Hungarica 28, 71–84.
Kirby, S.H., Kronenberg, A.K., 1987. Rheology of the lithosphere: selected topics. Reviews of Geophysics and Space Physics 25, 1219–1244.
Kissling, E., Spakman, W., 1996. Interpretation of tomographic images of uppermost mantle structure: Examples from the western and central alps. Journal of Geodynamics 21, 97–111.
Klein, R., Barr, M., 1987. Regional State of Stress in Western Europe. In: Stephansson, O. (Ed.), Proceedings of the International Symposium on Rock Stress and Rock Stress Measurements. Centek, Lulea, Sweden, pp. 33–45.
Klett, M., Eichhorst, F., Schäfer, A., 2002. Facies interpretation from well-logs applied to the Tertiary Lower Rhine Graben fill. Geologie en Mijnbouw 81, 167–176.
Kohl, T., Bächler, D., Rybach, L., 2000. Steps towards a comprehensive thermo-hydraulic analysis of the HDR test site Soultz-sous Forets. Proceedings World Geothermal Congress, Kyushu, pp. 2671–2676.
Kooi, H., Cloetingh, S.A.P.L., 1989. Intraplate stresses and the tectono-stratigraphic evolution of the Central North Sea. American Association of Petroleum Geology Memoir, 46: 541–558.
Kooi, H., Cloetingh, S.A.P.L., Remmelts, G., 1989. Intraplate stresses and the stratigraphic evolution of the North Sea Central Graben. Geologie en Mijnbouw 68, 49–72.
Kostrov, V.V., 1974. Seismic moment and energy of earthquakes, and seismic flow of rocks. Izv. Russian Academy of Sciences. Physics of the Solid Earth 1, 23–44.
Koulakov, I., Kaban, M.K., Tesauro, M., Cloetingh, S., 2009. P en S velocity anomalies in the upper mantle beneath Europe from tomographic inversion of ISC data. Geophysical Journal International 179, 345–366.
Kukkonen, I.T., Peltonen, P., 1999. Xenolith-controlled geotherm for the central Fennoscandian Shield: implications for lithosphere–asthenosphere relations. Tectonophysics 304, 301–315.
Kusznir, N.J., Park, R.G., 1987. The extensional strength of the continental lithosphere; its dependence on geothermal gradient, and crustal composition and thickness. Geological Society Special Publication 28, 35–52.
Lambert, J., Winter, T., Dewez, T.J.B., Sabourault, P., 2005. New hypotheses on the maximum damage area of the 1356 Basel earthquake (Switzerland). Quaternary Science Reviews 24, 381–399.
Lankreijer, A., Mocanu, V., Cloetingh, S.A.P.L., 1997. Lateral variations in lithosphere strength in the Romanian Carpathians: constraints on basin evolution. Tectonophysics 272, 269–290.
Le Pichon, X., Bergerat, F., Roulet, M., 1988. Plate kinematics and tectonics leading to the Alpine belt formation — a new analysis. Special Paper of the Geological Society of America 218, 111–132.
Lenkey, L., 1999. Geothermics of the Pannonian Basin and its bearing on the tectonics of basin evolution, PhD Thesis, Vrije Universiteit, Amsterdam, 215 pp.
Lister, G.S., Banga, G., Feenstra, A., 1984. Metamorphic core complexes of cordilleran-type in the Cyclades, Aegean Sea, Greece. Geology 12, 221–225.
Lucazeau, F., Vasseur, G., Bayer, R., 1984. Interpretation of heat flow in the French Massif Central. Tectonophysics 103, 99–119.
Mancktelow, N.S., Grasemann, B., 1997. Time-dependent effects of heat advection and topography on cooling histories during erosion. Tectonophysics 270, 167–195.
Mareschal, J.C., Jaupart, C., 2004. Variations of surface heat flow and lithospheric thermal structure beneath the North American craton. Earth and Planetary Science Letters 223, 65–77.
Marotta, A.M., Bayer, U., Scheck, M., Thybo, H., 2001. The stress field below the NE German Basin: effects induced by the Alpine collision. Geophysical Journal International 144, 8–12.
Martin, M., Ritter, J.R.R., CALIXTO working group, 2005. High-resolution teleseismic body-wave tomography beneath SE Romania—I. Implications for three-dimensional versus one-dimensional crustal correction strategies with a new crustal velocity model. Geophysical Journal International 162, 448–460.
Martinod, J., Davy, P., 1994. Periodic instabilities during compression of the lithosphere: 2. Analogue experiments. Journal of Geophysical Research 99, 12057–12069.
McKenzie, D.P., 1967. Some remarks on heat flow and gravity anomalies. Journal of Geophysical Research 72, 6261–6273.
McKenzie, D.P., 1978. Some remarks on the development of sedimentary basins. Earth and Planetary Science Letters 40, 25–32.
McKenzie, D., Bickle, M.J., 1988. The volume and composition of melt generated by extension of the lithosphere. Journal of Petrology 29, 625–697.
McKenzie, D., Jackson, J., Priestley, K., 2005. Thermal structure of oceanic and continental lithosphere. Earth and Planetary Science Letters 233, 337–349.
Meghraoui, M., Camelbeeck, T., Vanneste, K., Brondeel, M., Jongmans, D., 2000. Active faulting and paleoseismology along the Bree fault, Lower Rhine Graben (Belgium). Journal of Geophysical Research 105, 13809–13841.
Meghraoui, M., Delouis, B., Ferry, M., Giardini, D., Huggenberger, P., Spottke, I., Granet, M., 2001. Active faulting in the Upper Rhine Graben and palaeoseismic identification of the 1356 Basel earthquake. Science 293, 2070–2073.
Meissner, R., Wever, T., Fluh, E., 1987. The Moho of Europe—implications for crustal development. Annales Geophysicae 5 (357–364).
Merle, O., Michon, L., 2001. The formation of the West European Rift: a new model as exemplified by the Massif Central area. Bulletin de la Société Géologique de France 172, 213–221.
Meyer, B., Lacassin, R., Brulhet, J., Mouroux, B., 1994. The Basel 1356 earthquake: which fault produced it? Terra Nova 6, 54–63.
Michon, L., van Balen, R.T., Merle, O., Pagnier, H., 2003. The Cenozoic evolution of the Roer Valley Rift system integrated at a European scale. Tectonophysics 367, 101–126.
Moeck, I., Kwiatek, G., Zimmermann, G., 2009. Slip tendency analysis, fault reactivation potential and induced seismicity in a deep geothermal reservoir. Journal of Structural Geology 31, 1174–1182 DOI:10.1016/j.jsg.2009.06.012.
Moisio, K., Kaikkonen, P., Beekman, F., 2000. Rheological structure and dynamical response of the DSS profile BALTIC in the SE Fennoscandian Shield. Tectonophysics 320, 175–194.
Montelli, R., Nolet, G., Dahlen, F.A., Masters, G., Robert Engdahl, E., Hung, S.-H., 2004. Finite-frequency tomography reveals a variety of plumes in the mantle. Science 303, 338–343.
Mooney, W.D., Laske, G., Masters, T.G., 1998. CRUST 5.1: a global crustal model at 5°×5°. Journal of Geophysical Research 103, 727–747.
Morgan, P., Fernàndez, M., 1992. Neogene vertical movements and constraints on extension in the Catalan Coastal Ranges, Iberian Peninsula, and the Valencia trough (western Mediterranean). Tectonophysics 203, 185–201.
Müller, W.H., Blümling, P., Becker, A., Clauss, B., 1987. Die Entkoppelung des tektonischen Spannungsfeldes an der Jura-Überschiebung. Eclogae Geologicae Helvetiae 80, 473–489.
Müller, B., Zoback, M.L., Fuchs, K., Mastin, L., Gregersen, S., Pavoni, N., Stephansson, O., Ljunggren, C., 1992. Regional patterns of tectonic stress in Europe. Journal of Geophysical Research 97, 11783–11803.
Müller, W.H., Naef, H., Graf, H.R., 2002. Geologische Entwicklung der Nordwestschweiz, Neotektonik und Langzeitszenarien Zürcher Weinland. NAGRA Technischer Bericht, Wettingen, p. 237. 99-08.
NEIC, 2004. http://earthquake.usgs.gov/regional/neic/.
Nelson, K.D., 1992. Are crustal thickness variations in old mountain belts like the Appalachians a consequence of lithospheric delamination? Geology 20, 498–502.
Nivière, B., Winter, T., 2000. Pleistocene northwards fold propagation of the Jura within the southern Upper Rhine Graben; seismotectonic implications. Global and Planetary Change 27, 263–288.
Norden, B., Förster, A., Balling, N., 2008. Heat flow and lithospheric thermal regime of the northeast German Basin. Tectonophysics 460 (1–4), 215–229.
Nyblade, A.A., Pollack, H.N., 1993. A global analysis of heat flow from Precambrian terrains: implications for the thermal structure of Archean and Proterozoic lithosphere. Journal of Geophysical Research 98, 12207–12218.
Panza, C., Mueller, S., Calganile, G., 1980. The gross features of the lithosphere–asthenosphere system in Europe from seismic surface waves and body waves. Pure and Applied Geophysics 118, 1209–1213.
Panza, G.F., Suhadolc, P., Chiaruttini, C., 1986. Exploitation of broad-band networks through broad-band synthetic seismograms. Annales Geophysicae 4, 315–328.
Pascal, C., van Wijk, J.W., Cloetingh, S.A.P.L., Davies, G.R., 2002. Effect of lithosphere thickness heterogeneities in controlling rift localization: numerical modeling of the Oslo Graben. Geophysical Research Letters 29, 1355.
Pascal, C., Cloetingh, S., 2009. Gravitational potential stresses and stress field of passive continental margins: Insights from the south-Norway shelf. Earth and Planetary Science Letters 277, 464–473.
Pasquale, V., Verdoya, M., Chiozzi, P., 2001. Heat flux and seismicity in the Fennoscandian Shield. Physical of the Earth and Planetary Interiors 126, 147–162.
Pérez-Gussinyé, M., Reston, T.J., 2001. Rheological evolution during extension at nonvolcanic rifted margins: onset of serpentinization and development of detachments leading to continental breakup. Journal of Geophysical Research 106, 3961–3975.
Pérez-Gussinyé, M., Watts, A.B., 2005. The long-term strength of Europe and its implications for plate forming processes. Nature 436, 381–384.
Philippe, Y., Coletta, B., Deville, E. and Mascle, A., 1996. The Jura fold-and-thrust belt: a kinematic model based on map-balancing. In: P.A. Ziegler and F. Horvath (Editors), Peri-Tethys Memoir 2: Structure and Prospects of Alpine Basins and Forelands. Mém. Mus. natn. Hist. nat., pp. 235–261.
Piromallo, C., Morelli, A., 2003. P wave tomography of the mantle under the Alpine–Mediterranean area. Journal of Geophysical Research 108, 2065.
Plenefisch, T., Bonjer, K.P., 1997. The stress field in the Rhine Graben area inferred from earthquake focal mechanisms and estimation of frictional parameters. Tectonophysics 275, 71–97.
Plomerová, J., Babuška, V., Vecsey, L., Kouba, D., TOR Working Group, 2002. Seismic anisotropy of the lithosphere around the Trans-European Suture Zone (TESZ) based on teleseismic body-wave data of the Tor experiment. Tectonophysics 360, 89–114.
Pollack, H.N., Chapman, D.S., 1977. On the regional variation of heat flow, geotherms, and lithospheric thickness. Tectonophysics 38, 279–296.
Poudjom Djomani, Y.H., Fairhead, J.D., Griffin, W.L., 1999. The flexural rigidity of Fennoscandia: reflection of the tectonothermal age of the lithospheric mantle. Earth and Planetary Science Letters 174, 139–154.

Praus, O., Pěčová, J., Petr, V., Babuška, V., Plomerová, J., 1990. Magnetotelluric and seismological determination of the lithosphere–asthenosphere transition in Central Europe. Physical of the Earth and Planetary Interiors 60, 212–228.
Prodehl, C., Mueller, S., Haak, V., 1995. The European Cenozoic Rift System. In: Olsen, K.H. (Ed.), Continental Rifts: Evolution, Structure, Tectonics, Developments in Geotectonics. Elsevier, Amsterdam.
Ranalli, G., Rybach, L., 2005. Heat flow, heat transfer and lithosphere rheology in geothermal areas: features and examples. Journal of Volcanology and Geothermal Research 148 (1–2), 3–19.
Ratschbacher, L., Frisch, W., Linzer, H.-G., Merle, O., 1991. Lateral extrusion in the Eastern Alps. Tectonics 10, 257–271.
Reigber, C., Schwintzer, P., Stubenvoll, R., Schmidt, R., Flechtner, F., Meyer, U., König, R., Neumayer, H.-K., Förste, Ch., Barthelmes, F., Zhu, S.Y., Balmino, G., Biancale, R., Lemoine, J.-M., Meixner, H., Raimondo, J.C., 2006. A High Resolution Global Gravity Field Model Combining CHAMP and GRACE Satellite Mission and Surface Data: EIGENCG01C. Scientific Technical Report STR06/07, Potsdam.
Reston, T.J., 1990. The lower crust and the extension of the continental lithosphere; kinematic analysis of BIRPS deep seismic data. Tectonics 9, 1235–1248.
Ritter, J.R.R., Jordan, M., Christensen, U.R., Achauer, U., 2001. A mantle plume below the Eifel volcanic fields, Germany. Earth and Planetary Science Letters 186, 7–14.
Robertson, A.H.F., Grasso, M., 1995. Overview of the Late Tertiary–Recent tectonic and palaeo-environmental development of the Mediterranean region. Terra Nova 7, 114–127.
Roca, E., 2001. The northwest Mediterranean Basin (Valencia Trough, Gulf of Lions andLiguro-P rovencal basins); structure and geodynamic evolution. In: P.A. Ziegler, W. Cavazza, A.H.F. Robertson and S. Crasquin-Soleau (Editors), Peri-Tethys Memoir 6, Peri-Tethyan rift/Wrench Basins and Passive Margins. Mém. Mus. Nat. Hist. Nat, Paris, pp. 671–706.
Roca, E., Sans, M., Cabrera, L., Marzo, M., 1999. Oligocene to Middle Miocene evolution of the central Catalan margin (northwestern Mediterranean). Tectonophysics 315, 209–233.
Rondeel, H.E., Everaars, J.S.L., 1993. Spanning in noordoost Nederland, een breakoutanalyse, in Eindrapport Multidisciplinair Onderzoek naar de Relatie Tussen Gaswinning en Aardbevingen in Noord-Nederland, Het Koninklijk Neder. Meteorol. Inst, De Bilt, Netherlands.
Royden, L.H., 1988. Late Cenozoic tectonics of the Pannonian Basin system. In: L.H. Royden and F. Horvath (Editors), The Pannonian basin: a study in basin evolution. AAPG Memoir, pp. 27–48.
Royden, L., Keen, C.E., 1980. Rifting process and thermal evolution of the continental margin of Eastern Canada determined from subsidence curves. Earth and Planetary Science Letters 51, 343–361.
Royden, L.H., Dövényi, P., 1988. Variations in Extensional Styles at Depth across the Pannonian Basin System. In: Royden, L.H., Horváth, F. (Eds.), Amer. Assoc. Petr. Geol. Mem., 45, pp. 235–255.
Royden, L.H., Horváth, F., Rumpler, J., 1983a. Evolution of the Pannonian basin system: 1. Tectonics. Tectonics 2, 63–90.
Royden, L.H., Horváth, F., Nagymarosy, A., Stegena, L., 1983b. Evolution of the Pannonian basin system: 2. Subsidence and thermal history. Tectonics 2, 91–137.
Rudnick, R.L., Fountain, D.M., 1995. Nature and composition of the continental crust: a lower crustal perspective. Reviews of Geophysics 33, 267–309.
Rudnick, R.L., McDonough, W.F., O'Connell, R.J., 1998. Thermal structure, thickness and composition of continental lithosphere. Chemical Geology 145, 395–411.
Sachsenhofer, R., 2001. Syn- and post-collisional heat flow in the Cenozoic Eastern Alps. International Journal of Earth Sciences 90, 579–592.
Sachsenhofer, R.F., Lankreijer, A., Cloetingh, S.A.P.L., Ebner, F., 1997. Subsidence analysis and quantitative basin modelling in the Styrian Basin (Pannonian Basin System, Austria). Tectonophysics 272, 175–196.
Sandiford, M., McLaren, S., 2006. Thermo-mechanical controls on heat production distributions and the long-term evolution of the continents. In: Brown, M., Rushmer, T. (Eds.), Evolution and differentiation of the continental crust. Cambridge University Press, pp. 67–91.
Sandiford, M., Frederiksen, S., Braun, J., 2003. The long-term thermal consequences of rifting: implications for basin reactivation. Basin Research 15, 23–43.
Sanjuan, B., Pinault, J.-L., Rose, P., Gerard, A., Brach, M., Baribant, G., Crouzet, C., Foucher, J.-L., Gautier, A., Touzelet, S., 2006. Tracer testing of the geothermal heat exchanger at Soultz-sous-Forêts (France) between 2000 and 2005. Geothermics 35, 622–653.
Schoenwiesner-Bozkurt, C., 2006. Presentation of Geothermal Project "Unterhaching", Germany. In: Kaltschmitt, M., Le Bel, L. (Eds.), ENGINE workshop 5 "Electricity generation from Enhanced Geothermal Systems", Strasbourg, France.
Schumacher, M.E., 2002. Upper Rhine Graben: role of preexisting structures during rift evolution. Tectonics 21, 1006.
Shapiro, N.M., Ritzwoller, M.H., 2002. Monte-Carlo inversion for a global shear velocity model of the crust and upper mantle. Geophysical Journal International 151, 88–105.
Shudofsky, G.N., Cloetingh, S.A.P.L., Stein, S., Wortel, R., 1987. Unusually deep earthquakes in East Africa: constraints on the thermo mechanical structure of a continental rift system. Geophysical Research Letters 14, 741–744.
Sittler, C., 1969. Le fosse Rhénan en Alsace aspect structural et histoire géologique. Revue de Geographie Physysique et Geologie Dynamique 2, 465–494.
Sleep, N.H., 2005. Evolution of the continental lithosphere. Annual Review of Earth and Planetary Sciences 33, 369–393.
Sleep, N.H., 2006. Mantle plumes from top to bottom. Earth-Science Reviews 77, 231–271.
Sobolev, S.V., Zeyen, H., Stoll, G., Werling, F., Altherr, R., Fuchs, K., 1996. Upper mantle temperatures from teleseismic tomography of French Massif Central including effects of composition, mineral reactions, anharmonicity, anelasticity and partial melt. Earth and Planetary Science Letters 139, 147–163.
Spadini, G., Cloetingh, S.A.P.L., Bertotti, G., 1995. Thermo-mechanical modeling of the Tyrrhenian Sea: Lithospheric necking and kinematics of rifting. Tectonics 14, 629–644.
Spakman, W., 1990. The Structure of the Lithosphere and Mantle beneath the Alps as Mapped by Delay Time Tomography. In: Freeman, R., Giese, P., Mueller, S. (Eds.), EuropeanGeotraverse (EGT) Project: integrative studies. European Science Foundation, Strassbourg, pp. 213–220.
Spakman, W., van der Lee, S., van der Hilst, R., 1993. Travel-time tomography of the European–Mediterranean mantle down to 1400 km. Physical of the Earth and Planetary Interiors 79, 3–74.
Stephenson, R.A., 1989. Beyond First-Order Thermal Subsidence Models for Sedimentary Basins? In: Cross, T.A. (Ed.), Quantitative Dynamic Stratigraphy. Prentice-Hall, EnglewoodCliffs, NJ, pp. 113–125.
Stephenson, R.A., Cloetingh, S.A.P.L., 1991. Some examples and mechanical aspects of continental lithospheric folding. Tectonophysics 188, 27–37.
Taylor, S.R., McLennan, S.M., 1985. The Continental Crust: its Composition and Evolution. Blackwell, Cambridge, p. 312.
ter Voorde, M., Bertotti, G., 1994. Thermal effects of normal faulting during rifted basin formation. 1. A finite difference model. Tectonophysics 240, 133–144.
ter Voorde, M., Cloetingh, S.A.P.L., 1996. Numerical modelling of extension in faulted crust: effects of localized and regional deformation on basin stratigraphy. In: Buchanan, P.G., Nieuwland, D. (Eds.), Modern Developments in Structural Interpretation, Validation and Modelling: Geol. Soc. London Spec. Publ. , pp. 283–296.
ter Voorde, M., van Balen, R.T., Bertotti, G., Cloetingh, S.A.P.L., 1998. The influence of a stratified rheology on the flexural response of the lithosphere to (un)loading by extensional faulting. Geophysical Journal International 134, 721–735.
ter Voorde, M., de Bruijne, C.H., Cloetingh, S.A.P.L., Andriessen, P.A.M., 2004. Thermal consequences of thrust faulting: simultaneous versus successive fault activation and exhumation. Earth and Planetary Science Letters 223, 395–413.
ter Voorde, M., Gaspar-Escribano, J.M., Juez-Larré, J., Roca, E., Cloetingh, S.A.P.L., Andriessen, P., 2007. Thermal effects of linked lithospheric and upper crustal–scale processes: Insights from numerical modeling of the Cenozoic Central Catalan Coastal Ranges (NE Spain). Tectonics 26, TC5018.
Tesauro, M., Hollenstein, C., Egli, R., Geiger, A., Kahle, H.-G., 2005. CGPS and broad-scale deformation across the Rhine Graben and the Alps. International Journal of Earth Sciences 94, 525–537.
Tesauro, M., Hollenstein, C.h., Egli, R., Geiger, A., Kahle, H.G., 2006. Analysis of central western Europe deformation using GPS and seismic data. Journal of Geodynamics 42, 194–209.
Tesauro, M., Kaban, M.K., Cloetingh, S.A.P.L., Hardebol, N.J., Beekman, F., 2007. 3D strength and gravity anomalies of the European lithosphere. Earth and Planetary Science Letters 263, 56–73.
Tesauro, M., Kaban, M., Cloetingh, S.A.P.L., 2008. EuCRUST-07: a new reference model for European crust. Geophysical Research Letters 35, L05313.
Tester, J.W., Anderson, B.J., Batchelor, A.S., Blackwell, D.D., DiPippo, R., Drake, E.M., Garnish, J., Livesay, B., Moore, M.C., Nichols, K., Petty, S., Toksoz, M.N., Veatch, R.W., Baria, R., Augustine, C., Murphy, E., Negraru, P., Richards, M., 2007. Impact of enhanced geothermal systems on US energy supply in the twenty first century. Philosophical Transactions of the Royal Society A 365, 1057–1094.
Turcotte, D.L., Oxburgh, E.R., 1967. Finite amplitude convection cells and continental drift. Journal of Fluid Mechanics 28, 29–42.
Ustaszewski, K., Schumacher, M.E., Schmid, S., Nieuwland, D., 2005. Fault reactivation in brittle viscous wrench systems—dynamically scaled analogue models application to the Rhine–Bresse transform zone. Quaternary Science Reviews 24, 363–380.
Vakarcs, G., Vail, P.R., Tari, G., Pogácsás, G., Mattick, R.E., Szabó, A., 1994. Third-order Middle Miocene–Early Pliocene depositonal sequences in the prograding delta complex of the Pannonian basin. Tectonophysics 240, 81–106.
van Balen, R.T., van Bergen, F., De Leeuw, C., Pagnier, H., Simmelink, H., van Wees, J.D., Verweij, J., 2000. Modelling subsidence, compaction, heatflow and hydrocarbon generation and migration in the West Netherlands Basin, the Netherlands. Geologie en Mijnbouw 79, 29–44.
van Balen, R.T., Houtgast, R.F., Cloetingh, S.A.P.L., 2005. Neotectonics of The Netherlands: a review. Quaternary Science Reviews 24, 439–454.
van der Beek, P., Cloetingh, S., 1992. Lithospheric flexure and the tectonic evolution of the Betic Cordilleras (SE Spain). Tectonophysics 203, 325–344.
van der Beek, P., Cloetingh, S.A.P.L., Andriessen, P., 1994. Mechanism of extensional basin formation and vertical motions at rift flanks: constrains from tectonic modelling and fission track thermochronology. Earth and Planetary Science Letters 121, 417–433.
van der Pluim, B.A., Craddock, J.P., Graham, B.R., Harris, J.H., 1997. Paleostress in cratonic North America: implications for deformation of continental interiors. Science 277, 794–796.
van Eck, T., Davenport, C.A., 1994. Seismotectonics and seismic hazard in the Roer Valley Graben; with emphasis on the Roermond earthquake of April 13, 1992. Geologie en Mijnbouw 73, 91–92.
van Wees, J.D., Stephenson, R.A., 1995. Quantitative Modelling Of Basin and Rheological Evolution of the Iberian Basin (Central Spain): Implications for Lithospheric Dynamics of Intraplate Extension and Inversion. In: Cloetingh, S.A.P.L., D'Argenio, B., Catalano, R., Horvath, E., Sassi, W. (Eds.), Interplay of Extension and Compression in Basin Formation: Tectonophysics, pp. 163–178.
van Wees, J.D., Cloetingh, S.A.P.L., 1996. 3D flexure and intraplate compression in the North Sea Basin. Tectonophysics 266, 343–359.
van Wees, J.D., Beekman, F., 2000. Lithosphere rheology during intraplate basin extension and inversion. Tectonophysics 320, 219–242.
van Wees, J.D., Stephenson, R.A., Ziegler, P.A., Bayer, U., McCann, T., Dadlez, R., Gaupp, R., Narkiewicz, M., Bitzer, F., Scheck, M., 2000. On the origin of the Southern Permian Basin, Central Europe. Marine and Petroleum Geology 17, 43–59.

van Wees, J.-D., van Bergen, F., David, P., Nepveu, M., Beekman, F., Cloetingh, S.A.P.L., Bonte, D., 2009. Probabilistic tectonic heat flow modelling for basin maturation: assessment method and applications. Marine and Petroleum Geology 26, 536–551.
van Wijk, J.W., Cloetingh, S.A.P.L., 2002. Basin migration caused by slow lithospheric extension. Earth and Planetary Science Letters 198, 275–288.
Vauchez, A., Tommasi, A., Barruol, G., 1998. Rheological heterogeneity, mechanical anisotropy and deformation of the continental lithosphere. Tectonophysics 296, 61–86.
Ventura, B., Lisker, F., 2003. Long-term landscape evolution of the north-eastern margin of the Bohemian Massif: apatite fission track data from the Erzgebirge (Germany). International Journal of Earth Sciences 92, 691–700.
Villemin, T., Alvarez, F., Angelier, J., 1986. The Rhinegraben: extension, subsidence and shoulder uplift. Tectonophysics 128, 47–50.
Vosteen, H.-D., Rath, V., Clauser, C., Lammerer, B., 2006. A review of the thermal regime of the Eastern Alps with respect to the effects of paleoclimate and exhumation. Tectonophysics 414, 157–167.
Watts, A.B., Torné, M., 1992. Subsidence history, crustal structure, and thermal evolution of the Valencia trough: a young extensional basin in the Western Mediterranean. Journal of Geophysical Research 97 (B13), 20021–20041.
Watts, A.B., Burov, E., 2003. Lithospheric strength and its relationship to the elastic and seismogenic layer thickness. Earth and Planetary Science Letters 213, 113–131.
Wenzel, F., Sperner, B., Lorenz, F., Mocanu, V., 2002. Geodynamics, tomographic images and seismicity of the Vrancea region (SE–Carpathians, Romania). Stephan Mueller Special Publication Series 3, 95–104.
White, R.S., McKenzie, D.M., 1995. Mantle plumes and flood basalts. Journal of Geophysical Research 100, 17543–17585.
Wijbrans, J.R., van Wees, J.D., Stephenson, R.A., Cloetingh, S.A.P.L., 1993. Pressuretemperature timeevoltion of the high pressure metamorphic complex of Sifnos Greece. Geology 21, 443–446.
Willingshofer, E., Cloetingh, S.A.P.L., 2003. The lithospheric strength of the Eastern Alps and its relationship to neotectonics. Tectonics 22, 1075.
Willingshofer, E., Andriessen, P., Cloetingh, S.A.P.L., Neubauer, F., 2001. Detrital fission track thermochronology of upper Cretaceous synorogenic sediments in the South Carpathians (Romania); inferences on the tectonic evolution of a collisional hinterland. Basin Research 13, 379–395.
Wilson, M., Patterson, R., 2001. Intra-plate magmatism related to hot fingers in the upper mantle: evidence from the Tertiary–Quaternary volcanic province of western and central Europe. Geological Society of America Special Paper 352, 37–58.
Wortel, M.J.R., Spakman, W., 2000. Subduction and slab detachment in the Mediterranean–Carpathian region. Science 290, 1910–1917.
Worum, G., van Wees, J.D., Bada, G., van Balen, R.T., Cloetingh, S.A.P.L., Pagnier, H., 2004. Slip tendency analysis as a tool to constrain fault reactivation a numerical approach applied to 3-D fault models in the Roer Valley Rift System (Southeast Netherlands). Journal of Geophysical Research 109, B02401.
Yegorova, T.P., Starostenko, V.I., 2002. Lithosphere structure of Europe and Northern Atlantic from regional three-dimensional gravity modeling. Geophysical Journal International 151, 11–31.
Zeyen, H., Fernández, M., 1994. Integrated lithospheric modeling combining thermal, gravity, and local isostasy analysis: application to the NE Spanish Geotransect. Journal of Geophysical Research 99, 18089–18102.
Zeyen, H., Volker, F., Wehrle, V., Fuchs, K., Sobolev, S.V., Altherr, R., 1997. Styles of continental rifting; crust-mantle detachment and mantle plumes. Tectonophysics 278, 329–352.
Ziegler, P.A., 1988. Evolution of the Arctic–North Atlantic and the Western Tethys. American Association of Petroleum Geologists Memoir, 43, 198 pp.
Ziegler, P.A., 1989a. Geodynamic model for Alpine intraplate compressional deformation in western and central Europe. In: Cooper, M.A., Williams, G.D. (Eds.), Inversion tectonics. Geological Society Special Publicatio, London, pp. 63–85.
Ziegler, P.A., 1989b. Evolution of the North Atlantic; an overview. American Association of Petroleum Geologists Memoir, 46: 111–129.
Ziegler, P.A., 1990. Geological Atlas of Western and Central Europe, Shell International Petroleum Mij. B.V., distributed by Geological Society, 2nd Ed. Publishing House, Bath, London, p. 239.
Ziegler, P.A., 1992. European Cenozoïc rift system. Tectonophysics 208, 91–111.
Ziegler, P.A., 1994. Cenozoic rift systems of western and central Europe: an overview. Geologie en Mijnbouw 73, 99–127.
Ziegler, P.A., Cloetingh, S.A.P.L., 2004. Dynamic processes controlling evolution of rifted basins. Earth Science Reviews 64, 1–50.
Ziegler, P.A., Dèzes, P., 2005. Evolution of the lithosphere in the area of the Rhine Rift System. In: Behrmann, J.H., Granet, M., Schmid, S., Ziegler, P.A. (Eds.), EUCOR-URGENT Special Issue: International Journal of Earth Sciences, 94, pp. 594–614.
Ziegler, P.A., Dèzes, P., 2006. Crustal evolution of Western and Central Europe. In: Gee, D.G., Stephenson, R.A. (Eds.), European Lithosphere Dynamics: Geological Society of London, pp. 43–56.
Ziegler, P.A., Cloetingh, S.A.P.L., van Wees, J.D., 1995. Dynamics of intraplate compressional deformation: the Alpine foreland and other examples. Tectonophysics 252, 7–59.
Ziegler, P.A., van Wees, J.D., Cloetingh, S.A.P.L., 1998. Mechanical controls on collision-related compressional intraplate deformation. Tectonophysics 300, 103–129.
Ziegler, P.A., Cloetingh, S.A.P.L., Guiraud, R. and Stampfli, G.M., 2001. Peri-Tethyan platforms; Constraints on dynamics of rifting and basin inversion. In: P.A. Ziegler, W. Cavazza, A.H.F. Robertson and S. Crasquin-Soleau (Editors), Peri-Tethys Memoir 6; Peri-Tethyan rift/wrench basins and passive margins. Mém. Mus. Nat. Hist. Nat, pp. 9–49.
Ziegler, P.A., Bertotti, G., Cloetingh, S.A.P.L., 2002. Dynamic processes controlling foreland development—the role of mechanical (de)coupling of orogenic wedges and foreland. EGU Special Publication 1, 17–56.
Ziegler, P.A., Schumacher, M., Dèzes, P., van Wees, J.D., Cloetingh, S.A.P.L., 2004. Post-Variscan evolution of the lithosphere in the Rhine Graben area: constraints from subsidence modelling. Geological Society, London, Special Publications 223, 289–317.
Ziegler, P.A., Schumacher, M., Dèzes, P., van Wees, J.D. and Cloetingh, S.A.P.L., 2006. Post-Orogenic Evolution of the Variscan Lithosphere in the area of the European Cenozoic Rift System. In: D.G. Gee and R.A. Stephenson (Editors), European Lithosphere. Dynamics. Geological Society Memoirs 32, London, pp. 97–112.
Zijerveld, L., Stephenson, R., Cloetingh, S.A.P.L., Duin, E., van den Berg, M.W., 1992. Subsidence analysis and modelling of the Roer Valley Graben (SE Netherland). Tectonophysics 208, 159–171.
Zoback, M.D., 2007. Reservoir Geomechanics. Cambridge University Press, 448 pp.